Characterization of a three-dimensional culture system representative of disease progression in high-grade serous ovarian cancer

Naya El Mokbel

Faculty of Medicine

Department of Pathology

McGill University, Montreal

August 2023

A thesis submitted to McGill University in partial fulfillment of the requirements of the degree of

Master of Science

Table of Contents

Abstract

Introduction: Globally, ovarian cancer is the third most common gynecologic cancer after cervical and uterine cancer and is associated with the worst prognosis and the highest mortality rate. Approximately 313,959 individuals were diagnosed and 207,252 died of the disease in 2020 around the world. High-grade serous ovarian cancer (HGSC) is the most common histological subtype that is usually diagnosed at advanced stages and accounts for a high number of mortalities. While most patients initially respond to front-line platinum-based chemotherapy, over time, almost all recur despite therapy and develop resistance to platinum agents. These patients may benefit from different initial therapies or combination therapies such as PARP inhibitors (PARPis). The development of preclinical models to assess therapeutic responses would enable individualized therapy for patients. High-throughput 3D culture in which cells are maintained in suspension which stimulates formation of a 3D structure has been found to be a faithful preclinical model of ovarian cancer. We hypothesize that compared to 2D culture environments, in which cells are grown on flat surfaces, 3D culture models would more closely represent the in-vivo environment and may provide a more accurate representation of response to various therapies. PEO1, PEO4 and PEO6 are cell lines of epithelial origin derived from a single patient with HGSC collected at different stages of disease from initial diagnosis to death, thus illustrating disease progression. The aim of this project was to compare the behavior of PEO1, PEO4 and PEO6 with respect to morphology, viability, metabolic activity, and drug response in 2D culture as compared to 3D culture.

Methods: PEO1, PEO4 and PEO6 cells were grown in flat-bottom cell culture plates (i.e., in 2D culture) and in ultra-low attachment round-bottom plates (i.e., in 3D culture). Live/Dead, apoptosis, proliferation, and ATP quantitation assays were performed in both culture settings and

characterized using microscope imaging, cytometry, and spectrophotometry methods. The cell lines were exposed to therapeutic agents used in HGSC: carboplatin (25 μM to 200 μM), paclitaxel (1.25 μM to 10 μM), and the PARP inhibitor, niraparib (2 μM to 16 μM).

Results: In flat-bottom plates, PEO1 and PEO4 cells form a 2D cellular adherent layer whereas PEO6 cells, in addition to having an adherent component, over time naturally form 3D floating structures. In contrast, when grown in ultra-low attachment plates, all cell lines formed a 3D structure with different compaction levels. In 2D culture, the three cell lines proliferate with only few apoptotic cells scattered randomly on the bottom of the plates. Conversely, in 3D culture, all cell lines mimicked poorly vascularized tumors by forming a multilayered spheroidal structure with an outer layer of live cells (i.e., active cell proliferation) and an inner core of apoptotic cells (i.e., dead). Furthermore, a pronounced differential capacity of the cells to produce ATP was observed in 3D culture while the ATP production in 2D culture was of similar magnitude. In flat- and ultra-low attachment plates, response of the cell lines to carboplatin, paclitaxel and niraparib followed a similar trend. However, lower sensitivity to the drugs was observed in the 3D model as compared to in the 2D model. The reduced drug sensitivity displayed by cells in the ultra-low attachment plates may be more reflective of the magnitude of the in-vivo drug response.

Conclusions: The 3D culture environment provides a level of complexity absent in 2D culture making it more reflective of the in-vivo cellular tumor behavior central to prediction of in-vivo therapeutic responses.

Résumé

Introduction: Au niveau mondial, le cancer de l'ovaire est le troisième cancer gynécologique le plus fréquent, après le cancer du col de l'utérus et de l'utérus, et il est associé au pire pronostic et au taux de mortalité le plus élevé. Environ 313 959 personnes ont été diagnostiquées et 207 252 sont décédées de la maladie en 2020 dans le monde. Le cancer de l'ovaire séreux de haut grade (HGSC) est le sous-type histologique le plus courant. Si la plupart des patients répondent initialement à une chimiothérapie de première intention à base de platine, au fil du temps, la quasi-totalité d'entre eux récidivent malgré le traitement et développent une résistance aux agents de platine. Ces patients peuvent bénéficier de thérapies initiales différentes ou de thérapies combinées telles que les inhibiteurs de PARP. Le développement de modèles précliniques pour évaluer les réponses thérapeutiques permettrait d'individualiser les traitements. La culture 3D dans laquelle les cellules sont maintenues en suspension, ce qui stimule la formation d'une structure 3D, s'est avérée être un modèle préclinique fidèle du cancer de l'ovaire. Nous émettons l'hypothèse que, par rapport à la culture 2D, les modèles de culture 3D représenteraient plus fidèlement l'environnement in-vivo et pourraient fournir une représentation plus précise de la réponse à diverses thérapies. PEO1, PEO4 et PEO6 sont des lignées cellulaires d'origine épithéliale dérivées d'une seule patiente atteinte de HGSC et prélevées à différents stades de la maladie, du diagnostic initial au décès, illustrant ainsi la progression de la maladie. L'objectif de ce projet était de comparer le comportement des cellules PEO1, PEO4 et PEO6 en ce qui concerne la morphologie, la viabilité, l'activité métabolique et la réponse aux médicaments en culture 2D par rapport à la culture 3D.

Méthodes: Les cellules PEO1, PEO4 et PEO6 ont été cultivées dans des plaques de culture cellulaire à fond plat (en culture 2D) et dans des plaques à fond rond à fixation ultra-faible (en culture 3D). Des essais de Mort/Vivant, d'apoptose, de prolifération et de quantification de l'ATP

ont été réalisés dans les deux contextes de culture. Les lignées cellulaires ont été exposées à des agents thérapeutiques utilisés pour le HGSC: carboplatine (25 μM à 200 μM), paclitaxel (1,25 μM à 10 μM) et l'inhibiteur PARP, niraparib (2 μM à 16 μM).

Résultats: Dans les plaques à fond plat, les cellules PEO1 et PEO4 forment une couche cellulaire adhérente en 2D, tandis que les cellules PEO6, en plus d'avoir une composante adhérente, forment naturellement au fil du temps des structures flottantes en 3D. En revanche, lorsqu'elles sont cultivées sur des plaques à fixation ultra-faible, toutes les lignées cellulaires forment une structure 3D avec différents niveaux de compaction. En culture 2D, les trois lignées cellulaires prolifèrent avec seulement quelques cellules apoptotiques dispersées au hasard sur le fond des plaques. En culture 3D, toutes les lignées cellulaires imitent les tumeurs mal vascularisées en formant une structure sphéroïdale multicouche avec une couche externe de cellules vivantes (c'est-à-dire avec une prolifération cellulaire active) et un noyau interne de cellules apoptotiques (c'est-à-dire mortes). Une capacité différentielle prononcée des cellules à produire de l'ATP a été observée en culture 3D, alors que la production d'ATP en culture 2D était d'une ampleur similaire. Dans les plaques à fixation plate et ultra-faible, la réponse des lignées cellulaires au carboplatine, au paclitaxel et au niraparib a suivi une tendance similaire. Toutefois, une sensibilité moindre aux médicaments a été observée dans le modèle 3D par rapport au modèle 2D.

Conclusions: L'environnement de culture en 3D offre un niveau de complexité absent dans la culture en 2D, ce qui permet de mieux refléter le comportement cellulaire in-vivo de la tumeur, essentiel à la prédiction des réponses thérapeutiques in-vivo.

Acknowledgements

I would like to thank Dr. Alicia Goyeneche for providing feedback and advice on a daily basis, and for explaining and demonstrating various new laboratory techniques. I would like to thank the other members of the Telleria laboratory, Benjamin Forgie, Rewati Prakash, Farah Abdalbari and Elvis Martínez Jaramillo as well as the other members of the Leung laboratory, Erica Mandato, Simane Warsame, Hila Trabizian and Chelsea Zhou for providing advice, making suggestions and helping with troubleshooting when necessary. In particular, I would like to thank Benjamin Forgie, for introducing me to the basics of cell culture, for helping with the development of the luminescence reading protocol as well as with the establishment of the organoid protocol and generation of the first PDOs in the lab; Rewati Prakash, for helping with the development of the cell imaging protocols as well as with the establishment of the organoid protocol and generation of the first PDOs in the lab and Farah Abdalbari for performing the plating of PEO4 cells and the drug testing for the Caspase-3/7 positive control experiment. I would like to thank Chelsea Zhou for helping with gathering the clinical history of the patients for which organoids were generated; the Leung laboratory manager, Zahraa Qusairy, for helping with the organoid project and the gynecology oncology team at the McGill University Health Center for helping with the patient samples collection and analysis.

I would like to thank my research supervisors, Dr. Shuk On Annie Leung and Dr. Carlos Telleria for providing advice and support as well as for guiding my progression over the course of the project, and my research advisory committee members, Drs. Basile Tessier-Cloutier and Xing Zeng, for providing advice and feedback, as well as for assessing my progress. I would like to thank the members of the Department of Pathology of McGill University, Dr. Edith Zorychta, and

Dr. Hua Ling, and the Department as a whole, for funding my project as well as for overseeing the graduate student program of the department.

Additionally, I would like to thank Dr. Lorenzo Ferri and Julie Bérubé for providing help and knowledge in the establishment of our organoid development platform and Céline Domecq for helping with the generation of organoids.

This project was funded by the Graduate Excellence Award from the Department of Pathology of McGill University, the Research Institute of the McGill University Health Center Studentship Award, the Cedars Cancer Centre Henry Shibata Award, and the OvCAN program of Ovarian Cancer Canada.

Preface

This thesis is presented based on the manuscript-based thesis guidelines provided by McGill University and contains a manuscript in preparation for submission to Biochemical and Biophysical Research Communications. Chapter 1 is a literature review of ovarian cancer, cell culture models, specific ovarian cancer cell lines, and provides an introduction of the project (rationale, hypothesis, and aims). Chapter 2 reports our findings in comparing the behavior of PEO1, PEO4 and PEO6 cells in terms of morphology, viability, metabolic activity, and drug response in 2D culture versus 3D culture. Lastly, chapter 3 provides a specific discussion on the organoids part of the project and chapter 4 provides a general discussion of the findings, limitations, implications, and future directions. This thesis was written by myself with guidance from my supervisors, Dr. Shuk On Annie Leung and Dr. Carlos Telleria, as well as Dr. Alicia Goyeneche.

Contribution of Authors

This work was written in its entirety and edited by Naya El Mokbel. Prior to initial submission, this work was read and edited by Dr. Shuk On Annie Leung, Dr. Carlos Telleria and Dr. Alicia Goyeneche. Drs. Leung, Telleria and Goyeneche contributed to the design of experiments, data analysis and manuscript/thesis revision.

List of Figures

List of Tables

List of Protocols

List of Abbreviations

2D - Two-Dimensional

3D - Three-Dimensional

EdU - 5-Ethynyl-2′-deoxyuridine

BRCA1 - BReast CAncer gene 1

BRCA2 - BReast CAncer gene 2

CA125 - Cancer antigen 125

CCC - Clear cell carcinoma of the ovary

CT - Computerized tomography

CtIP - CtBP-interacting protein

DNA-PKCS - DNA-dependent protein kinase catalytic subunit

DSB - Double strand break

EC - Endometrioid carcinoma of the ovary

EMBRACE - Epidemiological Study of *BRCA1* and *BRCA2* mutation carriers

ER – Estrogen receptor

FIGO - International Federation of Gynecology and Obstetrics

HE4 - Human epididymis protein 4

HGSC - High-grade serous carcinoma

HRR - Homologous recombination DNA repair

IGF - Insulin-like growth factor

IL-8 - Interleukin 8

LGSC - Low-grade serous carcinoma

MCP-1- Monocyte chemotactic protein-1

MC - Mucinous carcinoma of the ovary

MMMT - Malignant mixed mullerian tumour

MRI - Magnetic resonance imaging

NHEJ - Non-homologous end joining

OS - Overall survival

P53 - Tumor protein p53

PARP - Poly (ADP-ribose) polymerase enzyme

PARPis - PARP inhibitors

PAX8 - Paired-box gene 8

PDOs - Patient-derived organoids

PDXs - Patient-derived xenografts

PFS - Progression-free survival

PD-1 - Programmed death 1

PD-L1 - Programmed death ligand 1

PR – Progesterone receptor

RANTES - Regulated on activation, normally T-cell expressed and secreted

ROS - Reactive oxygen species

SCOUTs - Secretory cell outgrowth

STIC - Serous tubal intraepithelial carcinoma

TAM – Tumor associated macrophages

TGF-β - Transforming growth factor-β

TIC - Tubal intraepithelial carcinoma

TVUS - Transvaginal ultrasound

ULAPs - Ultra-low attachment round-bottom cell culture plates

WT1 - Wilm's tumor gene 1

Chapter 1.
Literature Review and Introduction

1.1 Ovarian Cancer

1.1.1 Epidemiology

Globally, ovarian cancer is the third most common gynecologic cancer after cervical and uterine cancer and is associated with the worst prognosis and the highest mortality rate among all gynecological cancers[1-4]. Approximately 313,959 individuals were diagnosed and 207,252 died of the disease in 2020 worldwide[5]. In the United States, ovarian cancer accounts for 2.5% of all malignancies among women, but for more deaths than any other cancer of the female reproductive system[6, 7]; the lifetime risk of developing ovarian cancer is approximately 1.1%[8]. The high mortality rate results from lack of specific symptoms and lack of screening tools that results in 70% of ovarian cancer being diagnosed at advanced stages[1, 2, 9]. As a result, less than one-half of patients survive for more than five years after diagnosis[1, 6, 10]. In Canada, approximately 45% of patients diagnosed with ovarian cancer will survive for at least 5 years[11]. Age-adjusted rates for new ovarian cancer cases have decreased on average by 3.2% each year between 2010 and 2019[8]. Several factors may have contributed to this favorable trend, including the declining smoking prevalence, and increasing use of oral contraceptives, which may have a protective effect for ovarian cancer[12-14].

1.1.2 Classification

Ovarian cancer is not a homogeneous disease but rather a group of diseases each with different morphology and biological behavior[15] and is classified based on the cells from which it initiates[16]. The common cell types are epithelial cells (which account for around 90% of malignant tumors), germ cells, and stromal cells[16]. Based on histopathology, immunohistochemistry, and molecular genetic analysis, there are at least five main types of ovarian cancer of epithelial origin:

high-grade serous carcinoma (HGSC) which accounts for 70% of cases, endometrioid carcinoma (EC) which accounts for 10% of cases, clear-cell carcinoma of the ovary (CCC) which accounts for 10% of cases, low-grade serous carcinoma (LGSC) which accounts for less than 5% of cases, and mucinous carcinoma (MC) which accounts for 3% of cases (Fig.1.1)[15, 17]. Epithelial ovarian cancer can be further classified as type I and type II based on clinicopathologic factors[16]. Type I ovarian cancer includes LGSC, CCC, EC and MC whereas type II ovarian cancer consists of HGSC[16]. Type II is the most common histological subtype and is usually diagnosed at advanced stages and accounts for a high number of mortalities[16, 18].

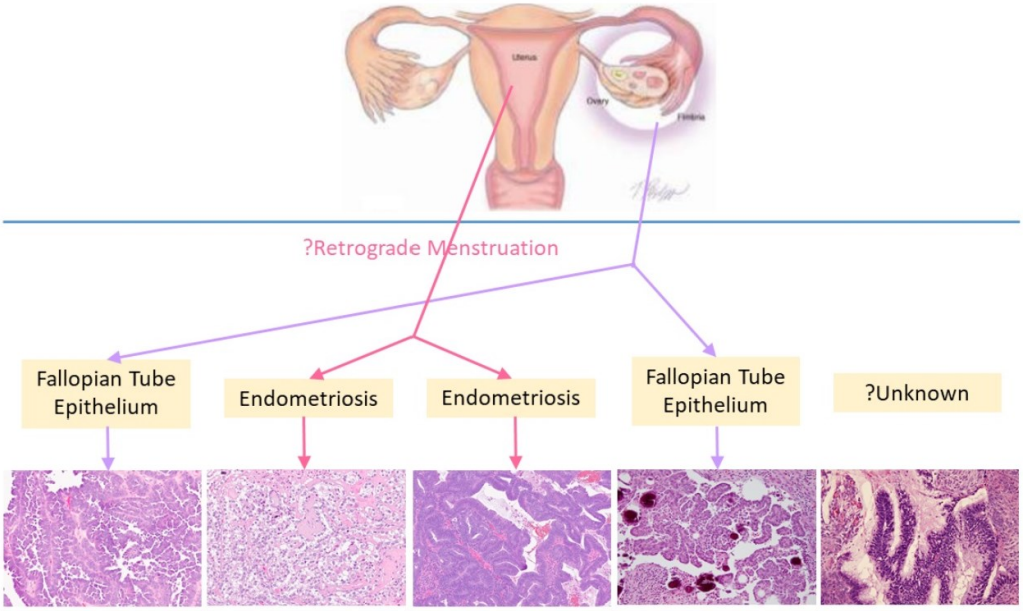

	High-Grade Serous Carcinoma	Clear Cell Carcinoma	Endometrioid Carcinoma	Low-Grade Serous Carcinoma	Mucinous Carcinoma
% of all Ovarian Carcinomas	~70%	~10%	~10%	<5%	<5%
Precursor Lesions	Serous tubal intraepithelial carcinoma (STIC)	Clear Cell Borderline Tumor	Endometrioid Borderline Tumor	Serous Borderline Tumor	Mucinous Borderline Tumor

Figure 1.1. Five major types of epithelial ovarian cancer. Other rare subtypes not listed include carcinosarcoma (Malignant Mixed Mullerian Tumour, MMMT), undifferentiated carcinoma and malignant Brenner tumour. Adapted from BC Cancer[19].

1.1.3 Staging

The International Federation of Gynecology and Obstetrics (FIGO) staging of ovarian cancer is based on surgical assessment of the cancer at initial diagnosis which may include hysterectomy, bilateral salpingo-oophorecotmy, omentectomy, removal of lymph nodes, biopsies and resection of other tumor sites, and collection of ascites fluid[20]. Staging allows one to describe the extent of tumor spread and to define groups of patients with similar prognoses[21]. The FIGO classification is divided into stages I, II, III and IV, and is further sub-divided into stages IA, IB, IC, IC1, IC2, IC3, IIA, IIB, IIIA1, IIIA2, IIIB, IIIC, IVA and IVB cancers.

Stage I ovarian cancer is relatively rare and is associated with excellent survival rates[22]. In stage IA, the tumor is limited to one ovary or fallopian tube (Fig.1.2A, yellow) while in stage IB, the tumor is limited to both ovaries or fallopian tubes (Fig.1.2A, blue). Stage IC1 indicates intraoperative spill when tumor cells are exposed into the sterile surgical field when otherwise no tumor cells are outside the affected organ site (Fig.1.2B)[22, 23]. Stage IC2 indicates preoperative rupture of the tissue around the tumor or the tumor being present on the ovarian or fallopian tube surface. In stage IC3, malignant cells are found in peritoneal washings or in ascites, which refers to the accumulation of fluid in the abdomen (Fig.1.2C)[22, 24].

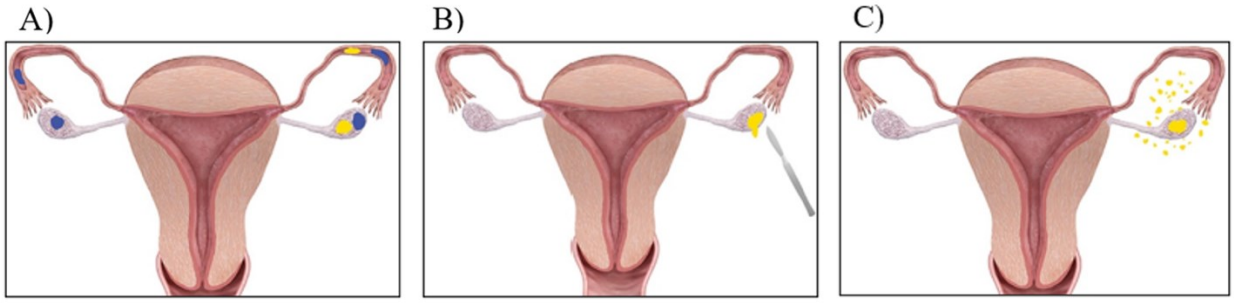

Figure 1.2. Stage I epithelial ovarian cancer. A) In stage IA, the tumor is limited to one ovary or fallopian tube (yellow) while in stage IB, the tumor is limited to both ovaries or fallopian tubes (blue). B) In Stage IC1, intraoperative spillage is noted. In stage IC2, preoperative rupture of the tumor or the tumor being present on the ovarian or fallopian tube surface is identified. C) In stage IC3, malignant cells are found in ascites or peritoneal washings. Adapted from Javadi *et al*[22].

In stage IIA, the tumor involves one or both ovaries or fallopian tubes extends to and/or is implanted on the uterus and/or the fallopian tubes (Fig.1.3)[22]. If it extends to other pelvic intraperitoneal tissues (below the pelvic rim), it is considered to be stage IIB. This group makes up less than 10% of tumors and is considered curable[22].

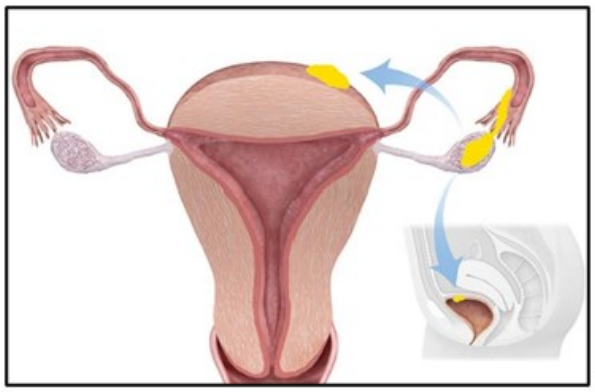

Figure 1.3. Stage II epithelial ovarian cancer. A) In stage IIA, the tumor involves one or both ovaries or fallopian tubes. In stage IIB, it extends to and/or is implanted on the uterus and/or the fallopian tubes. Adapted from Javadi *et al*[22].

The majority of ovarian cancers present as stage III with 84% as stage IIIC[22]. In stage III, the tumor involves one or both ovaries with spread to the peritoneum outside the pelvis and/or metastasis to the retroperitoneal lymph nodes. In stage IIIA1, there are positive retroperitoneal lymph nodes (Fig.1.4A). In stage IIIA2, microscopic, extrapelvic (above the pelvic rim) peritoneal

involvement is seen with or without positive retroperitoneal lymph nodes (Fig.1.4B). In stage IIIB or stage IIIC, macroscopic, extrapelvic (above the pelvic rim) peritoneal involvement is seen with or without positive retroperitoneal lymph nodes (Fig.1.4C). If the size of peritoneal metastases is 2 cm or smaller, it is classified as stage IIIB whereas if it is larger than 2 cm, it is considered stage IIIC[22].

Lastly, 12% to 21% of patients with ovarian cancer present distant metastatic disease, classified as stage IV[22]. In stage IVA, pleural effusion with positive cytology is present (Fig.1.5). In stage IVB cancer, hepatic and/or splenic parenchymal metastasis is seen as well as metastasis to extra-abdominal organs (Fig.1.5)[22].

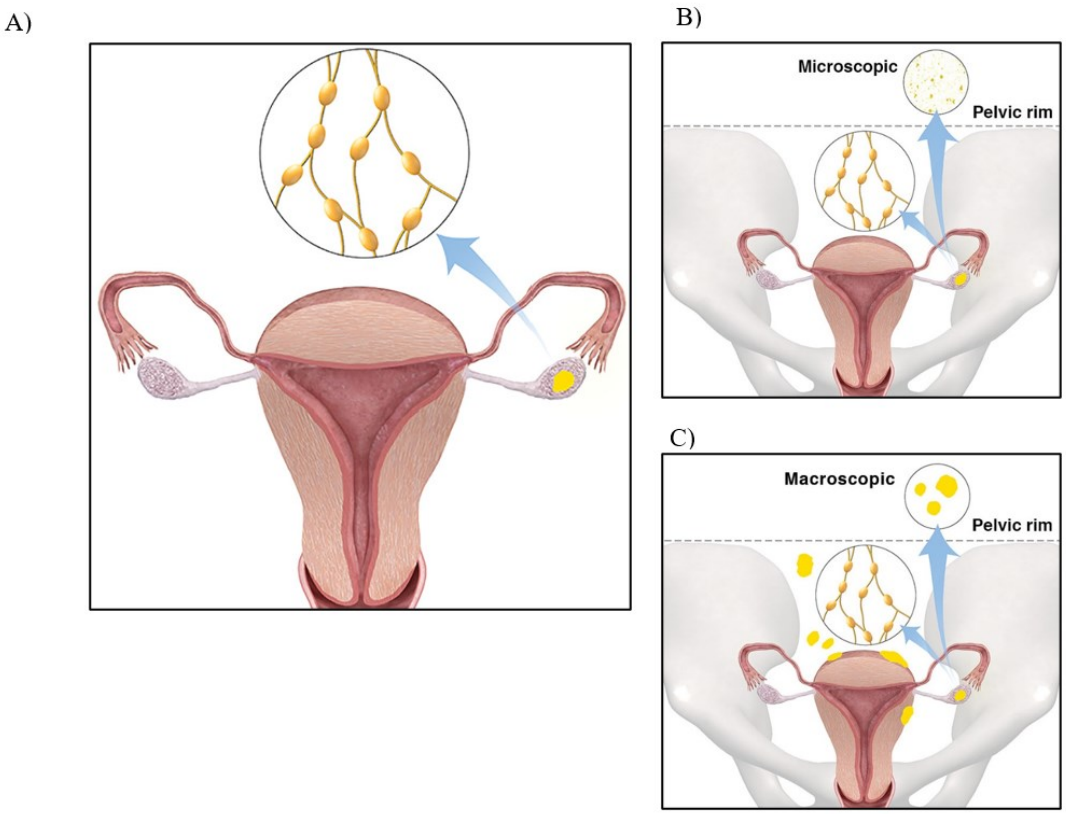

Figure 1.4. Stage III epithelial ovarian cancer. A) Stage IIIA1, the cancer shows positive retroperitoneal lymph nodes. B) Stage IIIA2, microscopic, extrapelvic (above the pelvic rim) peritoneal involvement is seen with or without positive retroperitoneal lymph nodes. C) When macroscopic, extrapelvic (above the pelvic rim) peritoneal involvement is seen with or without positive retroperitoneal lymph nodes, it is considered stage IIIB if the size of peritoneal metastases is 2 cm or smaller and stage IIIC if it is larger than 2 cm. Adapted from Javadi *et al*[22].

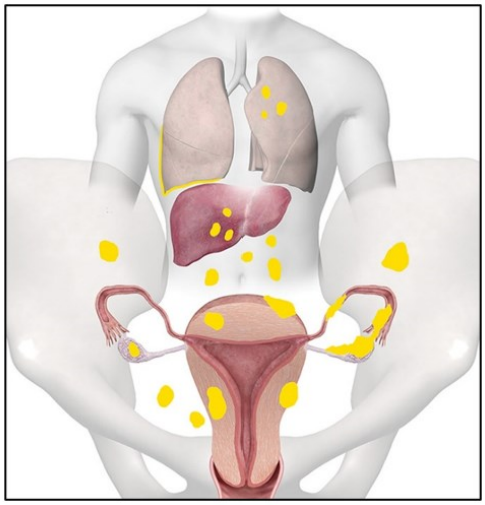

Figure 1.5. Stage IV epithelial ovarian cancer. In stage IVA, pleural effusion with positive cytology is present while in stage IVB, hepatic and/or splenic parenchymal metastasis is seen as well as metastasis to extra-abdominal organs. Adapted from Javadi *et al* [22].

1.1.4 Pathogenesis

There are three main theories postulated to explain the development of ovarian cancer: the gonadotropin theory, the continuous ovulation theory, and the theory involving the fallopian tube

as the origin of cells[25]; the most accepted origin for HGSC. The gonadotropin theory refers to the idea that the release of gonadotropins from the anterior pituitary activates hormonal receptors leading to the *over*-induction of the ovarian surface epithelium and stimulates healthy ovaries to secrete androgen and progesterone resulting in increased ovarian epithelium proliferation, and thus, development of malignancy[25]. In the continuous ovulation theory, constant ovulation results in accumulated damage to ovarian surface epithelium cells and increased induction of pro-inflammatory agents such as interleukin-8, monocyte chemotactic protein-1 (MCP-1), also known as CCL2, and RANTES (regulated on activation, normally T-cell expressed and secreted), also known as CCL5, which promote inflammation and consequently malignant transformation[25].

The third theory, which is the most widely accepted for HGSC, states that the cells of origin are actually from the fallopian tube epithelium and later on colonize the ovaries[25]. In the fallopian tube, secretory cell outgrowth (SCOUTs), an extended area of secretory cells, are thought to be the initial precursor lesion for HGSC[26]. SCOUTs then develop tumor protein p53 (p53) mutations which is referred to as "the p53 signature" (Fig.1.6) which then lead to serous tubal intraepithelial carcinoma (STIC) lesions, the immediate precursor of HGSC. P53 mutant cells activate tumor associated macrophages (TAMs) within STIC lesions leading them to secrete transforming growth factor-β (TGF-β). TGF-β then contributes to tumor progression. Reactive oxygen species (ROS), interleukin 8 (IL-8) and insulin-like growth factor (IGF) released during ovulation, are also thought to cause increased DNA damage leading to increased proliferation of STIC and development into HGSC[26].

There are pathologic and clinical evidence to support the idea that STIC lesions progress to HGSC arising from the secretory cells of the fallopian tube [26]. STIC lesions share the same morphological features as HGSC[20]. The lesions present continuous non-ciliated tubal epithelial

cells with nuclear enlargement, loss of cellular polarity, mitotic figures and p53 mutations identical to those found in HGSC. Approximately 40% of HGSC are accompanied by these types of lesions[26]. Patients with a BReast CAncer gene 1 (*BRCA1*) or BReast CAncer gene 2 (*BRCA2*) mutation are often advised to consider prophylactic bilateral salpingo-oophorectomy (prophylactic oophorectomy), in which the ovaries and fallopian tubes are removed, after age 35 or after childbearing is complete[27, 28]. This procedure reduces the risk of ovarian cancer substantially in these patients and reduces the risk of breast cancer if performed prior to menopause due to decreased circulating estrogen [27, 29, 30]. A study estimating the likelihood of occult cancer diagnosis at prophylactic oophorectomy in 159 *BRCA1* or *BRCA2* carriers has identified the fallopian tube as a source of early serous carcinoma[27, 31]. It was found that approximately 6% of *BRCA1* carriers and 2% of *BRCA2* carriers undergoing prophylactic salpingo-oophorectomy have occult carcinomas and a significant proportion of these appeared to originate in the fallopian tube[27]. A study exploring the relationship of tubal intraepithelial carcinoma (TIC) to pelvic serous carcinomas found that overall, 71% and 48% of ovarian serous carcinomas had endosalpinx involvement or TIC, respectively[31]. TIC has been found to coexist with all forms of pelvic serous carcinoma and to be a plausible origin for many of these tumors.

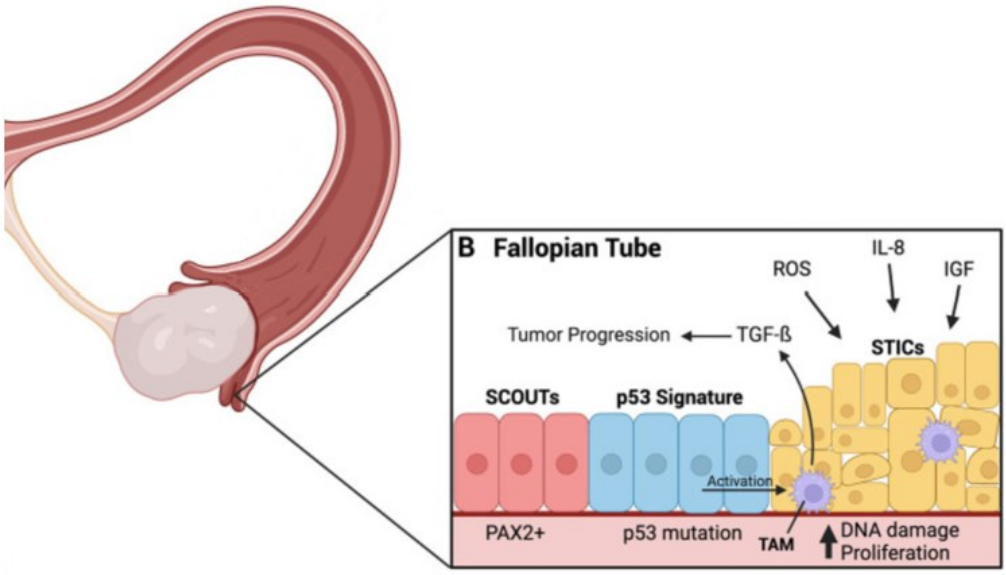

Figure 1.6. Development of ovarian cancer from the secretory cells of the fallopian tube. The involvement of SCOUTs, p53 signature and STIC lesions in the development of HGSC. Adapted from Ritch *et al*[26].

1.1.5 DNA Repair and the *BRCA1/2* Genes in Ovarian Cancer

DNA damage repair is essential to eliminate mutations that could result in cell death or abnormal cell function such as uncontrollable growth[32]. One of the most significant alterations to DNA can occur through a double strand break (DSB) and if left unrepaired, it is lethal to a cell. Non-homologous end joining (NHEJ) and homologous recombination DNA repair (HRR) are the two main repair mechanisms. NHEJ is the simplest and fastest and the predominant DSB repair mechanism in most mammalian cells [33, 34].

During NHEJ, the protein complex, the Ku70/80 heterodimer, binds to both ends of the broken DNA molecule[35]. The DNA-Ku scaffold attracts the DNA-dependent protein kinase catalytic subunit (DNA-PKCS) to the DSB. This kinase leads to the formation of a synaptic complex which brings both DNA ends together. Once the two DNA ends have been tethered in a protein complex consisting of Ku and DNA-PKCS, non-ligatable DNA termini must be processed before final repair of the DSB can take place. The ligase IV/XRCC4 complex catalyses ligation of the processed DNA ends and this ligation reaction may be enhanced by the presence of the recently discovered XLF/Cernunnos protein. During HRR, sister chromatids are used as a template for repairing double-stranded DNA breaks and interstrand crosslinks[36]. HRR pathways also support the recovery of stalled replication forks during DNA replication. Successful HRR depends on several properly functioning key proteins, such as the BRCA1 and BRCA2 proteins.

BRCA1 is a tumor suppressor protein central to several macromolecular complexes which drive HRR[36]. After DNA is resected by the MRN protein complex (MRE11-RAD50-NBS1 protein complex) and the CtBP-interacting protein (CtIP), BRCA1 reaches sites of double-stranded DNA breaks to participate in DNA damage signaling and coordinate DNA damage repair (Fig.1.7A)[37, 38]. During the DNA synthesis phase of the normal cell cycle progression, if DNA is damaged, the BRCA1 protein complexes recruit BRCA2 protein complexes to initiate strand invasion and/or homology-directed repair (Fig.1.7B)[36]. BRCA1 is thus thought to be part of a larger complex molecule that plays a role in DNA surveillance for DSB damage while BRCA2 likely has a more direct role in repair by assisting protein complexes in attaching to the repair site[32].

Mutations inherited from parents are known as germline mutations while those acquired and identified in the tumor are referred to as somatic mutations[39]. *BRCA1* is located on chromosome 17q21 and *BRCA2* on 13q12.3[40, 41]. Germline mutations in *BRCA1/2* are highly

penetrant mutations which are found in 13% to 15% of ovarian cancers, leading to germline genetic testing being universally recommended for all women with non-mucinous epithelial ovarian cancer[42-44]. Patients with germline mutations in *BRCA1* and/or *BRCA2* have an increased risk of developing breast or ovarian cancer[32]. *BRCA1* germline mutations are approximately four times more common in ovarian cancer patients than *BRCA2* mutations[45].

BRCA1- and *BRCA2*-associated hereditary breast and ovarian cancer is inherited in an autosomal dominant manner[46]. The diagnosis of *BRCA1*- and *BRCA2*-associated hereditary breast and ovarian cancer is established by performing molecular genetic testing for potential identification of a heterozygous germline pathogenic variant in *BRCA1* or *BRCA2*. Once a cancer-predisposing *BRCA1* or *BRCA2* germline variant has been identified, prenatal and preimplantation genetic testing can be performed if desired. Somatic *BRCA1/2* mutations are found in an additional 5% to 7% of ovarian cancers and have been found to be early events in carcinogenesis[44, 47, 48]. Somatic *BRCA1/2* mutations have been associated with similar clinical outcomes compared with germline *BRCA1/2* mutations[44, 49]. It has been suggested that a reasonable approach would be to conduct targeted germline and/or tumor *BRCA1/2* mutation testing, and use homologous recombination deficiency assays to guide treatment in patients who are subsequently found to be *BRCA1/2* wild type[44]. Since early knowledge of *BRCA1/2* mutation and homologous recombination deficiency status is crucial to select an appropriate management plan for patients with advanced ovarian cancer, it has been suggested that such testing should be performed as soon as possible after the diagnosis is made.

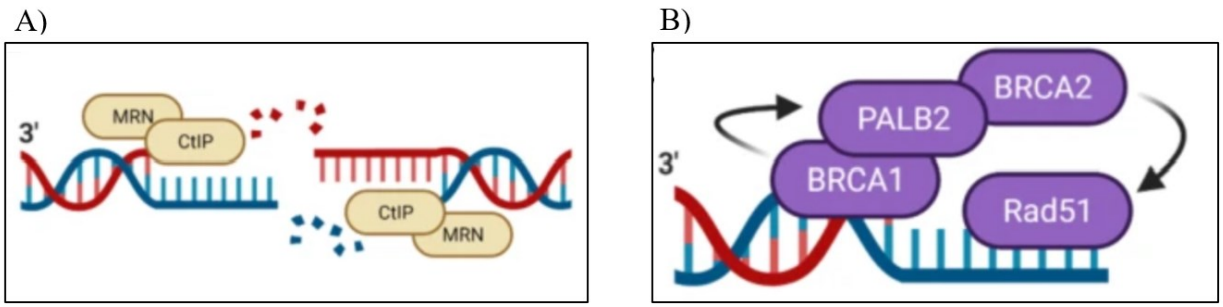

Figure 1.7. Homologous recombination DNA repair. A) MRN and CtIP resecting DNA. B) BRCA1 protein complexes recruit BRCA2 protein complexes to initiate strand invasion and/or homology-directed repair forming the HRR repair complex. Adapted from Creeden et al[36].

1.1.6 Clinical Approach

1.1.6.1 Symptoms

Symptoms of ovarian cancer are non-specific and are often mistaken for normal changes associated with ageing, menopause, and gastrointestinal disease such as bloating, nausea, changes in bowel habits, increase in abdominal girth, among others[50]. Consequently, there is often a delay in referrals and diagnosis, with 50% of patients not being referred directly to gynaecological cancer clinics and diagnosis frequently occurring when the cancer has reached late stages[20, 50, 51]. This is due to both patients and general practitioners failing to recognise the presenting symptoms of ovarian cancer[50, 51]. In a study aiming to identify symptoms of and diagnostic factors for ovarian cancer, persistent abdominal distension, postmenopausal bleeding, appetite loss and early satiety have been found to be associated with ovarian cancer while fluctuating distension has not been found to be associated with ovarian cancer[50].

1.1.6.2 Protective and Risk Factors

Factors that can decrease the total number of ovulatory cycles such as pregnancy and breastfeeding, late menarche and early menopause reduce the risk for ovarian cancer[52, 53]. The use of oral contraceptives has also been found to be a protective factor for ovarian cancer and the widespread use of it during recent decades has been postulated to be one of the reasons for the decreasing incidence of ovarian cancer[53, 54]. Use of oral contraceptives in the general population is associated with approximately 50% risk reduction in ovarian cancer[55-59]. In a multicenter case–control study, the use of oral contraceptives was associated with a reduction in the risk of ovarian cancer of 20% for up to three years of use and 60% for six or more years of use among women with a mutation in the *BRCA1* or *BRCA2* gene[60]. The relationship between oral contraceptives use and mucinous ovarian cancer is unclear[53].

Ovarian cancer risk increases with aging and peaks between the ages of 50 and 80 years old[52, 53]. Non-reproductive factors which can influence the risk of ovarian cancer include alcohol, caffeine, smoking and body size (height or body mass index)[1, 53, 61]. A family history of breast or ovarian cancer is a strong risk factor for ovarian cancer[6, 25, 53]. Familial risk is associated with mutations in *BRCA1* or *BRCA2*, which confers a 59% and 16.5% risk of developing ovarian cancer by the age of 70 respectively in the Epidemiological Study of *BRCA1* and *BRCA2* mutation carriers (EMBRACE) in the UK[6, 25, 53].

1.1.6.3 Initial Clinical Evaluation

Determining the history of the presenting symptoms and assessing risk factors including personal and family history of gynecologic and other cancers are important components of the

initial evaluation[10, 20]. A complete physical examination including abdominal examination, pelvic examination and a rectovaginal examination with the bladder empty is important to evaluate for pelvic and abdominal masses, ascites (i.e., fluid shift), and omental masses may be palpable [10, 20]. It should be noted that physical examination has limited accuracy, especially in obese patients. Auscultation of the lungs may reveal decreased air entry suggestive of pleural effusion in advanced disease. Examination of the lower extremities may reveal edema indicative of third-spacing and/or suspicion of deep vein thrombosis with swelling, erythema, and pain.

1.1.6.4 Imaging and Biopsy

Patients with suspected ovarian cancer based on clinical presentation or with a pelvic mass should undergo transvaginal ultrasonography, which can assess ovarian architecture and vascularity, differentiate cystic from solid masses, and detect ascites[10]. It can also provide information on the size, location, and level of complexity of the ovarian mass which can help clinicians to determine the level of suspicion for cancer[20]. Although ultrasound is useful in the initial workup, further imaging is often needed. The sensitivity of Doppler ultrasound in the detection of peritoneal metastases is low at 69%, compared with 95% for magnetic resonance imaging (MRI) and 92% for computerized tomography (CT) in patients with stages III and IV cancer [22, 62]. Ultrasound is also limited by the operator experience[22, 63].

CT is the recommended imaging modality for staging ovarian cancer [22, 64] as it provides information on the size of the primary tumor, size and location of any peritoneal implants and lymph nodes which is useful to determine resectability (Fig.1.8 and 1.9A)[22, 65]. Also, CT is used frequently to detect persistent or recurrent ovarian carcinoma and to monitor tumor response to

therapy [22, 66]. However, CT is limited in detecting small peritoneal metastases[22, 62, 67]. It can depict tumor implants larger than 1 cm with sensitivity of 85% to 93% and specificity of 91% to 96%, but the sensitivity decreases to 25% to 50% in detecting implants that are 1 cm or smaller. CT is particularly useful in patients with large amounts of ascites, which is often encountered in advanced ovarian cancer (Fig.1.9B)[22]. CT has also been used to predict the outcome of primary cytoreductive surgery of advanced ovarian cancer[22, 68, 69]. It is crucial to determine which patients will benefit from surgery to minimize the number of patients undergoing unnecessary surgery. In one study, peritoneal thickening, peritoneal implants (2 cm or larger), bowel mesentery involvement (2 cm or larger), suprarenal paraaortic lymph nodes (1 cm or larger), omental extension (spleen, stomach, or lesser sac), pelvic sidewall involvement, and enlargement of the ureter due to a backup of urine were most strongly associated with poor surgical outcome (Fig.1.10).

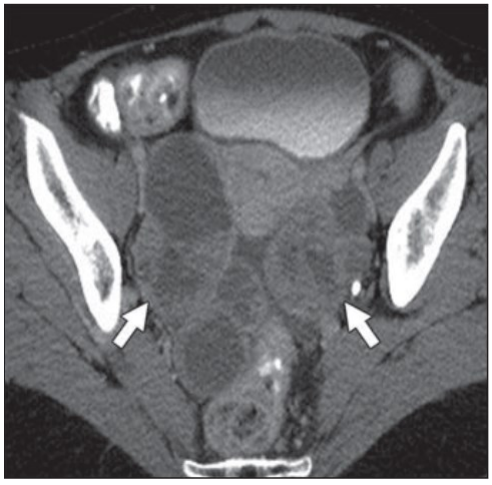

Figure 1.8. 54-year-old woman with stage IIA high-grade serous ovarian carcinoma. The axial CT image shows bilateral ovarian cystic and solid masses (arrows). Histology evaluation showed that the tumors were involved with the fallopian tubes. Adapted from Javadi *et al*[22].

A) B)

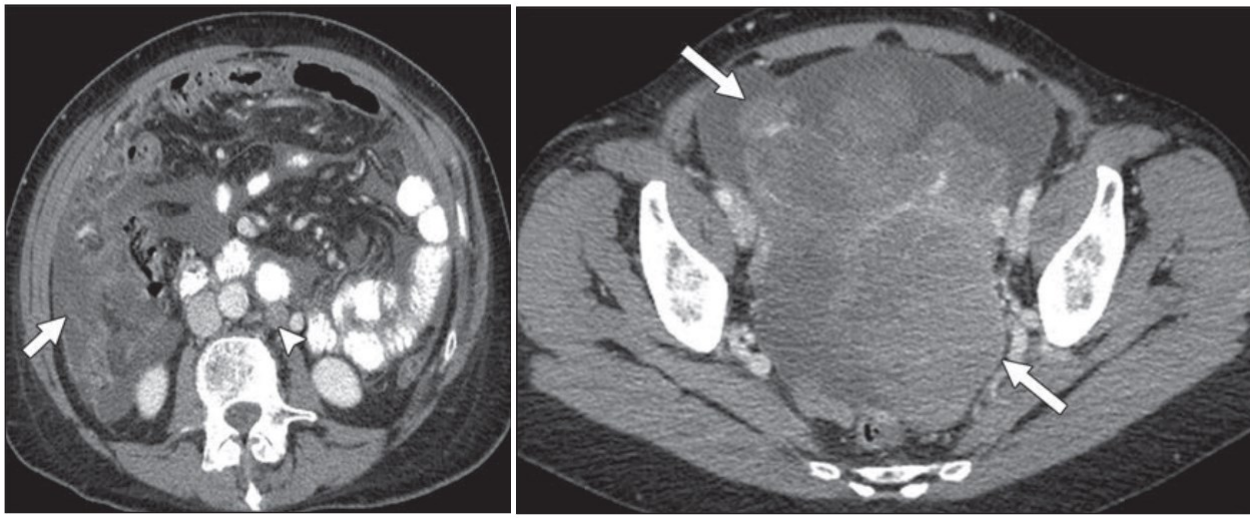

Figure 1.9. 71-year-old woman with stage IIIC ovarian cancer. A) The axial CT image shows enlarged retroperitoneal lymph node (arrowhead) and malignant ascites (arrow). B) The axial CT image shows metastatic ovarian cancer in pelvis and malignant ascites (arrows). Adapted from Javadi *et al*[22].

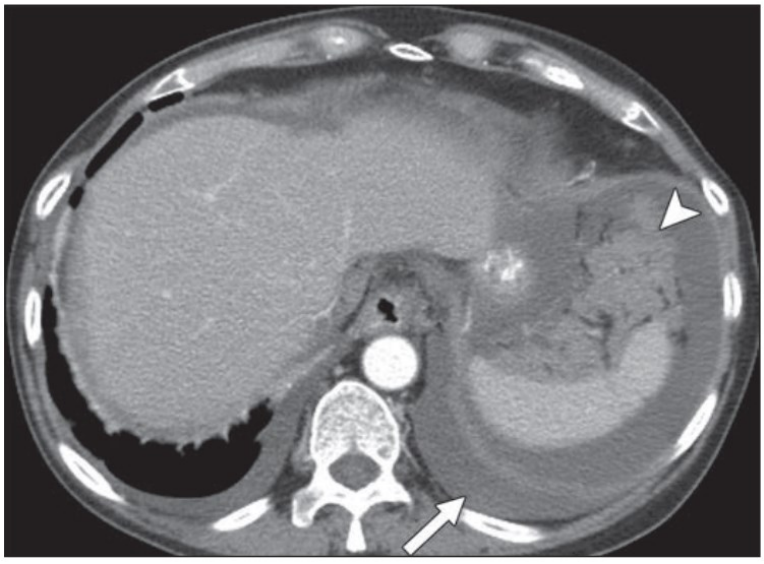

Figure 1.10. 67-year-old woman with stage IVB high-grade serous carcinoma of ovary. The axial CT image shows left malignant pleural effusion (arrow) and omental caking (i.e., a thickened greater omentum) anterior to the spleen (arrowhead) consistent with omental metastases. Adapted from Javadi *et al*[22].

MRI provides excellent tissue differentiation and can be used for characterization of indeterminate lesions seen on CT or ultrasound[22, 70, 71]. Lesions containing fat or blood products can be easily differentiated using MRI. MRI has staging accuracy like conventional CT[22, 72]. It can accurately identify invasion of pelvic organs due to its superior soft-tissue contrast resolution. In patients who are being considered for cytoreductive surgery, preoperative imaging of the abdomen and pelvis plays an important role in determining the extent of peritoneal disease[22, 73]. In a study, for predicting resectability, MRI had sensitivity of 95%, specificity of 70%, and accuracy of 88% compared with 55%, 86%, and 63%, respectively, for CT. However, some studies suggest that there is no statistically significant difference between CT and MRI for the depiction of recurrent ovarian cancer[22, 74].

Positron emission tomography/Computerized tomography is limited in characterizing ovarian masses but is particularly helpful in detecting recurrent disease[22, 75-81]. In summary, clinically, ultrasound, and CT are most commonly used for initial diagnosis whereas MRI and positron emission tomography are used for detection of recurrence. Although imaging plays a significant role in diagnosing ovarian cancer, to confirm a diagnosis, a tissue biopsy must be performed[20, 22, 82].

1.1.6.5 Serum Biomarkers

The tumour biomarker CA125 has been used as the primary biomarker for ovarian cancer[83, 84]. It was first identified by Bast, Knapp, and colleagues in 1981 in their work to develop a monoclonal antibody (OC125) against this antigen[84, 85]. CA125 contains two major antigenic domains, A and B, which bind the monoclonal antibodies OC125 and M11, respectively[84]. CA125 is a high molecular weight glycoprotein found in healthy ovaries, but blood levels commonly increase in patients with ovarian cancer[86]. Serum levels of CA125 are often used to monitor response to chemotherapy, relapse, and disease progression in ovarian cancer patients[84]. However, it is not as reliable when used as a diagnostic tool as there are many benign processes that can cause an elevated CA125 level, both gynecological (e.g., menstruation, fibroids, endometriosis) and non-gynecological (e.g., inflammatory bowel disease, congestive heart failure, liver failure)[86]. There is an inverse relationship between serum CA125 levels and survival in ovarian cancer[86]. Decreasing levels generally indicate a positive response to therapy, while increasing levels indicate tumor recurrence and poor overall survival. CA125 levels less than 35 units per milliliter are considered "normal"[86]. Levels are more frequently elevated in advanced disease and in some tumor types than others[86]. Elevated CA125 levels were found in more than 90% of patients with advanced stage ovarian cancer and in only 50% of patients with stage I disease[84].

Numerous studies have confirmed the usefulness of CA125 levels in monitoring the patients with a history of ovarian cancer with a rise in CA125 levels found to precede clinically detectable recurrence by approximately three to four months[84]. Even though CA125 has been the most promising biomarker for screening ovarian cancer, it does not have an acceptable accuracy in population-based screening for ovarian cancer and a few prospective studies indicated the inadequate sensitivity of CA125 in the setting of ovarian cancer screening in asymptomatic

populations[83, 84]. A study assessing the efficacy of annual CA125 and transvaginal ultrasound (TVUS) scan as surveillance for ovarian cancer found that ovarian screening by annual TVUS and CA125 is inefficient at detecting early-stage ovarian cancer in both high-risk and population risk women[87]. Another study found that while many individuals with *BRCA1* or *BRCA2* pathogenic variants undergo TVUS and CA125 surveillance testing, abnormal surveillance testing led to diagnosis of ovarian cancer in only a limited number of cases[88]. As such, the use of CA125 and ultrasound surveillance in the clinical setting for ovarian cancer detection in women with *BRCA1* or *BRCA2* pathogenic variants is limited.

Human epididymis protein 4 (HE4) is a new biomarker which is being evaluated for diagnosing ovarian malignant tumors [89, 90]. It is weakly expressed in the epithelium tissues of respiratory and reproductive organs [90, 91]. However, it is overexpressed in ovarian tumors, especially in endometrioid ovarian cancer. Data have shown that HE4 might be more reliable than CA125 for diagnosing ovarian epithelial cancer [90, 92-94].

HE4 and CA125 have levels that vary in different patient populations, and thus, the combination of HE4 and CA125 could have multiple advantages[83]. For example, HE4 values vary in smokers and contraceptive users, while CA125 values are less affected in these patient populations [83, 95]. Unlike CA125, HE4 levels are not significantly changed in endometrioma. HE4 levels increase with age, and thus, postmenopausal patients tend to have higher HE4 levels. [83, 90, 96]. CA125, in contrast, exhibits higher levels in premenopausal patients with benign conditions. Such difference between HE4 and CA125 expression patterns may account for the superior performance of HE4 in premenopausal patients and that of CA125 in postmenopausal patients.

1.1.7 Treatments

Surgery in combination with carboplatin and paclitaxel is the standard of care for patients with newly diagnosed ovarian cancer. Newer or experimental strategies to improve both up-front and second-line or later treatment include the addition of biologic agents to chemotherapy and the use of combination strategies that employ anti-vascular agents, PARP inhibitors (PARPis), and immunotherapies, and the use of new agents such as antibody-drug conjugates[97, 98].

1.1.7.1 Surgery

The extent of surgery is determined by the stage of cancer and patient factors[20]. For example, patients with more-advanced cancer might undergo bilateral oophorectomy where both ovaries are removed while young patients with stage I disease who wish to preserve fertility might undergo unilateral oophorectomy of the affected ovary only or unilateral salpingo-oophorectomy where only one ovary and fallopian tube are removed[10, 20].

Cytoreductive (i.e., debulking) surgery is the basis of treatment of ovarian cancer and residual disease at the end of surgery is one of the most important prognostic factors[22]. The volume of residual disease after cytoreductive surgery is inversely proportional with survival[22]. Cytoreductive surgery is considered complete if no residual disease is visible, optimal if there is less than 1 cm in maximum diameter of residual cancer, and suboptimal if there is more than or equal to 1 cm in size of residual cancer[20, 22]. Patients with complete cytoreductive surgery have significant improvements in outcomes compared with patients with remaining postoperative visible disease[20].

Currently, established guidelines recommend primary cytoreduction surgery followed by postoperative (adjuvant) chemotherapy with carboplatin and paclitaxel (Fig.1.11)[99, 100]. In a pharmacokinetic analysis of the combination of cisplatin and paclitaxel, paclitaxel clearance has been found to apparently be sequence dependent[101]. Patients administered cisplatin prior to paclitaxel had lower clearances and greater clinical toxicity than patients receiving paclitaxel before cisplatin, suggesting that administration of paclitaxel before a platinum-based agent is more beneficial[101]. For patients with epithelial ovarian cancer and resectable disease, primary cytoreductive surgery followed by six to eight cycles of intravenous paclitaxel and carboplatin every three weeks is recommended[102].

In patients with advanced ovarian cancer for whom primary surgery would result in significant gross residual disease and/or in patients with poor overall performance status, significant comorbidities, treatment can begin with preoperative (neoadjuvant) chemotherapy followed by interval debulking surgery[99, 100]. For patients with stage III or IV epithelial ovarian cancer who may have a high-risk profile for primary cytoreductive surgery, neoadjuvant chemotherapy with three to four cycles of intravenous three-weekly paclitaxel and carboplatin before and after interval debulking surgery is an option[102]. The purpose of preoperative therapy is to reduce the tumor burden and increase the likelihood of complete resection[99].

Several randomized controlled trials compared primary debulking surgery versus neoadjuvant chemotherapy and interval debulking surgery, namely EORTC, CHORUS, JCOG and SCORPION clinical trials[103-106]. The data from these trials concluded that neoadjuvant chemotherapy followed by interval debulking surgery is not inferior, nor superior to primary debulking surgery followed by chemotherapy as a treatment option for patients. Complete removal

of all macroscopic disease is the key surgical goal, whether surgery is performed before or after initial chemotherapy treatment.

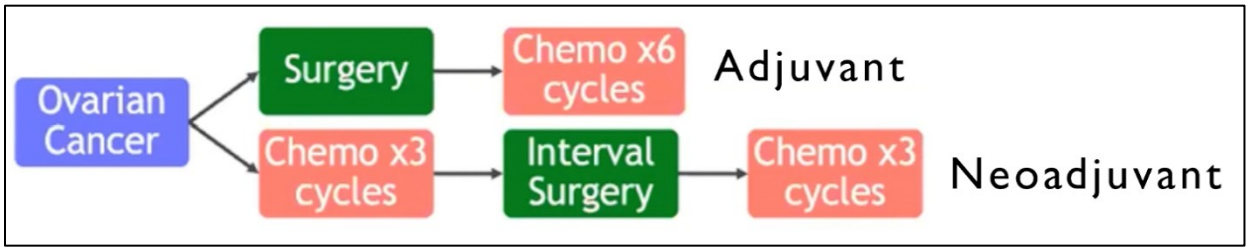

Figure 1.11. Ovarian cancer patients' treatment routes. Primary cytoreduction surgery followed by postoperative chemotherapy with carboplatin and paclitaxel is the adjuvant route. Preoperative chemotherapy followed by interval debulking surgery is the neoadjuvant route. Adapted from Arab *et al*[100].

1.1.7.2 Systemic Chemotherapy

Platinum compounds have formed the basis for chemotherapy in ovarian cancer for several decades[99]. Cisplatin was initially used as the main chemotherapeutic drug[99]. However, its adverse effects, specifically nephrotoxicity and ototoxicity, led to the development of second-generation platinum compounds such as carboplatin[99]. Carboplatin has the advantage of being as effective as cisplatin, but with fewer adverse effects, especially in terms of nephrotoxicity[99].

Carboplatin gets activated once it crosses the cell membrane[107]. Inside the cell, the molecule undergoes hydrolysis leading it to become positively charged. This allows carboplatin to interact with nucleophilic molecules within the cell, including DNA, RNA and proteins, generating the formation of adducts of platinum. The linkage between DNA and carboplatin can produce crosslinking between strands of DNA referred to as interstrand and intrastrand cross-links. Such

cross-links are the most cytotoxic effect because they lead to the generation of errors during DNA replication. Consequently, the cells are prevented from completing mitosis, and thus, undergo the induction of apoptosis.

Taxanes, specifically paclitaxel, also constitute an important part of ovarian cancer treatment. Microtubules are composed of tubulin subunits. In healthy cells, microtubules exist in a dynamic state where tubulin subunits are added and removed from the mature microtubules[108]. Paclitaxel suppresses microtubule spindle dynamics by binding to the polymeric tubulin, thereby preventing tubulin disassembly. Since microtubules are crucial for the formation of the mitotic spindle involved in mitosis, by disturbing the microtubules' dynamic states, paclitaxel blocks the mitotic metaphase to anaphase transitions[108, 109]. The inhibition of mitosis consequently leads to the induction of apoptosis[108].

Even though different ovarian cancer histologic subtypes respond differently to chemotherapy, carboplatin and paclitaxel became the standard first-line chemotherapy combination more than 20 years ago[15, 110]. In a randomized, phase III trial comparing paclitaxel plus cisplatin with paclitaxel plus carboplatin in patients with advanced ovarian cancer, the paclitaxel plus carboplatin regimen achieved comparable efficacy to the paclitaxel plus cisplatin regimen but was associated with better tolerability and quality of life[111]. A randomized clinical trial showed that compared with every-3-weeks or weekly carboplatin–paclitaxel regimens, single-agent carboplatin was less active with significantly worse survival outcomes in vulnerable older patients with ovarian cancer[112]. Such finding suggests that a conventional doublet regimen should be considered for all patients with ovarian cancer.

1.1.7.3 Platinum Resistance

A central issue surrounding platinum compounds use is the development of platinum resistance, defined as recurrence within 6 months of the last platinum administration[113]. Although most patients initially respond well to a platinum regimen, most progress despite therapy and develop resistance rendering the recurrence of disease incurable[99]. Platinum-resistant ovarian cancer has a median survival of 9 to 12 months and less than 15% respond to subsequent chemotherapy[114, 115].

The development of resistance to platinum-based chemotherapy is a major clinical challenge in cancer treatment since the cellular response that confers resistance to platinum agents is multifactorial and poorly understood[107]. It has been observed that the intracellular mechanisms by which cells become resistant to platinum derivatives such as carboplatin include improved tolerance to nuclear damage leading to a reduction in apoptosis and reduced accumulation of intracellular metal.

The most studied mechanisms underlying HGSC platinum resistance include p53 and genome wide mutations, epigenetic changes, and dysfunctional DNA repair[33, 115-121]. Possibly working together, these genetic mechanisms lead to genomic instability that allows cancer cells to adapt and survive DNA damage caused by platinum chemotherapy. The presence of cancer stem cells and epithelial-to-mesenchymal transition is also associated with platinum resistance in HGSC[115, 122-124]. Platinum chemotherapy is most effective on proliferating cells which are part of most rapidly growing cancer. Therefore, it is hypothesized that populations of latent cancer stem cells and mesenchymal-like cells are less likely to respond to platinum chemotherapy. In addition to changes to the genome and phenotype of HGSC cancer cells, the tumor microenvironment, such

as immune cell infiltration, angiogenesis, and hypoxia, have also been implicated in platinum chemoresistance.

The treatment of patients with resistant disease remains a challenge[98]. At this time, single non-platinum chemotherapy agents remain the standard of care for patients with platinum-resistant disease with or without addition of the antiangiogenic agent, bevacizumab, which is approved by the United States Food and Drug Administration in this setting. Antiangiogenic agents, PARP inhibitors, and immune checkpoint inhibitors have demonstrated variable tumor efficacy in clinical trials. Overcoming resistance to therapy will require many different approaches and trials are still ongoing to identify the most effective treatment for patients with resistant disease.

1.1.7.4 PARP Inhibitors and Clinical Trials Supporting Their Use

PARPis are usually given after frontline platinum-based chemotherapy as maintenance therapy to prevent or delay recurrence, particularly for patients with homologous recombination deficiency. BRCA-dependent DNA double-strand break repair mechanisms can compensate for dysfunctional DNA single-strand break repair mechanisms[36]. PARPis inhibit the poly (ADP-ribose) polymerase enzyme (PARP) and trap it on single-strand breaks (Fig.1.12). Consequently, DNA single-strand breaks accumulate and are converted to double-strand breaks. In non-cancerous cells, HRR can repair DNA lesions and maintain cell viability[36]. However, in HRR-deficient cancer cells, DNA damage accumulates resulting in cell death[125]. Although BRCA1 and BRCA2 associated HGSCs have been shown to respond to PARPis, with the aim of optimizing efficacy and tolerability of the therapeutic regimen for ovarian cancer, other drugs have also been developed and under study for first-line and maintenance therapies[126].

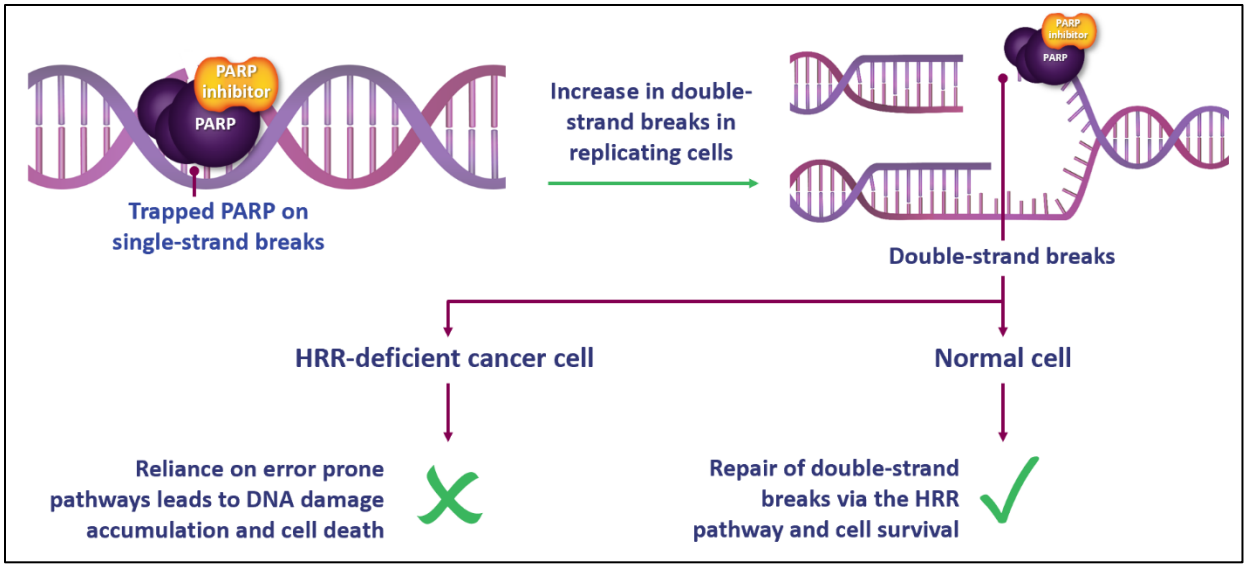

Figure 1.12. PARPis mechanism of action. PARPis exert their cytotoxic effects through a synthetic lethal pathway, thereby killing tumor cells with defects in homologous recombination and/or in the protection of stalled replication forks. Adapted from O'Connor [125]

The aim of the SOLO-1 clinical trial was to evaluate the efficacy of olaparib as maintenance therapy in patients with newly diagnosed advanced ovarian cancer and a BRCA1/2 mutation (Table 1.1) [127]. Before the SOLO-1 clinical trial, most patients with newly diagnosed advanced ovarian cancer had a relapse within three years after standard treatment with surgery and platinum-based chemotherapy. The benefit of olaparib in relapsed disease was previously established, but the benefit of olaparib as maintenance therapy in newly diagnosed disease was uncertain[127, 128]. In SOLO-1, it was found that the use of maintenance therapy with olaparib provided a substantial benefit with regard to progression-free survival (PFS) among patients with newly diagnosed advanced ovarian cancer and a *BRCA1/2* mutation, with a 70% lower risk of disease progression or death with olaparib compared to placebo[127]. PFS refers to the time from

treatment initiation until disease progression or worsening[129]. The Kaplan–Meier estimate of the rate of freedom from disease progression and from death at 3 years was 60% in the olaparib group versus 27% in the placebo group (hazard ratio for disease progression or death, 0.30; 95% confidence interval, 0.23 to 0.41; $p<0.001$)[127]. Based on the SOLO-1 data, olaparib received approval as maintenance therapy among patients with newly diagnosed advanced ovarian cancer and a *BRCA1/2* mutation.

The aim of the SOLO-2 clinical trial was to confirm olaparib efficacy as maintenance therapy in patients with platinum-sensitive, relapsed ovarian cancer and a *BRCA1/2* mutation who had received at least two lines of previous chemotherapy (Table 1.1)[130]. The SOLO-2 trial demonstrated the beneficial effects of using olaparib as maintenance therapy with improved median PFS (19.1 months; 95% CI, 16.3 to 25.7) versus placebo (5.5 months [5.2-5.8]; hazard ratio, 0.30; 95% CI, 0.22 to 0.41; $p<0.0001$). Apart from anaemia, toxicities with olaparib were low grade and manageable.

The aim of the SOLO-3 clinical trial was to evaluate olaparib versus non-platinum chemotherapy in patients with germline BRCA-mutated platinum-sensitive relapsed ovarian cancer who had received at least two prior lines of platinum-based chemotherapy (Table 1.1) [131]. The SOLO-3 trial demonstrated the benefits of using olaparib in comparison with non-platinum chemotherapy (median PFS 13.4 months in the olaparib group versus 9.2 months in the non-platinum chemotherapy group; hazard ratio, 0.62; 95% confidence interval, 0.43 to 0.91; $p = 0.013$).

Another PARPi, niraparib, was studied in the PRIMA clinical trial[132]. Structural differences and distinct pharmacokinetic properties exist between niraparib and olaparib. Niraparib is a selective inhibitor of PARP1 and PARP2, while olaparib is a more potent inhibitor of PARP1, but

is less selective[133, 134]. Niraparib had been thought to be beneficial among patients with recurrent ovarian cancer after platinum-based chemotherapy, regardless of the presence or absence of *BRCA* mutations[132]. However, the efficacy of niraparib in patients with newly diagnosed advanced ovarian cancer after a response to first-line platinum-based chemotherapy was unknown. The PRIMA trial demonstrated improved PFS with niraparib in patients with newly diagnosed advanced ovarian cancer who responded to platinum-based chemotherapy (Table 1.1), regardless of the presence or absence of homologous-recombination deficiency. Among the patients with tumors with homologous-recombination deficiency, the median PFS was significantly longer in the niraparib group than in the placebo group (21.9 months vs. 10.4 months; hazard ratio for disease progression or death, 0.43; 95% confidence interval, 0.31 to 0.59; $p<0.001$). In the overall population, the corresponding progression-free survival was 13.8 months in the niraparib group and 8.2 months in the placebo group (hazard ratio, 0.62; 95% confidence interval, 0.50 to 0.76; $p<0.001$). At the 24-month analysis, the rate of overall survival (OS) was 84% in the niraparib group and 77% in the placebo group (hazard ratio, 0.70; 95% confidence interval, 0.44 to 1.11). OS refers to the duration of patient survival from the time of treatment initiation[129]. The most common adverse events were anemia, thrombocytopenia, and neutropenia[132].

The VELIA trial assessed efficacy of veliparib added to first-line chemotherapy with carboplatin and paclitaxel and continued as maintenance monotherapy in patients with high-grade serous ovarian carcinoma (Table 1.1)[135]. It was found that, across all trial populations, a regimen of carboplatin, paclitaxel and veliparib therapy followed by veliparib maintenance therapy led to significantly longer PFS than carboplatin and paclitaxel combination therapy alone. In the *BRCA*-mutation cohort, the median PFS was 34.7 months in the veliparib-throughout group in which patients received chemotherapy plus veliparib followed by veliparib maintenance and 22.0 months

in the control group in which patients received chemotherapy plus placebo followed by placebo maintenance (hazard ratio for progression or death, 0.44; 95% confidence interval, 0.28 to 0.68; p<0.001). In the cohort with homologous-recombination deficiency (which included the *BRCA*-mutation cohort), it was 31.9 months and 20.5 months, respectively (hazard ratio, 0.57; 95% confidence interval, 0.43 to 0.76; p<0.001). In the intention-to-treat population (i.e., in all the patients who had undergone randomization), it was 23.5 months and 17.3 months (hazard ratio, 0.68; 95% confidence interval, 0.56 to 0.83; p<0.001).

Study Design	SOLO-1	SOLO-2	SOLO-3	PRIMA	VELIA
Treatment Groups	Olaparib **vs** Placebo	Olaparib **vs** Placebo	Olaparib **vs** Pegylated liposomal Doxorubicin, Paclitaxel, Gemcitabine or Topotecan	Niraparib **vs** Placebo	Veliparib-throughout group: Carboplatin/paclitaxel + Veliparib followed by Veliparib maintenance **vs** Veliparib-combination-only group: Carboplatin/paclitaxel + Veliparib followed by placebo maintenance **vs** Control group: Carboplatin/paclitaxel + placebo followed by placebo maintenance
Study Population	*BRCA* mutation	*BRCA* mutation At least two lines of previous chemotherapy	Germline *BRCA* mutation At least two lines of previous platinum-based chemotherapy	All comers Responded to first-line platinum-based chemotherapy	All comers
Newly Diagnosed or Recurrent Cancer	Newly diagnosed advanced	Recurrent Platinum-sensitive	Recurrent Platinum-sensitive	Newly diagnosed advanced	Newly diagnosed advanced
Aim of the Study	**Primary end point:** PFS **Secondary end point:** OS .	**Primary end point:** PFS	**Primary end point:** Objective response rate in the measurable disease analysis set assessed by blinded independent central review **Secondary end point:** PFS assessed by BICR in the intent-to-treat population.	**Primary end point:** PFS in patients with HRD tumors and in those in overall population **Secondary end point:** OS .	**Primary end point:** PFS **Secondary end points:** OS in veliparib-throughout group vs. in control group PFS and OS in the veliparib-combination-only group vs. in control group,
PFS/OS	**Kaplan–Meier estimate of rate of freedom from disease progression and from death at 3 years:** 60% in the olaparib group vs. 27% in the placebo group	**Median PFS:** 19.1 months in olaparib group vs. 5.5 months in placebo group	**PFS:** 13.4 months in olaparib group vs. 9.2 months in non-platinum chemotherapy	**Among patients with tumors with homologous-recombination deficiency, median PFS:** 21.9 months in niraparib group vs. 10.4 months in placebo group **In overall population, PFS:** 13.8 months in niraparib group vs. 8.2 months in placebo group **OS:** 84% in niraparib group vs. 77% in placebo group	**In BRCA-mutation cohort, median PFS:** 34.7 months in veliparib-throughout group vs. 22.0 months in control group **In HRD cohort , median PFS:** 31.9 months in veliparib-throughout group vs. 20.5 months in control group **In intention-to-treat population, median PFS:** 23.5 months in veliparib-throughout group vs. 17.3 months in control group
Toxicity	Grade 3 or 4 was anemia (in 22% of patients) and neutropenia (in 9%)	Most common grade 3 or higher were anemia (in 19% of patients), fatigue or asthenia (in 4%) and neutropenia (in 5%)	Most common grade 3 or higher was anemia (in 21.3% of patients)	Grade 3 or higher were anemia (in 31.0% of patients), thrombocytopenia (in 28.7%), and neutropenia (in 12.8%)	Nausea in veliparib-throughout group (in 80% of patients). 90% were grade 1 or 2.

Table 1.1. Summary of the SOLO-1, SOLO-2, SOLO-3, PRIMA and VELIA clinical trials study design

1.1.7.5 Emerging Studies of PARPi

Niraparib was the first selective PARPi approved in the United States and Europe for maintenance treatment in patients with recurrent ovarian cancer regardless of mutation status[136]. Preclinical evidence suggests that niraparib synergizes with anti-PD-1 therapy. Pembrolizumab is a humanized monoclonal antibody against programmed death 1 (PD-1) that has increased activity in tumors that express programmed death ligand 1 (PD-L1)[137]. In the TOPACIO/KEYNOTE-162 trial, niraparib in combination with pembrolizumab has shown efficacy in recurrent, platinum-resistant ovarian cancer[136].

Hypoxia impairs homologous recombination leading to cell death, and thus, inhibiting angiogenesis through anti-angiogenic agents to induce hypoxia could lead to synergy with PARPis[136]. Niraparib in combination with the anti-angiogenic agent bevacizumab is under study for the treatment of recurrent platinum-sensitive ovarian cancer in the AVANOVA trial and advanced ovarian cancer following response on frontline platinum-based chemotherapy in the OVARIO trial[136].

Most recently, there is interest in the use of PARPi in the neoadjuvant setting. OPAL-C is an ongoing phase 2 randomized clinical trial comparing niraparib versus carboplatin/paclitaxel doublet chemotherapy as neoadjuvant treatment, in patients with homologous recombination-deficient stage III/IV ovarian cancer (study NCT03574779)[138]. The key inclusion criteria are patients aged 18 years and older with measurable disease according to the Response Evaluation Criteria in Solid Tumors v1.1, with newly diagnosed stage III/IV high-grade nonmucinous epithelial ovarian, fallopian tube, or peritoneal cancer, that are eligible for neoadjuvant platinum-taxane doublet chemotherapy followed by interval debulking surgery, have a prior completion of one run-in cycle of carboplatin-paclitaxel treatment and have tumors that are homologous

recombination-deficient. The primary endpoint is pre-interval debulking surgery unconfirmed overall response rate defined as the investigator-assessed percentage of patients with unconfirmed complete or partial response on study treatment before interval debulking surgery per the Response Evaluation Criteria in Solid Tumors v1.1. The secondary endpoints are PFS, PFS rate at 12, 18, and 24 months, OS and the time to first subsequent treatment. The exploratory endpoint is the pathological complete response. All adverse events will be assessed for intensity according to the Common Terminology Criteria for Adverse Events. Enrollment is ongoing and is expected to conclude in March 2024. The primary analysis is anticipated to be completed in September 2024, and the final analysis in May 2026.

1.2 Preclinical Models to Study New Therapeutic Approaches

Although the use of carboplatin in combination with paclitaxel as first-line therapy in ovarian cancer has undergone refinements, optimizing the efficacy and tolerability of new therapies is necessary to improve patient survival. Therefore, further pre-clinical studies and in-vivo models are needed to determine the efficacy of emerging therapeutic agents [126, 127, 130, 131]. The establishment of a preclinical model that recapitulate tumor pathophysiology in-vivo is necessary to acquire a deeper understanding of the therapeutic response of HGSC[139]. Several preclinical models exist with each their strengths and challenges as described below.

1.2.1 In-Vivo Model

1.2.1.1 Patient-Derived Xenografts

Patient-derived xenografts (PDXs) models are generated by the implantation of fresh human tumor tissues into immunodeficient mice[140]. PDXs are derived from patients and the model is implemented in-vivo, which is known to be more accurate and reliable compared with that in vitro[141]. PDXs resemble the tumor of the patient in cellular complexity and retain tumor heterogeneity. Therefore, PDXs may be an ideal model to simulate actual human disease for cancer research[141]. The main advantage of PDXs compared to in vitro cell culture is the possibility of studying cancer cells in their microenvironment and assessing the involvement of fibroblasts, endothelial cells and leukocytes in tumour biology and response to treatments[142, 143]. In this way, PDX has been valuable in elucidating the mechanisms and advanced our knowledge of biology of various tumors[139, 144]. However, they have low implantation-take rates, a long duration of immune reconstitution, and are expensive to generate. The duration of survival and treatment schedules for patients is one of the considerable factors for personalized medicine applications[145]. It usually takes two to eight months to develop a PDX model for a preclinical study and in many cases, this length of time is too long to inform clinical decisions for individual patients[145]. Furthermore, since the intrinsic genetic material and cellular characteristics of tumor tissue is altered after three generations, the PDX model is not suitable for continuous amplification[141].

1.2.2 In-Vitro Models

1.2.2.1 Two-Dimensional (2D) Cell Culture

2D cell culture contributed to the advancement of several areas of research and remains a predominant preclinical method of study[139, 144]. 2D cell culture is a model that is relatively simple, economical, and convenient for high-throughput drug studies. However, it provides an oversimplified version of tumors that does not mimic essential in-vivo cellular organization and interactions since in flat-bottom cell culture plates, cells tend to adhere to the bottom surface of the plate forming a flat layer of cells. For example, a study found that the carboplatin sensitivity of 2D epithelial ovarian carcinoma cell cultures differed from the in-vivo response[146].

1.2.2.2 Three-Dimensional (3D) Cell Culture

1.2.2.2.1 Spheroid Culture

High-throughput 3D culture of epithelial ovarian cancer cells has been found to be a strong preclinical model of disease for in-vitro experiments that bridges the gap between 2D cell culture and animal models [139, 147]. Cells grown in such 3D environment mimic poorly vascularized in-vivo tumors' multilayered structure and their nutrients, pH, and oxygen concentration gradients[148]. In round-bottom plates (i.e., 3D culture), the ultra-low attachment environment forces cells in suspension to naturally aggregate, and thus, form 3D spheroidal structures more closely resembling in-vivo tumors[149]. It has been demonstrated that cells cultured in 3D preserve a more significant number of cellular functions than cells cultured in 2D and that both models differ in terms of drug efficacy suggesting that the 3D culture model is superior to 2D monolayers in the search for new therapeutic targets[150, 151]. A study found that the carboplatin response of 3D

epithelial ovarian carcinoma spheroids improved the correlation with the in-vivo response compared to 2D cultures[146].

The generation of 3D spheroids can be performed using different methods such as ultra-low attachment round-bottom cell culture plates (ULAPs), hanging droplet method, or agitation-based approach[149]. 3D spheroids can be formed by placing them in ULAPs since the natural aggregation of cells in suspension will lead them to form spheroidal structures (Fig.1.13A)[149]. The hanging-droplet method consists of placing a hanging droplet on the underside of a plate lid. The cells are then clustered into spheroids through the action of gravity. Similar to the ULAP method, the hanging-droplet method allows for the easy formation of spheroids for any downstream analyses (Fig.1.13B)[149]. In the agitation-based approach, cells are seeded onto plates that have agarose on the bottom of the culture vessel and incubated with constant agitation. However, since this technique exposes cells to additional shear forces, the cell biology and viability may be affected (Fig.1.13C)[149].

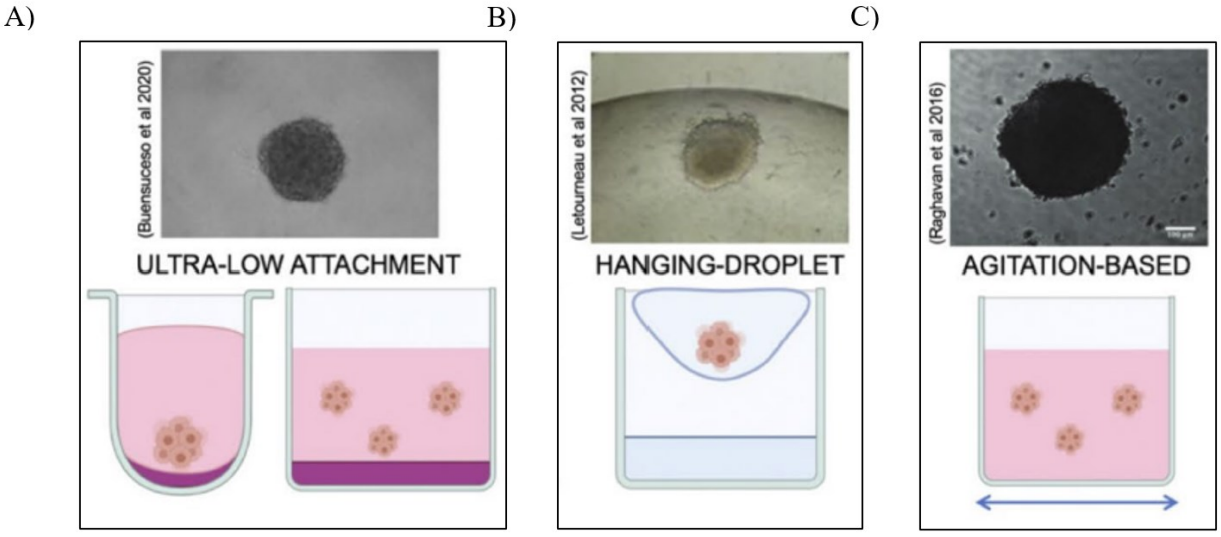

Figure 1.13. Methods for 3D spheroids generation. A) Generation of spheroids using ULAPS. B) Generation of spheroids using the hanging-droplet method. C) Generation of spheroids using the agitation-based approach. Adapted from Tomas *et al*[149].

1.2.2.2.2 Patient-Derived Organoids (PDOs)

The organoid model, which contains a more complex diversity of cell types, has been shown to partially resemble the parent organ in both structure and function, as well as histologically and genetically [152-154]. However, organoids lack immune cells and blood vessels and are a costly model to generate[154, 155]. Establishment of a PDO model is time-consuming and technically difficult, thereby necessitating further exploration[141].

The generation of organoids can be performed using different methods, namely the submerged method, the air-liquid interface method, the bioreactor method, and the organoid-on-a-chip method[139]. The submerged method is initiated by mechanical and enzymatic digestion of primary tumor tissue, followed by embedding cells into a specific matrix such as Matrigel, and culturing medium, supplemented with a cocktail of growth factors and hormones for long-term maintenance (Fig.1.14). This submerged method generally represents epithelial-only organoids and does not include stroma[139]. Tumor–stroma interactions are a key feature of most solid tumors and drive tumor progression, metastasis, and drug resistance leading to treatment failure[156]. Therefore, the ability of 3D in vitro models to recapitulate the complex interactions between tumor and stromal cells could allow for more accurate testing of anticancer therapies.

In the air–liquid interface method, tissue is minced into smaller fragments and embedded in a layer of collagen, which is assembled in a cell culture insert (Boyden chamber) that has a layer

of acellular collagen (Fig.1.15)[139]. The cell culture insert is placed in a culture dish with media. By being embedded in extra-cellular matrix gels in an upper surface of the cell culture inserts with a porous membrane underneath, cells have an increased oxygen supply compared to an epithelial-only submerged organoid method. The air-liquid interface method allows the propagation of organoids both with epithelial and stromal cells. The distinct advantage of the method is that it not only includes stromal cells but can also retain the tumor microenvironment for an extended period of time.

In the bioreactor method, tissue fragments are embedded in basement membrane extract and then transferred into a bioreactor (Fig.1.16) [139]. The continuous agitation in this method provides better absorption of nutrients and oxygen compared to the two aforementioned static methods.

Lastly, the organoid-on-a-chip method uses microfluidic chips which allow culture of organoids in a chamber connected to an inlet that can circulate culture media (Fig.1.17)[139]. In the design of a vascularized organoid-on-chip model, the fabricated microfluidic chip has a central chamber with perfusable microvasculature in a hydrogel compartment and adjacent chambers for loading fragments from cancer cell lines or patient tumor samples. Capillaries in the porous gel that are outgrown from the vascular chamber into the tumor chamber allow interconnection of the two chambers. The efficient delivery of nutrients and/or drugs to the tumor tissue through the vascular network helps to maintain structures physiologically active for a long time. This organoid-on-chip method could allow the development of organoids that model organ physiology in vitro better than those developed using the previous methods mentioned. This method also has the advantage of potentially simulating multi-organ interactions by interconnecting different microfluidic organ-on-a-chip with each other to build body-on-a-chip models. These micro-

physiological systems can be harnessed to study cancer multi-organ metastasis. However, organ-on-a-chip models developed so far utilized either primary cells or cancer cell lines which cannot resemble the cellular complexity of organs and tumors.

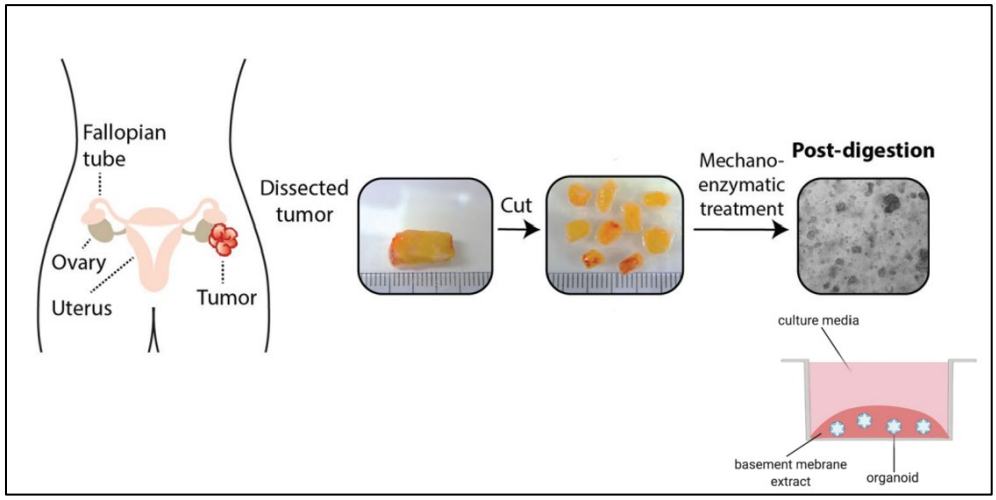

Figure 1.14. The submerged method. Adapted from Gunti *et al* and Kopper *et al*[139, 157].

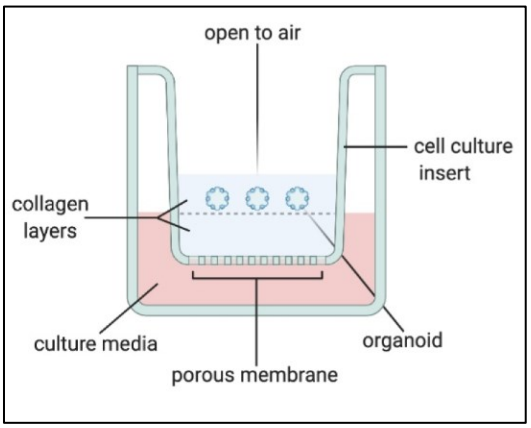

Figure 1.15. The air–liquid interface method. Adapted from Gunti *et al*[139].

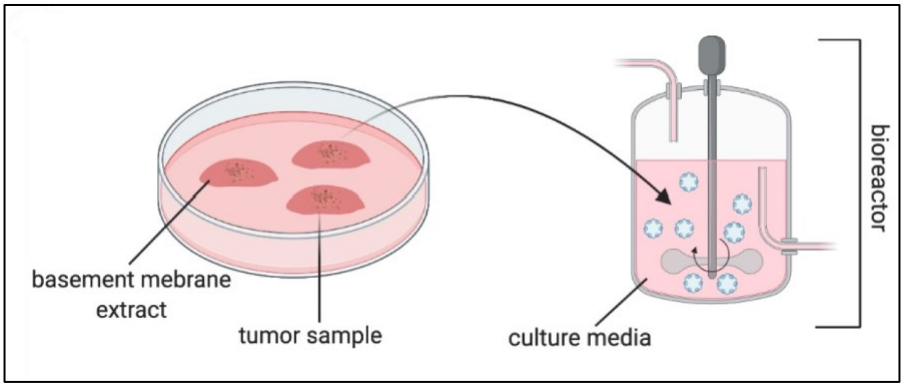

Figure 1.16. The bioreactor method. Adapted from Gunti *et al*[139].

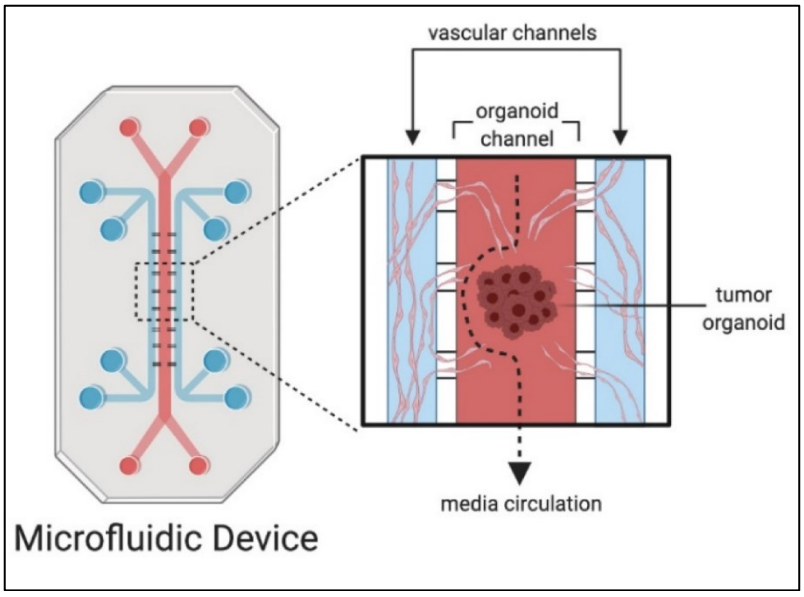

Figure 1.17. The organoid-on-a-chip method. Adapted from Gunti *et al*[139].

1.3 Specific Ovarian Cancer Cell Lines

Ovarian cancer cell lines of epithelial origin that have the advantage of illustrating disease progression, and thus, that could be useful in in-vitro studies are PEO1, PEO4, and PEO6. The three cell lines were established sequentially from the same patient and initially reported in 1988[158]. PEO1 were derived from the ascites of a patient diagnosed with HGSC. PEO1 cells were collected 22 months after cisplatin, 5-fluorouracil and chlorambucil treatment and the patient continued to show response to cisplatin treatment. PEO4 cells were taken from the same patient after relapse occurred 10 months later and consequently are considered platinum resistant, and PEO6 cells, also platinum resistant, were collected three months later, following further cisplatin treatment that had produced no beneficial effects[158, 159]. The three cell lines were reported to have high genetic fidelity to HGSC by having multiple copy number alterations consistent with the origin of HGSC. Despite originating from the same patient, PEO1, PEO4 and PEO6 cells were shown to have karyotype divergence (i.e., different chromosomal morphology)[158]. PEO1 have also been found to be *BRCA2* mutants while PEO4 and PEO6 were BRCA wild-type[160].

Not many studies involving the three cell lines in 2D culture are present in the literature and even less involving the cell lines in 3D culture. For example, in 2D culture, a study has reported the accumulation of platinum drugs in the cell lines[159]. In 3D culture, a study has demonstrated the cell lines' capacity to form foci and to develop multicellular structures as well as their orthotopic tumorigenicity in immunosuppressed mice[158]. A study has also characterized the metastatic capabilities of the cell lines, in both 2D and 3D assays, and the ability of cytostatic concentrations of mifepristone to inhibit them[161]. Mifepristone is a synthetic steroid that acts as anti-glucocorticoid and anti-progestin and that has been found to be a potential treatment option for ovarian cancer.

1.4 Rationale, Hypothesis and Objectives of Current Study

As most early-phase clinical trial designs rely heavily on preclinical data, it is important to consider variations that exist between experimental models when performing drug screening or therapeutic response prediction studies, especially in the era of personalized medicine, to accurately select a preclinical model for use[146].

Since 2D culture is a widely used cell culture method and that 3D culture is an emerging and constantly evolving model, both were compared in this project using ovarian cancer cell lines of epithelial origin that illustrate disease progression. Acquiring a better understanding of the variations that exist between both cell culture models by analysing the cellular behavior across different disease states in the different culture conditions, may allow for a more accurate selection of a cell culture model for clinically relevant data collection. The range of disease state represented by PEO1, PEO4 and PEO6 cells along with their *BRCA* statuses could influence treatment response and thus make these cell lines of choice to compare 2D and 3D culture environments as representations of in-vivo conditions.

We hypothesize that when compared to 2D culture settings, the 3D culture model will more closely represent the in-vivo environment and may provide a more accurate representation of response to various therapies. The following project aims to compare the behavior of PEO1, PEO4 and PEO6 cells in terms of morphology, viability, metabolic activity, and drug response in 3D versus 2D culture, two in-vitro models used in ovarian cancer research. While several methods can be used for spheroids formation as described above, allowing spheroids to form in ULAPs greatly facilitates numerous assays such as cell viability assays, transferring spheroids and performing drug treatments[149]. Therefore, in this project, flat-bottom cell culture plates were used for 2D culture and ULAPs were used as the 3D culture method.

Chapter 2.

Manuscript in preparation for submission to Biochemical and Biophysical Research Communications as a short communications paper

Characterization of a Three-Dimensional Culture System Representative of Disease Progression in High-Grade Serous Ovarian Cancer

2.1 Abstract

High-grade serous ovarian cancer is the most common ovarian cancer histological subtype and is usually diagnosed at advanced stages accounting for a high number of mortalities. Over time, almost all ovarian cancer patients eventually recur despite therapy and develop resistance to platinum agents. These patients may benefit from the use of PARP inhibitors. The development of preclinical models to assess therapeutic responses would enable individualized therapy for patients. 3D culture has been found to be a faithful preclinical model of ovarian cancer. The aim of this study was to compare the behavior of PEO1, PEO4 and PEO6 ovarian cancer cells in terms of morphology, viability, metabolic activity, and drug response in 3D culture versus 2D culture. In flat-bottom plates (i.e., in 2D culture), PEO1 and PEO4 form a 2D cellular adherent layer whereas PEO6 cells, in addition to a flat layer of cells, naturally form 3D floating structures if given time. In contrast, when grown in ultra-low attachment round-bottom plates (i.e., in 3D culture), all cell lines formed 3D structures with different compaction levels. In 2D culture, the three cell lines are mostly proliferative with only few apoptotic cells scattered randomly on the bottom of the plates. Conversely, in 3D culture, the cell lines mimicked poorly vascularized tumors by forming a multilayered structure with an outer layer of live cells, where there is active cell proliferation, and an inner core of apoptotic cells. A pronounced differential capacity between the cells to produce ATP was observed in 3D culture while similar magnitude of production was observed in 2D culture. The response of the cells to carboplatin, paclitaxel and niraparib in flat- and round-bottom plates followed a similar trend with lower sensitivity to the drugs observed in the 3D culture setting. The 3D culture environment seems to provide a level of complexity absent in 2D culture making it more likely reflective of the in-vivo cellular tumor behavior central to assessment of therapeutic responses.

2.2 Introduction

Ovarian cancer is the fourth most common gynecologic cancer and is associated with a high mortality rate[1]. High-grade serous (HGSC) is the most common histological subtype of ovarian cancer that is usually diagnosed at advanced stages and accounts for a high number of mortalities[2]. The initial treatment includes platinum-based chemotherapy either before (neoadjuvant) or after (adjuvant) surgical debulking[3]. While most patients initially respond well to a platinum-based chemotherapy regimen, over time, almost all ovarian cancer patients eventually recur despite therapy and develop resistance to platinum agents[3]. These patients may benefit from different initial therapies such as PARP inhibitors (PARPis).

PARPis exert their cytotoxic effects by trapping the poly (ADP-ribose) polymerase enzyme on single-strand breaks resulting in an increase in double-strand breaks in replicating cells. Consequently, the reliance of homologous recombination repair-deficient cancer cells on error prone DNA repair pathways leads to DNA damage accumulation and cell death[4]. Clinical trials have demonstrated that BRCA1 and BRCA2 associated HGSCs, and a subset of sporadic HGSCs, respond to PARPis[5-10]. However, with the aim of optimizing efficacy and tolerability of novel therapeutic regimens in ovarian cancer, further pre-clinical studies are needed to determine the efficacy of PARPis as frontline therapeutic agents.

The establishment of a preclinical model of disease to acquire a deeper understanding of the therapeutic response of HGSC became a point of focus in ovarian cancer research as the lack of preclinical models that recapitulate tumor pathophysiology in-vivo slowed the accurate assessment of drug efficacy and toxicity[11]. Two-dimensional (2D) cell culture contributed to the advancement of several areas of research and remains a predominant preclinical method[11, 12]. It is a model that is relatively simple, economical, and convenient for high-throughput drug studies. However, it is

an oversimplified version of tumors that does not mimic essential in-vivo cellular organization and interactions since in flat-bottom cell culture plates, cells tend to adhere to the bottom surface of the plate forming a flat layer of cells.

Three-dimensional (3D) culture of epithelial ovarian cancer cells has been found to be a strong preclinical model of disease for in-vitro experiments that bridges the gap between 2D cell culture and animal models[11, 13]. Cells grown in such 3D environment mimic poorly vascularized in-vivo tumors' multilayered structure and their nutrients, pH, and oxygen concentration gradients[14]. In round-bottom plates (i.e., 3D culture), the ultra-low attachment environment forces cells in suspension to naturally aggregate, and thus, form 3D spheroidal structures similar to in-vivo tumors[15]. It has been demonstrated that cells cultured in 3D preserve a more significant number of cells functions than cells cultured in 2D and that both models differ in terms of drug efficacy suggesting that the 3D culture model is superior to 2D monolayers in the search for new therapeutic targets[16, 17]. Thus, we hypothesize that compared to 2D culture settings, the 3D culture model more closely represents the in-vivo environment and may provide a more accurate representation of response to various therapies.

PEO1, PEO4 and PEO6 cells were collected from a single patient with HGSC after initial treatment with cisplatin, 5-fluorouracil, and chlorambucil[18]. PEO1 cells were isolated from ascites of the patient after she had recurrence more than 22 months following the first treatment. PEO4 cells were isolated from ascites of the same patient after she developed resistance to the previous chemotherapeutics, whereas PEO6 cells were isolated from ascites collected prior to the death of the patient.

Although multiple studies have compared 2D and 3D culture settings, only a few have done so in epithelial ovarian cancer cell lines. Comparison of both culture settings using epithelial

ovarian cancer cell lines from the same patient that illustrate disease progression and have different BRCA statuses has not been performed yet.

This study aims to compare the human ovarian adenocarcinoma behavior of PEO1, PEO4 and PEO6 cells in terms of morphology, viability, metabolic activity, and drug response in 3D culture versus 2D culture.

2.3 Materials and Methods

2.3.1 Cell Culture Plates and Cultured Cell Lines

For 3D cell culture, 96-well transparent (Corning Incorporated, Kennebunk, ME, USA) or white (S-BIO, Hudson, NH, USA) ultra-low attachment round-bottom plates (ULAPs) were the plating type of choice since allowing cellular spheroidal structures to form in round-bottom plates facilitates the process of transferring structures and performing cell viability assays and drug treatments[15]. For 2D cell culture, cell culture-treated flat-bottom T75 flasks (Thermo Fisher Scientific, Rochester, NY, USA) and 96-well flat-bottom plates (Corning Incorporated, Kennebunk, ME, USA) were used.

The cell line models used for culture were PEO1, PEO4 and PEO6. They are derived from a single patient with HGSC and illustrate disease evolution as they were longitudinally obtained along disease progression[14]. More precisely, PEO1 cells are chemosensitive and were obtained during the early stage of the disease following chemotherapeutic treatment, PEO4 cells were obtained following ovarian cancer recurrence and are chemoresistant, while PEO6 cells, also chemoresistant, were obtained prior to the death of the patient, and thus, represent the latest stage of the disease. The cells were originally obtained from Dr. Taniguchi (Fred Hutchinson Cancer

Center, University of Washington, Seattle, WA, USA) with the written consent of the originator, Dr. Langdon (Edinburgh Cancer Research Centre, Edinburgh, UK)[19]. PEO1 have been found to be *BRCA2* mutants while PEO4 and PEO6 BRCA wild-type[20]. The three cell lines were maintained in RPMI 1640 medium (Gibco, Grand Island, NY, USA) prepared in HyPure cell culture grade water (Cytiva, Logan, UT, USA) and supplemented with 10 mM HEPES (Corning), 100 IU penicillin and 100 µg/mL streptomycin (Corning), 2 mM dipeptide glutamine (Glutagro, Corning), 10 µg/mL insulin (Gibco), 1 mM sodium pyruvate (Corning), 5% fetal bovine serum (Corning), 5% bovine serum (Corning) and 23.8 mM sodium bicarbonate (Millipore Sigma) at a constant temperature of 37 °C in a humidified atmosphere of 5% CO_2. Media was changed every 48 to 72 hours when cells were cultured in cell culture-treated flat-bottom T75 flasks.

For all experiments except the morphological analysis, ATP quantitation assay and positive controls, the three cell lines were plated in 96-well flat-bottom plates with 5,000 cells per well and in ULAPs with 5,000 cells per well. For the ATP quantitation assay, cells representing the three cell lines were plated in a 96-well flat-bottom plate with 10,000 cells per well and in ULAPs with 5,000 cells per well. Double the number of cells per well was plated in the flat-bottom plate than in the ULAPs to maximize the number of cells that adhere to the bottom of the flat-bottom plate during the 24 hours incubation period. For the Live/Dead assay positive control in 2D, PEO1, PEO4 and PEO6 cells were plated in 96-well flat-bottom plates with 5,000 cells per well. For the CellEvent Caspase-3/7 assay positive control in 2D, PEO1 and PEO4 cells were plated in 96-well flat-bottom plates with 5,000 cells per well. For the Live/Dead assay positive control in 3D, PEO6 cells were plated in an ULAP with 5,000 cells per well.

2.3.2 Morphological Analysis

The morphology of the cells in culture-treated flat-bottom flasks at one and five days after plating for PEO1 and PEO4 and at two and seven days for PEO6 was compared to determine their morphological adaptation in a 2D culture environment. The arrangement of the cells in an ultra-low attachment environment was compared one, four and seven days after plating by determining the compaction pattern of the 3D spheroidal structures formed by the cells. The cells were plated in 96-well ULAPs with 5,000 cells per well and three wells per cell line. After one, four and seven days in the plates, the average cross-sectional area of the PEO1, PEO4 and PEO6 spheroidal structures was calculated across three wells per cell line using the ToupView Software (OMAX, USA). The compaction pattern of the 3D spheroidal structures was determined by comparing the average cross-sectional areas at one and four days as well as at four and seven days after plating such that a decrease in average cross-sectional area with time represents getting more compact.

2.3.3 Cell Viability Assay

The viability of the cells was compared in a 2D and 3D culture environment using Live/Dead cell assay. After four days in the plates for 2D culture and four and seven days for 3D culture, Calcein-AM (live cells indicator), EthD-1 (dead cells indicator) (LIVE/DEAD Viability/Cytotoxicity Kit, Thermo Fisher Scientific, Eugene, OR, USA), and the NucBlue Live Cell Stain ReadyProbes reagent (nuclei indicator) (Thermo Fisher Scientific, Eugene, OR, USA) were added to the cells followed by imaging.

Regarding the positive control for the Live/Dead assay, after four days in the plates, the cells were fixed with a 4% PFA solution before undergoing the Live/Dead assay. Fixation of the cells

allows for penetration of the non-permeable dead indicator and disruption of the esterase activity indicator of cell viability.

2.3.4 Apoptosis Detection Assay

The cell death method of the cells was compared in 2D, and 3D culture by performing a CellEvent Caspase-3/7 assay. After three days in the plates for 2D culture and three and six days for 3D culture, the CellEvent Caspase-3/7 Green ReadyProbes reagent (Thermo Fisher Scientific, Eugene, OR, USA) was added to the cells. 24 hours later, caspase-3/7 activation was assessed and NucBlue was added to allow for nuclei detection through imaging.

We utilized known results on the effect of auranofin on activation of caspase-3/7 in PEO1 and PEO4 in 2D to confirm whether the caspase-3/7 reagent captures the feature of caspase-3/7 activation and is effective in our 3D model. Since the drug auranofin has been found to cause apoptosis in PEO1 and PEO4, a positive control in which the two cell lines were exposed to the drug was included[21, 22]. PEO1 and PEO4 cells were plated in three groups, namely a group exposed to the Caspase-3/7 Green Reagent and DMSO (Corning, Manassas, VA, USA) (i.e., the vehicle group), a group exposed to the Caspase-3/7 Green Reagent, DMSO and 2 μM of the drug auranofin and a group exposed to the Caspase-3/7 Green Reagent, DMSO and 4 μM of auranofin. Only PEO1 and PEO4 were used for the positive control because the known results on caspase-3/7 activation were done with auranofin on PEO1 and PEO4 and were not evaluated in PEO6[21, 22]. Since 2 μM and 4 μM were the concentrations found to have a positive effect on apoptosis in both cell lines, these were the concentrations used.

2.3.5 Proliferation Detection Assay

The proliferation levels of the cells were compared in 2D and in 3D culture using a Click-iT 5-Ethynyl-2′-deoxyuridine (EdU) Cell Proliferation assay (Click-iT EdU Alexa Fluor 594 Imaging Kit, Thermo Fisher Scientific, Eugene, OR, USA). The assay relies on the incorporation of a fluorescently labeled mimetic of the thymidine nucleotide, EdU, into newly synthesized DNA to indicate cells that are having DNA synthesis. After three days in the plates for 2D culture and three and six days for 3D culture, 10 µM of EdU dissolved in DMSO was added to the cells[18]. 24 hours later, the Click-iT cocktail containing an EdU reaction buffer, copper (III) sulfate, Alexa Fluor 594 Azide dye and a Click-iT EdU buffer additive as well as Hoechst (nuclei indicator) was added to the cells followed by imaging.

2.3.6 ATP Quantitation Assay

The metabolic activity of the cells in 2D and 3D were compared by performing a CellTiter-Glo Luminescent Cell Viability assay (Promega Corporation, Madison, WI, USA) and a CellTiter-Glo 3D Cell Viability assay (Promega Corporation, Madison, WI, USA). Cells representing the three cell lines were plated in a 96-well flat-bottom plate with 10,000 cells per well and in ULAPs with 5,000 cells per well. After 24 hours in the flat-bottom plate and four and seven days in the ULAPs, the CellTiter-Glo reagent was added to the cells followed by shaking on an orbital shaker and finally plate reading.

A negative control for the CellTiter-Glo assay was included by adding the CellTiter-Glo Reagent to three wells out of 96 without cells.

2.3.7 Drug Testing

The drug response of the cells in a 2D and 3D culture environment was compared by performing the Live/Dead and the CellTiter-Glo Luminescent 3D Cell Viability assays as described above. After four days in the ULAPs, the cells were exposed to the therapeutic agent carboplatin (25 μM, 50 μM, 100 μM or 200 μM), paclitaxel (1.25 μM, 2.5 μM, 5 μM or 10 μM) and the PARPi, niraparib (2 μM, 4 μM, 8 μM or 16 μM). The reason as to why the cell lines were kept for four days in the plates before drug exposure is because we wanted to assess the effect of the drugs at the healthier point of the spheroidal structures. Based on the known maximum effect of the tested drugs with ovarian cancer cells in 2D, three days following the initial drug exposure, the two assays were performed[23, 24].

In Liston *et al*'s paper, the listed Cmax for carboplatin is 135 μM, for paclitaxel is 4.27 μM and for olaparib is 13.1 μM[25]. The drug concentrations we utilized comprise lower and higher concentrations than the Cmax values presented in the paper of Liston *et al.* to ensure that clinically relevant concentrations are included. Since no data was available for niraparib, the Cmax of the PARPi, olaparib, was used instead.

2.3.8 Statistical Analysis and Replicates

For the ATP quantitation assay results analysis, data are presented as mean ± standard error of the mean (S.E.M.) and compared using one-way ANOVA followed by the Tukey's Multiple Comparison Test. For the cross-sectional areas and drug testing results analysis, data are presented as mean ± S.E.M.and compared using two-way ANOVA followed by the Dunnett's Multiple Comparison Test. For the CellEvent Caspase-3/7 assay green fluorescence units results and Click-

iT 5-Ethynyl-2′-deoxyuridine (EdU) Cell Proliferation assay red fluorescence units results for PEO1, PEO4 and PEO6 cells four and seven days after plating in 96-well ULAPs and the percentages of positive nuclear EdU results in 2D, statistical analysis was performed using unpaired *t*-test.

The experiments were done with four to seven replicates for each cell line in each experiment. In 2D, the Live/Dead assay at day four was performed once with four wells per cell line. In 3D, at days two, four and seven, it was performed twice, once with three wells per cell line and once with four wells per cell line. At days four and seven, it was performed once with seven wells per cell line and at day eight was performed once with 10 wells per cell line. In 2D, the CellEvent Caspase-3/7 assay at day four was performed once with 4 wells per cell line. In 3D, at days four and seven, it was performed once with four wells per cell lines and at days two, four and seven, it was performed once with four wells per cell line. In 2D, the Click-iT 5-Ethynyl-2′-deoxyuridine (EdU) Cell Proliferation assay at day four was performed once with 4 wells per cell line. In 3D, at days four and seven, the Click-iT assay was performed twice with four wells per cell line. In 2D, at 24 hours, the ATP quantitation experiment was performed once with five wells per cell line. In 3D, at days four and seven, the ATP assay was performed three times with five wells per cell line. In 2D, the drug testing experiment was performed once with 4 wells per drug concentration and vehicle group per cell line. In 3D, the drug testing experiment was performed twice with 4 wells per drug concentration and vehicle group per cell line.

In 2D, the Live/Dead assay positive control was performed once with four wells per cell line. The CellEvent Caspase-3/7 assay positive control was performed once with three wells per drug concentration and vehicle group per cell line. The CellTiter-Glo Cell Viability assay positive control was performed at each plate luminescence reading, and thus, was performed four times. In

3D, the Live/Dead assay positive control was performed once with two wells with PEO6. The CellTiter-Glo Cell Viability assay negative control was performed at each plate luminescence reading, and thus, was performed nine times with three wells with no cells every full plate reading.

2.3.9 Plate Imaging and Reading Parameters

For all experiments, the BioTek Cytation3 Imaging Reader in conjunction with the BioTek Gen5 Software were used to perform imaging and fluorescent and luminescent plate reading.

For the Live/Dead assay, the excitation and emission values set for green fluorescence reading were 494 nm and 516 nm respectively, for red fluorescence reading they were 528 nm and 617 nm respectively and for blue fluorescence reading they were 359 nm and 461 nm respectively. For the CellEvent Caspase-3/7 assay, the excitation and emission values set for green fluorescence reading were 502 nm and 530 nm respectively and for blue fluorescence they were 359 nm and 461 nm respectively. For the Click-iT 5-Ethynyl-2′-deoxyuridine (EdU) Cell Proliferation assay, the excitation and emission values set for red fluorescence reading were 590 nm and 615 nm respectively and for blue fluorescence they were 359 nm and 461 nm respectively.

For plate luminescence reading, a shaking step of 10 seconds was performed before reading.

2.4 Results

2.4.1 Morphological analysis

Morphological differences were observed between PEO1, PEO4 and PEO6 cells following imaging of the cell lines in T75 flasks. All cells grew forming monolayers and islands of uniform polygonal cells (Fig.2.1A)[26]. PEO1 cells had an elongated shape compared to PEO4 cells, and PEO6 cells tended to grow on top of each other.

In ULAP, all cell lines formed 3D structures with different compaction patterns along time (Fig.2.1B). For PEO1, PEO4 and PEO6 cells, the spheroidal structures get more compact from day 1 to day 4 since their average cross-sectional area decreases during this time (Fig.2.1C). The PEO1 structures have no change in compaction level from day 4 to day 7 while PEO4 and PEO6 structures get less compact from day 4 to day 7 since their average cross-sectional area increases during this time.

At day 4 and day 7, the average cross-sectional area of PEO1 is smaller than that of PEO4 which is smaller than that of PEO6 (Fig.2.1C).

2.4.2 Cell Viability Assay

In 2D, the three cell lines displayed a homogeneous and flat vital culture with minimum cell death (Fig.2.2A). In 3D, it was observed that all three cell lines display an outer layer of live cells at the periphery of the spheroidal structures and an inner layer of dead cells in the center, but at different time points (Fig.2.2B). Two days after plating, the structures of PEO1 and PEO4 cells had few dead (i.e., red) cells. Four days after plating, the structures had an almost fully developed

core of dead cells while seven days after plating, the structures had no visible dead cells in the center. Two days after plating, the structures of PEO6 cells had few dead (i.e., red) cells. Four and seven days after plating, the structures had no visible dead cells in the center. Calcein-AM (live cells) and EthD-1 (dead cells) fluorescence units graphs show that from two to seven days after plating, PEO1 cells have a decrease in the levels of live and dead cells while PEO4 cells have no significant change in the levels of live cells but have a decrease in the levels of dead cells (Fig.2.2B). Across the three time points, PEO6 cells appear to have no significant change in the levels of live and dead cells.

2.4.3 Apoptosis Detection

In 2D, for PEO1, PEO4 and PEO6 cells, only a few apoptotic cells were scattered randomly on the bottom of the plates (Fig.2.3A). In 3D, PEO1 apoptotic cell death was confined to the center of the spheroidal structure, PEO4 cell death was spread all over the spheroidal structure and PEO6 cell death tended to occur in the center of the spheroidal structure (Fig.2.3B). Green fluorescence relative units indicate that PEO1 apoptosis levels decrease from day four to day seven and do not change significantly during the same time period for PEO4 and PEO6 (Fig.2.3B).

2.4.4 DNA Synthesis Pattern

In 2D, DNA synthesis in PEO1, PEO4, and PEO6 cells across the plates' surface was detected as indicated by the purple fluorescence (i.e., a superposition of red and blue fluorescence) (Fig.2.3C). The percentages of positive nuclear EdU indicate that DNA synthesis levels in 2D of

PEO1 cells are higher than those of PEO4 and PEO6 cells, reaching statistic significance only with PEO4 cells (Fig.2.3C).

In 3D culture, the three cell lines were found to proliferate mostly in the outer layer of the cellular structures (Fig.2.3D). Averaging relative red fluorescence units indicate that DNA synthesis level of all three cell lines does not change significantly from day four to day seven (Fig.2.3D).

2.4.5 Metabolic Activity

In 2D, the three cell lines produced a similar level of ATP between approximately 3800 to 5000 relative luminescent units. However, PEO6 cells produced a significantly higher amount of ATP followed by PEO1 cells and then PEO4 cells 24 hours following plating (Fig.2.4A). In 3D, at day four and seven following plating, it was found that PEO6 cells produce approximately four times more ATP than PEO4 followed by PEO1 that produce approximately eight times less ATP than PEO6 (Fig.2.4B).

2.4.6 Drug Testing

The level of ATP produced by the control cells, without treatment, in both the 2D and 3D model was considered 100%. In 2D culture, all four concentrations of carboplatin appeared to reduce ATP levels in a concentration-dependent manner in PEO1 cells while only 100 μM and 200 μM caused a decrease of ATP in PEO4 cells (Fig.2.4C). The production of ATP in PEO6 cells seemed to be higher than control cells at 25 μM and 50 μM of carboplatin with no effect at 100

μM and a decrease below the control level only at 200 μM. The ATP levels in all three cell lines were found to be reduced by paclitaxel to a similar extent at the four concentrations used. Niraparib caused a decrease in ATP levels at 4 μM, 8 μM and 16 μM only in PEO1 cells, while none of the concentrations had a significant effect on PEO4 and PEO6 cells.

In 3D culture, the ATP production in PEO1 and PEO4 cells appeared to be reduced by 50 μM, 100 μM and 200 μM of carboplatin in a concentration-dependent manner, although to a lesser extent in PEO4 cells (Fig.2.4C). The production of ATP in PEO6 cells seemed to be higher than control cells at 25 μM, 50 μM and 100 μM of carboplatin with no effect at 200 μM. The levels of ATP in all three cell lines were found to be reduced by paclitaxel to a similar extent at the four concentrations used. Only 8 μM and 16 μM of niraparib caused a decrease in ATP levels in PEO1 cells while none of the concentrations had a significant effect on PEO4 and PEO6 cells. When the drug had an impact on cellular ATP production, it was found to be less effective in 3D than in 2D (Fig.2.4C).

2.5 Discussion

Our results suggest that the behavior of PEO1, PEO4 and PEO6 cells, in terms of morphology, viability, metabolic activity, and drug response, in 3D culture reflects more complex differences associated with the disease state that the cell lines represent, compared to a more homogeneous response associated with 2D culture.

In 2D culture, PEO1 and PEO4 cells form an adherent layer, while PEO6 cells tend to grow on top of each other and naturally form 3D floating structures if given time[18]. This highlights the complexity of the cells representing the tumor as the disease progresses[18].

For PEO1, PEO4 and PEO6 cells, the spheroidal structures get more compact from day one to day four. From day four to day seven, the PEO1 structures have no change in compaction level while PEO4 and PEO6 structures get less compact. Therefore, these results suggest that the three cell lines reach a maximum level of compaction at day four.

At day four and day seven, the average cross-sectional area of PEO1 is smaller than that of PEO4 which is smaller than that of PEO6. Considering that PEO1 cells represent the earliest and PEO6 cells the latest stage of disease, such average cross-sectional area pattern at day four and day seven could be associated with the disease state the cells represent where the more complex cells become, the less prone they are to get together.

While in 2D culture, no specific pattern of live and apoptotic cells has been observed, cells within the spheroids formed in 3D culture did have different levels of viability and death associated with their proliferative capacity and apoptotic state. In general, live proliferating cells are present at the periphery while apoptotic cells accumulate in the center. Such behavior correlates with findings in previous studies that highlight the similarity of such pattern to the cellular behavior of in-vivo tumors as limited nutrients and agents penetration in the center generates a healthy outer layer of cells with high proliferative ability and a hypoxic dead core[14, 27].

Green and red fluorescence intensities along the drawn white line passing through the spheroidal structures of PEO1, PEO4 and PEO6 cells 4 days after plating in 96-well ULAPs provide additional evidence regarding the formation of a multilayered structure with an outer layer of live cells and an inner core of dead cells (Fig.S2.1). For PEO1 and PEO4 cells, green fluorescence intensity tends to peak at the extremities of the white line (i.e., at the periphery of the spheroidal structures) and red fluorescence intensity tends to peak at the middle of the white line (i.e., at the center of the spheroidal structures). These results are expected, since four days after

plating, the PEO1 and PEO4 spheroidal structures had an almost fully developed core of dead cells. Four days after plating, the PEO6 spheroidal structure had no visible dead cells in the center. It is thus expected that no red fluorescence intensity peak appears in between the two peaks of green fluorescence intensity for PEO6.

For the Live/Dead positive control in 2D where cells were fixed with paraformaldehyde (i.e., killed in the process) four and seven days after plating in 96-well flat-bottom cell culture plates and the Live/Dead assay was performed, no live cells (i.e., green, fluorescent cells) were present. Only dead cells (i.e., purple, fluorescent cells due to a superposition of red and blue fluorescence) indicating fixed dead cells were present (Fig.S2.2). For the Live/Dead assay positive control in 3D, no live cells (i.e., green, fluorescent cells) were present, only dead cells (i.e., red, fluorescent cells) (Figure S2.3). These results are expected since fixation of the cells allows for penetration of the non-permeable dead indicator, and thus, for EthD-1 red fluorescence to be apparent and disruption of the esterase activity indicator of cell viability, and thus, for no Calcein-AM (sensitive to esterase activity) green fluorescence to be visible. Therefore, these results confirm that the Calcein-AM and EthD-1 combination of reagents used in the Live/Dead assay is reliable.

From four to seven days following plating, PEO1 appeared to have a decrease in apoptosis and viability with no significant change in proliferation levels and average cross-sectional area of the spheroidal structures formed for PEO1, suggesting a stagnant level of compaction. PEO4 and PEO6 cells appeared to have no significant changes in their apoptosis and proliferation levels from four to seven days after plating. However, the average cross-sectional area of the spheroidal structures formed for both cell lines increased during this period, suggesting a decrease in the level of compaction.

For the CellEvent Caspase-3/7 assay positive control results, as expected, the higher the concentration of auranofin administered, the higher the number of apoptotic cells (i.e., green, fluorescent cells) compared to the basal number of apoptotic cells of the vehicle group (Fig.S2.4)[21, 22].

Despite the varying complexities of the 2D and 3D cell culture models, the response of the cell lines to carboplatin, paclitaxel and niraparib in flat- and round-bottom plates followed a similar trend with lower sensitivity to the drugs observed in the 3D culture setting. Such decrease in drug sensitivity in 3D has been observed in previous studies and attributed to the reduced access of chemotherapy agents to internal cells in the un-vascularized 3D spheroids due to their structure characterized by a metabolite density gradient[17, 28-30].

The effect of carboplatin observed in PEO1, PEO4 and PEO6 cells in 2D and 3D culture correlates with the cell lines' expected behavior. PEO1 cells are chemosensitive while PEO4 and PEO6 cells are more chemoresistant. Therefore, it is expected that carboplatin will be more effective on PEO1 cells than on PEO4 and PEO6 cells. The effect of paclitaxel on the three cell lines in 2D and 3D culture is strong and independent of the concentrations used, yet is less effective in 3D than in 2D. Considering that PEO1 is mutant for *BRCA2* while PEO4 and PEO6 are BRCA wild-type and that *BRCA1* and *BRCA2* associated HGSCs have been found to respond to PARPis, the fact that niraparib only has an effect in PEO1 cells reinforces that the cells studied are a good model of disease progression [6-8, 20]. Moreover, the expected response on PARPis on PEO1 was stronger in 2D than in 3D, reflecting an advanced level of adaptation and poor response for PEO1 cells in the 3D model.

Measuring luminescence levels, and thus, ATP production levels of cells in a flat-bottom plate in which they adhere to the bottom allows us to determine the intrinsic ATP production levels

of the three cell lines when they are in a 2D environment. PEO1, PEO4 and PEO6 did have the ability to produce ATP in flat-bottom plates with similar biologically relevant levels. In 3D culture, a differential capacity of the cells to produce ATP was observed with PEO6 cells producing the highest amount of ATP followed by PEO4 and then PEO1 cells similarly at four and seven days after plating. Such differential capacity might reflect the in-vivo cellular adaptation based on the disease state that PEO6 cells represent. High ATP levels are key drivers of aggressive cancer cell phenotypes. ATP-high cancer cells show increases in many aggressive properties or behaviors, including anchorage-independence, metastasis, and antioxidant capacity[31]. Therefore, the ability of PEO6 cells to produce significantly higher levels of ATP than the other two cell lines in 3D culture could be linked to an increase in mitochondrial mass and to the aggressive disease state that they represent[31].

It was found that, from day four to day seven in ULAPs, PEO1 appeared to have a decrease in apoptosis with no significant change in proliferation level and compaction level of the spheroidal structures formed. We speculate that less cells were dying and the average cross-sectional area and proliferation level did not change because cells were arranging themselves on top of each other rather than next to one another. However, further investigation is needed to confirm this speculation.

It was found that, from day four to day seven in ULAPs, PEO4 and PEO6 have no significant changes in their apoptosis and proliferation levels and the spheroidal structures they form get less compact. Since PEO4 and PEO6 cells appear to have a similar behavior in terms of caspase-3/7 activation, proliferation level from day four to day seven and a similar response to niraparib potentially associated with their *BRCA* wildtype status, we speculate that an intrinsic characteristic of the cells related to the more advanced disease stage they represent could explain their similar

decreasing compaction pattern from day four to day seven. However, further investigation is required to assess the validity of our speculation.

Since PEO1 cells appeared to have a more visible and pronounced apoptotic core than PEO4 and PEO6 cells in 3D culture, taken together, morphological analysis, Live/Dead, apoptosis detection and ATP quantitation assays results in 3D suggest that as cells get more together, those in the center of the spheroidal structures have less access to components in the media, and thus, have a higher tendency to experience apoptotic cell death, are less metabolically active and are associated with less aggressive cancer cell phenotypes.

Such findings suggest that the 3D culture environment provides a level of complexity absent in 2D culture making it more reflective of the in-vivo cellular tumor behavior central to assessment of therapeutic responses.

2.6 Limitations

The percentages of positive nuclear EdU in 2D indicate that the level of DNA synthesis of PEO1 is significantly higher than that of PEO4. However, PEO1, PEO4 and PEO6 cells in 2D are known to have different doubling times with PEO1 cells being the fastest and PEO6 cells the slowest to divide[32]. This inconsistency between doubling times and DNA synthesis might be explained by a longer time spent in the G2/M phase of the cell cycle, during which cell division occurs, being longer for PEO4 and PEO6 than for PEO1 . However, further investigation is needed to determine whether our speculation is true.

2.7 Conclusion

As HGSC is the most aggressive ovarian cancer subtype and generally presents at an advanced stage with poor long-term survival, developing in-vitro models that are as faithful as possible to the in-vivo tumor behavior to accurately determine therapeutic efficacy of treatments, and thus, potentially increase patient survival is of vital importance.

2.8 References

[1] Momenimovahed Z, Tiznobaik A, Taheri S, Salehiniya H: Ovarian cancer in the world: epidemiology and risk factors. Int J Womens Health 2019, 11:287-99.
[2] Anzar N, Hasan MR, Akram M, Yadav N, Narang J: Systematic and validated techniques for the detection of ovarian cancer emphasizing the electro-analytical approach. Process Biochemistry 2020, 94:126-35.
[3] Lukanović D, Kobal B, Černe K: Ovarian Cancer: Treatment and Resistance to Pharmacotherapy. Reproductive Medicine 2022, 3:127-40.
[4] O'Connor MJ: Targeting the DNA Damage Response in Cancer. Mol Cell 2015, 60:547-60.
[5] Rose PG: First-Line Chemotherapy for Ovarian Cancer: Inferences From Recent Studies. Oncologist 2016, 21:1286-90.
[6] Moore K, Colombo N, Scambia G, Kim BG, Oaknin A, Friedlander M, Lisyanskaya A, Floquet A, Leary A, Sonke GS, Gourley C, Banerjee S, Oza A, Gonzalez-Martin A, Aghajanian C, Bradley W, Mathews C, Liu J, Lowe ES, Bloomfield R, DiSilvestro P: Maintenance Olaparib in Patients with Newly Diagnosed Advanced Ovarian Cancer. N Engl J Med 2018, 379:2495-505.
[7] Pujade-Lauraine E, Ledermann JA, Selle F, Gebski V, Penson RT, Oza AM, Korach J, Huzarski T, Poveda A, Pignata S, Friedlander M, Colombo N, Harter P, Fujiwara K, Ray-Coquard I, Banerjee S, Liu J, Lowe ES, Bloomfield R, Pautier P, Korach J, Huzarski T, Byrski T, Pautier P, Friedlander M, Harter P, Colombo N, Pignata S, Scambia G, Nicoletto M, Nussey F, Clamp A, Penson R, Oza A, Poveda Velasco A, Rodrigues M, Lotz J-P, Selle F, Ray-Coquard I, Provencher D, Prat Aparicio A, Vidal Boixader L, Scott C, Tamura K, Yunokawa M, Lisyanskaya A, Medioni J, Pécuchet N, Dubot C, de la Motte Rouge T, Kaminsky M-C, Weber B, Lortholary A, Parkinson C, Ledermann J, Williams S, Banerjee S, Cosin J, Hoffman J, Penson R, Plante M, Covens A, Sonke G, Joly F, Floquet A, Banerjee S, Hirte H, Amit A, Park-Simon T-W, Matsumoto K, Tjulandin S, Kim JH, Gladieff L, Sabbatini R, O'Malley D, Timmins P, Kredentser D, Laínez Milagro N, Barretina Ginesta MP, Tibau Martorell A, Gómez de Liaño Lista A, Ojeda González B, Mileshkin L, Mandai M, Boere I, Ottevanger P, Nam J-H, Filho E, Hamizi S, Cognetti F, Warshal D, Dickson-Michelson E, Kamelle S, McKenzie N, Rodriguez G, Armstrong D, Chalas E, Celano P, Behbakht K, Davidson S, Welch S, Helpman L, Fishman A, Bruchim I, Sikorska M, Słowińska A, Rogowski W, Bidziński M, Śpiewankiewicz B, Casado Herraez A, Mendiola Fernández C, Gropp-Meier M, Saito T, Takehara K, Enomoto T, Watari H, Choi CH, Kim B-G, Kim JW, Hegg R, Vergote I: Olaparib tablets as maintenance therapy in patients with platinum-sensitive, relapsed ovarian cancer and a BRCA1/2 mutation (SOLO2/ENGOT-Ov21): a double-blind, randomised, placebo-controlled, phase 3 trial. The Lancet Oncology 2017, 18:1274-84.
[8] Penson RT, Valencia RV, Cibula D, Colombo N, Leath CA, 3rd, Bidzinski M, Kim JW, Nam JH, Madry R, Hernandez C, Mora PAR, Ryu SY, Milenkova T, Lowe ES, Barker L, Scambia G: Olaparib Versus Nonplatinum Chemotherapy in Patients With Platinum-Sensitive Relapsed Ovarian Cancer and a Germline BRCA1/2 Mutation (SOLO3): A Randomized Phase III Trial. J Clin Oncol 2020, 38:1164-74.
[9] Gonzalez-Martin A, Pothuri B, Vergote I, DePont Christensen R, Graybill W, Mirza MR, McCormick C, Lorusso D, Hoskins P, Freyer G, Baumann K, Jardon K, Redondo A, Moore RG, Vulsteke C, O'Cearbhaill RE, Lund B, Backes F, Barretina-Ginesta P, Haggerty AF, Rubio-Perez MJ, Shahin MS, Mangili G, Bradley WH, Bruchim I, Sun K, Malinowska IA, Li Y, Gupta D, Monk BJ, Investigators PE-OG-: Niraparib in Patients with Newly Diagnosed Advanced Ovarian Cancer. N Engl J Med 2019, 381:2391-402.

[10] Coleman RL, Fleming GF, Brady MF, Swisher EM, Steffensen KD, Friedlander M, Okamoto A, Moore KN, Efrat Ben-Baruch N, Werner TL, Cloven NG, Oaknin A, DiSilvestro PA, Morgan MA, Nam J-H, Leath CA, Nicum S, Hagemann AR, Littell RD, Cella D, Baron-Hay S, Garcia-Donas J, Mizuno M, Bell-McGuinn K, Sullivan DM, Bach BA, Bhattacharya S, Ratajczak CK, Ansell PJ, Dinh MH, Aghajanian C, Bookman MA: Veliparib with First-Line Chemotherapy and as Maintenance Therapy in Ovarian Cancer. New England Journal of Medicine 2019, 381:2403-15.
[11] Gunti S, Hoke ATK, Vu KP, London NR, Jr.: Organoid and Spheroid Tumor Models: Techniques and Applications. Cancers (Basel) 2021, 13.
[12] Yang J, Huang S, Cheng S, Jin Y, Zhang N, Wang Y: Application of Ovarian Cancer Organoids in Precision Medicine: Key Challenges and Current Opportunities. Front Cell Dev Biol 2021, 9:701429.
[13] Heredia-Soto V, Redondo A, Berjon A, Miguel-Martin M, Diaz E, Crespo R, Hernandez A, Yebenes L, Gallego A, Feliu J, Hardisson D, Mendiola M: High-throughput 3-dimensional culture of epithelial ovarian cancer cells as preclinical model of disease. Oncotarget 2018, 9:21893-903.
[14] Millard M, Yakavets I, Zorin V, Kulmukhamedova A, Marchal S, Bezdetnaya L: Drug delivery to solid tumors: the predictive value of the multicellular tumor spheroid model for nanomedicine screening. Int J Nanomedicine 2017, 12:7993-8007.
[15] Tomas E, Shepherd TG: Insights into high-grade serous carcinoma pathobiology using three-dimensional culture model systems. Journal of Ovarian Research 2023, 16:70.
[16] Sainz-Arnal P, Pla-Palacín I, Sánchez-Romero N, Almeida M, Morini S, Solanas E, Lue A, Serrano-Aulló T, Baptista PM: Chapter 62 - Bioengineering of Liver Tissue. Principles of Regenerative Medicine (Third Edition). Edited by Atala A, Lanza R, Mikos AG, Nerem R. Boston: Academic Press, 2019. pp. 1101-13.
[17] Melissaridou S, Wiechec E, Magan M, Jain MV, Chung MK, Farnebo L, Roberg K: The effect of 2D and 3D cell cultures on treatment response, EMT profile and stem cell features in head and neck cancer. Cancer Cell Int 2019, 19:16.
[18] Goyeneche A, Lisio M-A, Fu L, Srinivasan R, Valdez Capuccino J, Gao Z-h, Telleria C: The Capacity of High-Grade Serous Ovarian Cancer Cells to Form Multicellular Structures Spontaneously along Disease Progression Correlates with Their Orthotopic Tumorigenicity in Immunosuppressed Mice. Cancers 2020, 12:699.
[19] Sakai W, Swisher EM, Jacquemont C, Chandramohan KV, Couch FJ, Langdon SP, Wurz K, Higgins J, Villegas E, Taniguchi T: Functional restoration of BRCA2 protein by secondary BRCA2 mutations in BRCA2-mutated ovarian carcinoma. Cancer Res 2009, 69:6381-6.
[20] Cooke SL, Ng CK, Melnyk N, Garcia MJ, Hardcastle T, Temple J, Langdon S, Huntsman D, Brenton JD: Genomic analysis of genetic heterogeneity and evolution in high-grade serous ovarian carcinoma. Oncogene 2010, 29:4905-13.
[21] Abdalbari FH, Goyeneche AA, Martinez-Jaramillo E, Sabri S, Telleria CM: Abstract 1014: Repurposing the anti-rheumatic gold compound auranofin for high-grade serous ovarian cancer therapy. Cancer Research 2021, 81:1014-.
[22] Abdalbari FH, Telleria CM: The gold complex auranofin: new perspectives for cancer therapy. Discov Oncol 2021, 12:42.
[23] Świerczewska M, Sterzyńska K, Ruciński M, Andrzejewska M, Nowicki M, Januchowski R: The response and resistance to drugs in ovarian cancer cell lines in 2D monolayers and 3D spheroids. Biomedicine & Pharmacotherapy 2023, 165:115152.

[24] Mon MT, Yodkeeree S, Punfa W, Umsumarng S, Lekwanavijit S, Siriaunkgul S, Suprasert P, Limtrakul P: Relationships of Ex-Vivo Drug Resistance Assay and Cytokine Production with Clinicopathological Features in the Primary Cell Culture of Thai Ovarian and Fallopian Tube Cancer Patients. Asian Pac J Cancer Prev 2017, 18:3063-71.
[25] Liston DR, Davis M: Clinically Relevant Concentrations of Anticancer Drugs: A Guide for Nonclinical Studies. Clin Cancer Res 2017, 23:3489-98.
[26] Langdon SP, Lawrie SS, Hay FG, Hawkes MM, McDonald A, Hayward IP, Schol DJ, Hilgers J, Leonard RC, Smyth JF: Characterization and properties of nine human ovarian adenocarcinoma cell lines. Cancer Res 1988, 48:6166-72.
[27] Mitrakas AG, Tsolou A, Didaskalou S, Karkaletsou L, Efstathiou C, Eftalitsidis E, Marmanis K, Koffa M: Applications and Advances of Multicellular Tumor Spheroids: Challenges in Their Development and Analysis. International Journal of Molecular Sciences 2023, 24:6949.
[28] Muguruma M, Teraoka S, Miyahara K, Ueda A, Asaoka M, Okazaki M, Kawate T, Kuroda M, Miyagi Y, Ishikawa T: Differences in drug sensitivity between two-dimensional and three-dimensional culture systems in triple-negative breast cancer cell lines. Biochem Biophys Res Commun 2020, 533:268-74.
[29] Jensen C, Teng Y: Is It Time to Start Transitioning From 2D to 3D Cell Culture? Front Mol Biosci 2020, 7:33.
[30] Ciucci A, Buttarelli M, Fagotti A, Scambia G, Gallo D: Preclinical models of epithelial ovarian cancer: practical considerations and challenges for a meaningful application. Cellular and Molecular Life Sciences 2022, 79:364.
[31] Fiorillo M, Ozsvari B, Sotgia F, Lisanti MP: High ATP Production Fuels Cancer Drug Resistance and Metastasis: Implications for Mitochondrial ATP Depletion Therapy. Front Oncol 2021, 11:740720.
[32] Ritch SJ, Noman ASM, Goyeneche AA, Telleria CM: The metastatic capacity of high-grade serous ovarian cancer cells changes along disease progression: inhibition by mifepristone. Cancer Cell International 2022, 22:397.

2.9 List of Figures

A)

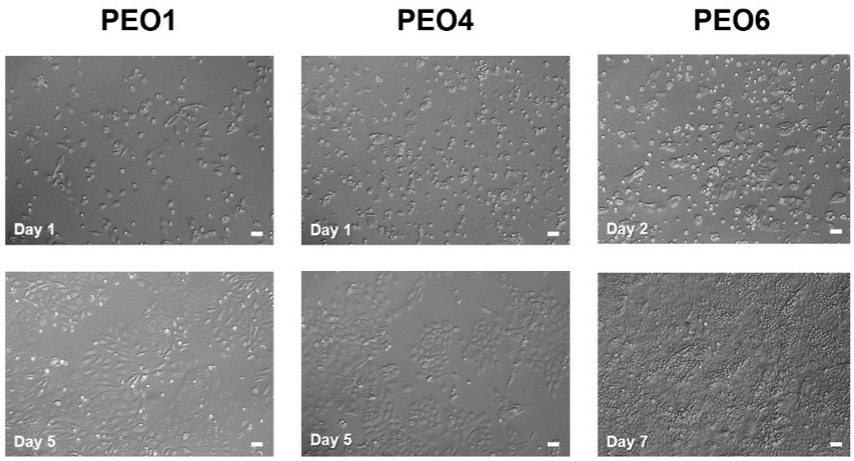
PEO1
PEO4
PEO6
Day 1
Day 1
Day 2
Day 5
Day 5
Day 7

B)

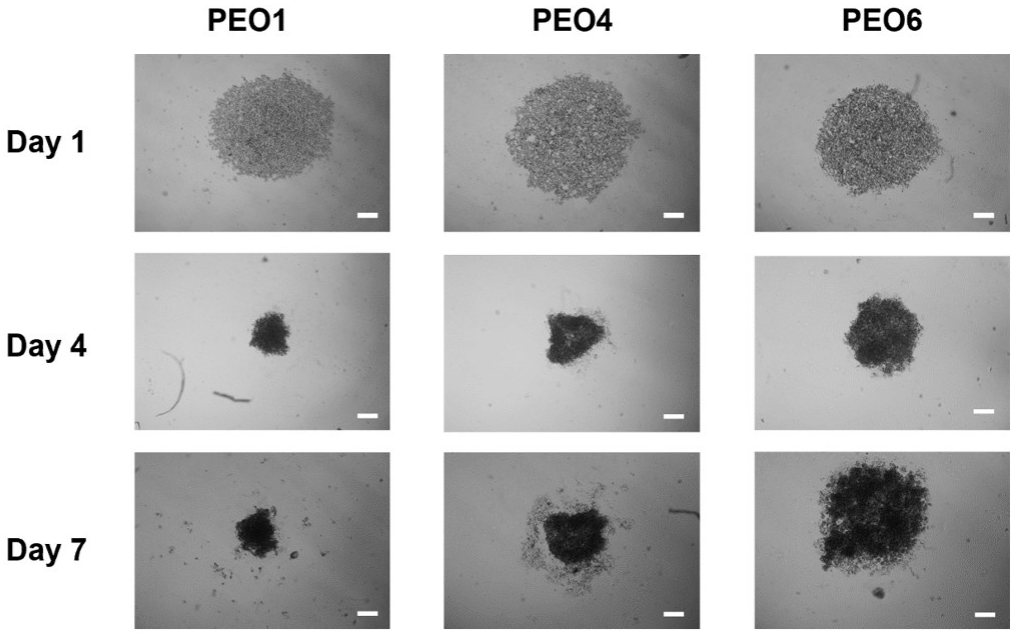
PEO1
PEO4
PEO6
Day 1
Day 4
Day 7

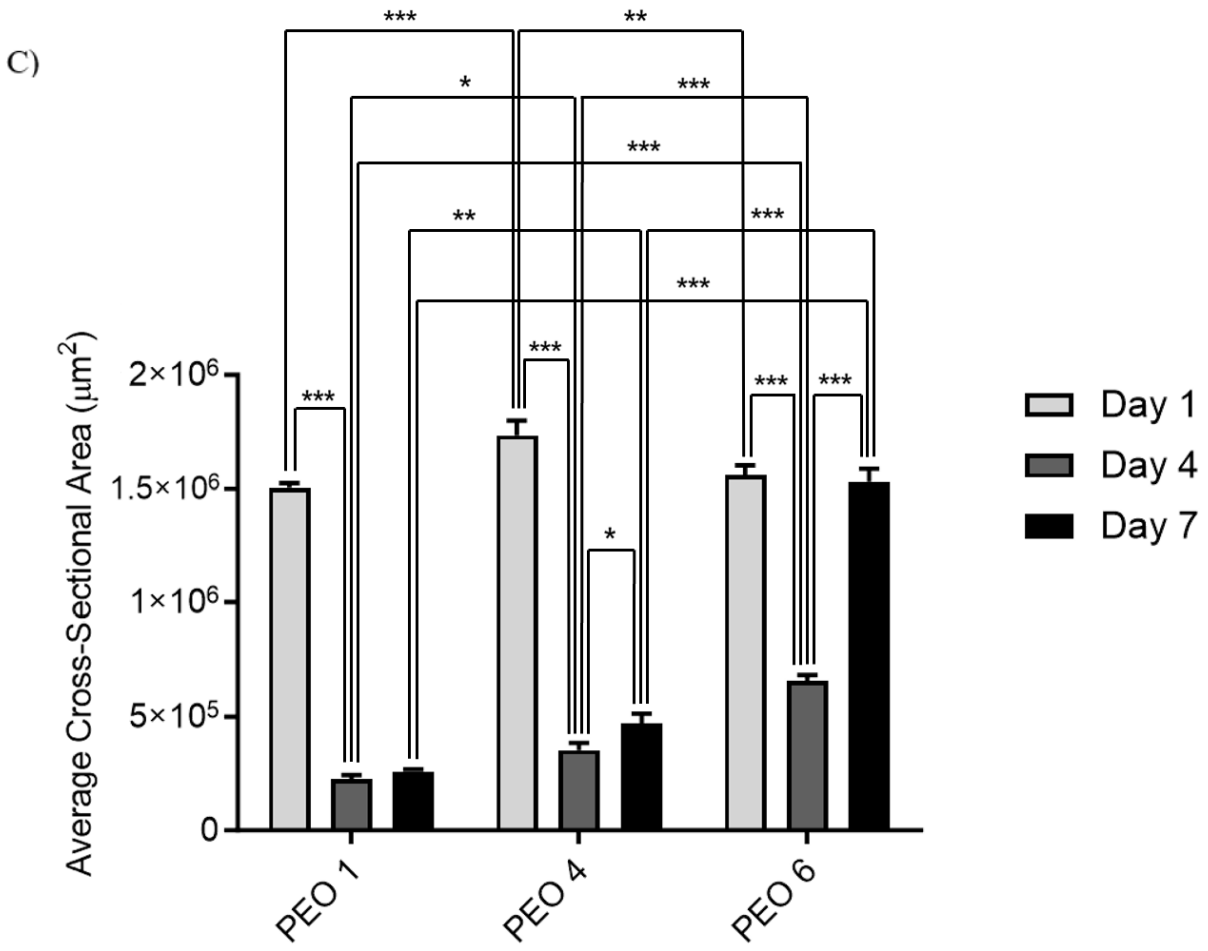

Figure 2.1. Morphological comparison of PEO1, PEO4 and PEO6 cells in 2D and 3D cultures. A) PEO1 and PEO4 cells one and five days after plating in cell culture-treated flat-bottom T75 flasks and PEO6 cells two- and seven-days following plating. Scale bars = 50 μm. B) PEO1, PEO4 and PEO6 cells one, four and seven days after plating in 96-well ULAPs. Scale bars = 200 μm. C) Average cross-sectional area of PEO1, PEO4 and PEO6 spheroidal structures one, four and seven days after plating in ULAPs.

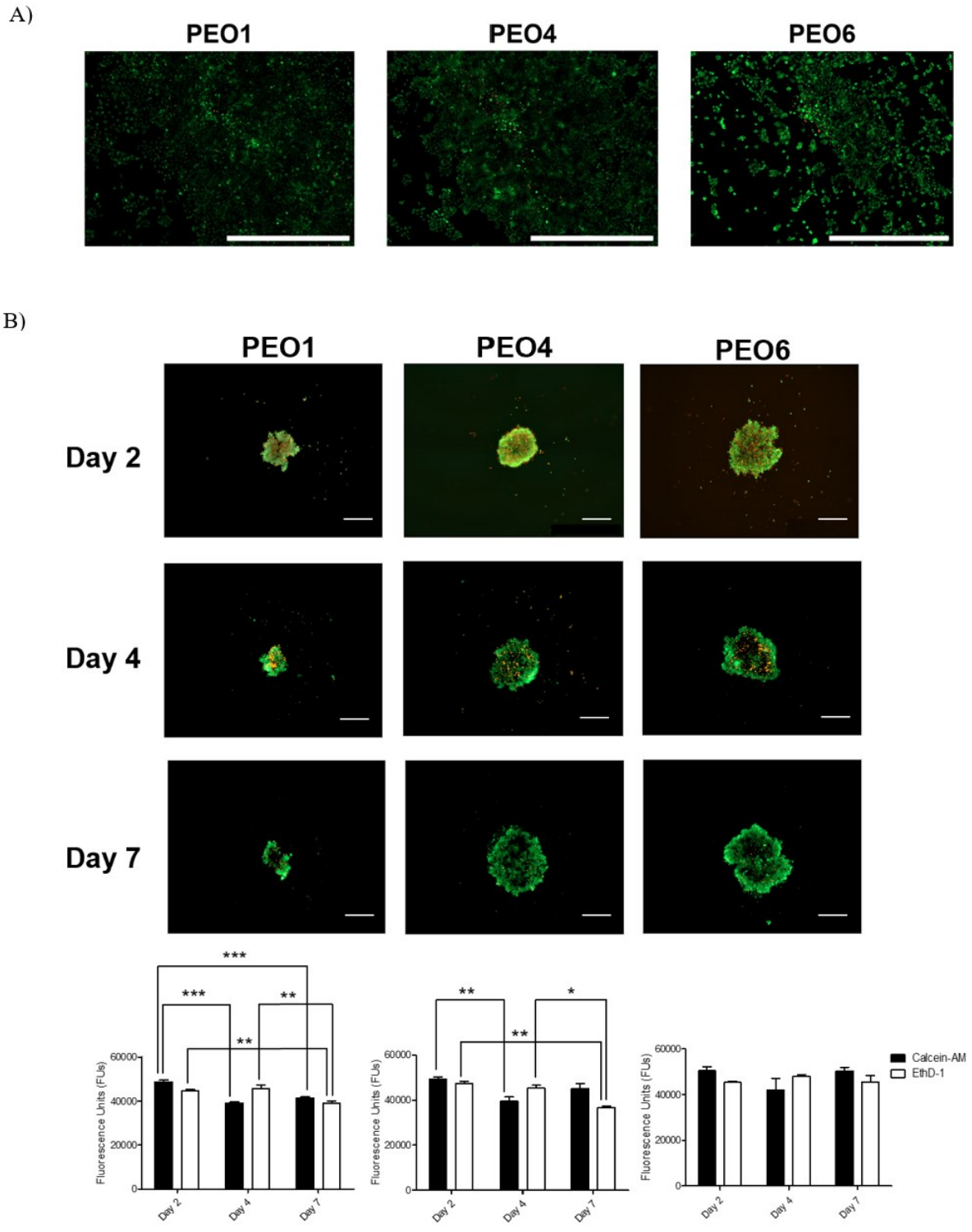

Figure 2.2. Comparison in terms of viability of PEO1, PEO4 and PEO6 cells in 2D and 3D cultures. A) Live/Dead 2D results of PEO1, PEO4 and PEO6 cells four days after plating in 96-

well flat-bottom plates. Green fluorescence indicates live cells and red fluorescence indicates dead cells. Scale bars = 1000 µm. B) Live/Dead 3D results of PEO1, PEO4 and PEO6 cells two, four and seven days after plating in 96-well ULAPs. Green fluorescence indicates live cells and red fluorescence indicates dead cells. Green (Calcein-AM) and red (EthD-1) fluorescence units indicative of levels of live and dead cells respectively are presented in the graphs. Scale bars = 500 µm.

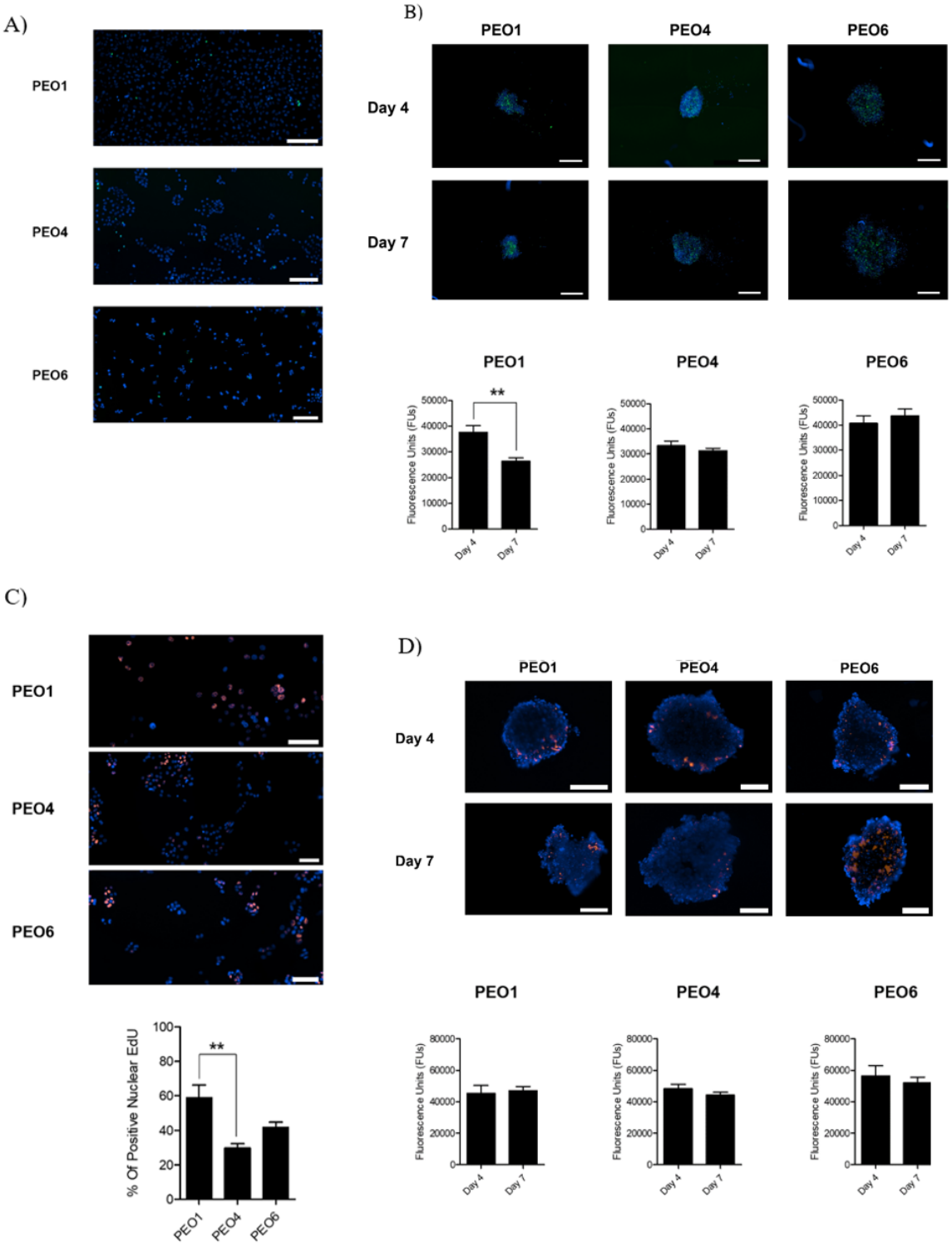
A)
PEO1
PEO4
PEO6
B)
PEO1
PEO4
PEO6
Day 4
Day 7
PEO1
PEO4
PEO6
**
Fluorescence Units (FUs)
50000
40000
30000
20000
10000
0
Day 4
Day 7
C)
PEO1
PEO4
PEO6
% Of Positive Nuclear EdU
100
80
60
40
20
0
**
PEO1
PEO4
PEO6
D)
PEO1
PEO4
PEO6
Day 4
Day 7
PEO1
PEO4
PEO6
Fluorescence Units (FUs)
80000
60000
40000
20000
0
Day 4
Day 7

Figure 2.3. Comparison in terms of cell death and proliferation of PEO1, PEO4 and PEO6 cells in 2D and 3D cultures. A) CellEvent Caspase-3/7 assay 2D results in PEO1, PEO4 and PEO6 cells four days after plating in 96-well flat-bottom cell culture plates. Green fluorescence was used as the apoptosis indicator and blue fluorescence for nuclear staining. Scale bars = 200 μm. B) Caspase-3/7 assay 3D results in PEO1, PEO4 and PEO6 cells four and seven days after plating in 96-well ULAPs. Scale bars = 500 μm. The graphs represent the CellEvent Caspase-3/7 assay green fluorescence units results indicative of apoptosis levels for PEO1, PEO4 and PEO6 cells four and seven days after plating in 96-well ULAPs. ns means $p > 0.05$ and ** means $p < 0.01$. C) Click-iT 5-Ethynyl-2′-deoxyuridine (EdU) Cell Proliferation assay 2D results of PEO1, PEO4 and PEO6 cells four days after plating in 96-well flat-bottom cell culture plates. Red fluorescence was used as the proliferation indicator and blue fluorescence for nuclear staining. Therefore, a purple color (i.e., a superposition of red and blue fluorescence) indicates proliferating cells. The percentages of positive nuclear EdU indicative of DNA synthesis levels of PEO1, PEO4 and PEO6 cells four days after plating in 96-well flat-bottom cell culture plates are shown in the graph. ns means $p > 0.05$ and ** means $p < 0.01$. Scale bars = 100 μm. D) Cell Proliferation assay 3D results of PEO1, PEO4 and PEO6 cells four and seven days after plating in 96-well ULAPs. Scale bars = 200 μm. The graphs represent the Cell Proliferation assay red fluorescence units results indicative of proliferation levels of PEO1, PEO4 and PEO6 cells four and seven days after plating in 96-well ULAPs. ns means $p > 0.05$.

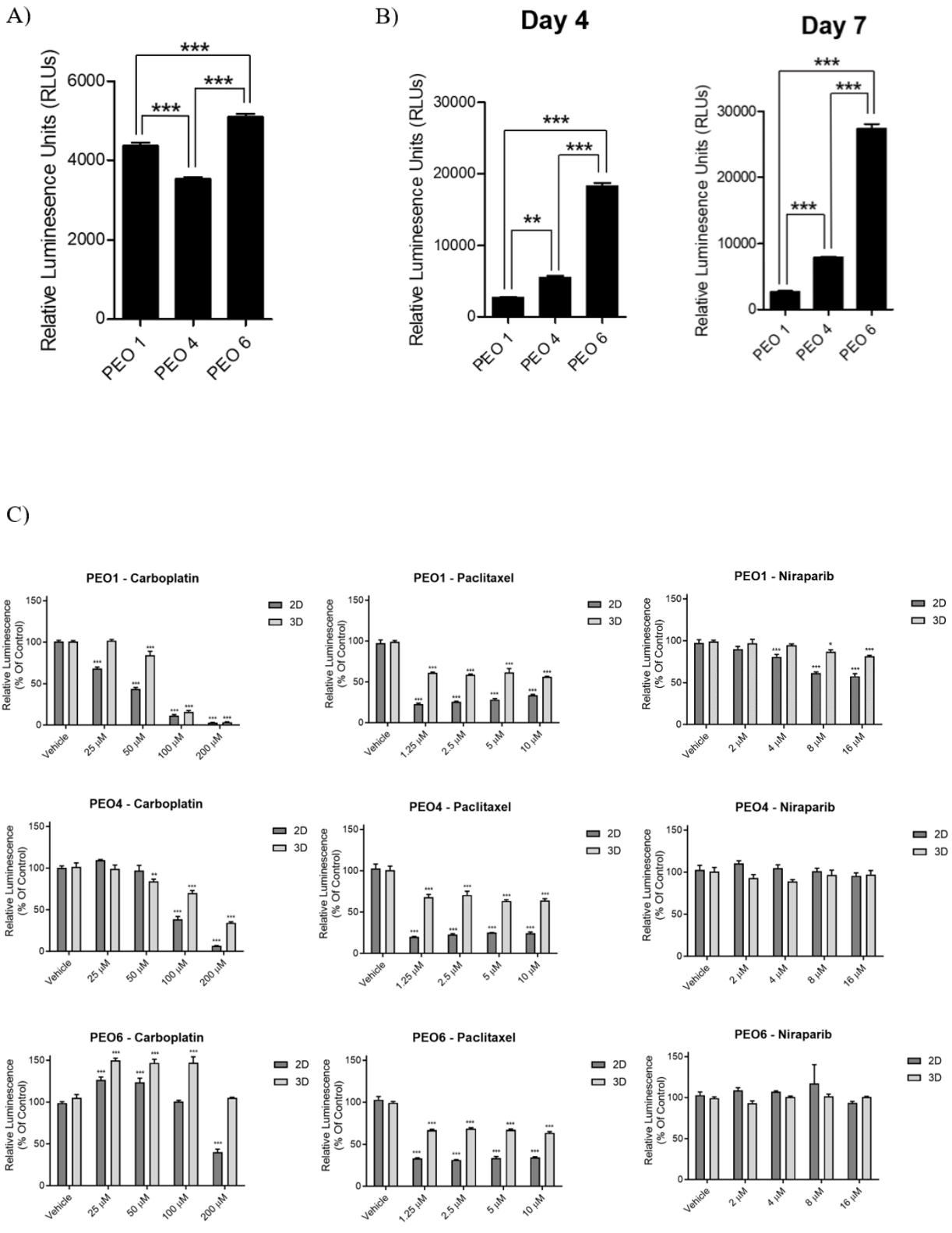
A)
Relative Luminesence Units (RLUs)
6000
4000
2000
0
***
***
***
PEO 1
PEO 4
PEO 6
B)
Day 4
Relative Luminesence Units (RLUs)
30000
20000
10000
0
**
***
***
PEO 1
PEO 4
PEO 6
Day 7
Relative Luminesence Units (RLUs)
30000
20000
10000
0
***
***
***
PEO 1
PEO 4
PEO 6
C)
PEO1 - Carboplatin
PEO1 - Paclitaxel
PEO1 - Niraparib
PEO4 - Carboplatin
PEO4 - Paclitaxel
PEO4 - Niraparib
PEO6 - Carboplatin
PEO6 - Paclitaxel
PEO6 - Niraparib
Relative Luminescence (% Of Control)
2D
3D
Vehicle
25 µM
50 µM
100 µM
200 µM
1.25 µM
2.5 µM
5 µM
10 µM
2 µM
4 µM
8 µM
16 µM

Figure 2.4. Comparison in terms of metabolic activity and drug response of PEO1, PEO4 and PEO6 cells in 2D and 3D cultures. A) PEO1, PEO4 and PEO6 cells 2D ATP production levels reflected by the generated luminescence levels 24 hours after plating in 96-well flat-bottom cell culture plates. *** means $p < 0.001$. B) PEO1, PEO4 and PEO6 cells ATP production levels reflected by the generated luminescence levels four and seven days after plating in 96-well ULAPs. ** means $p < 0.01$ and *** means $p < 0.001$. C) PEO1, PEO4 and PEO6 cells' drug response to carboplatin, paclitaxel and niraparib through ATP production levels in flat-bottom plates and ultra-low attachment round-bottom plates. ns means $p > 0.05$, * means $p < 0.05$, ** means $p < 0.01$ and *** means $p < 0.001$.

2.10 Supplementary Figures

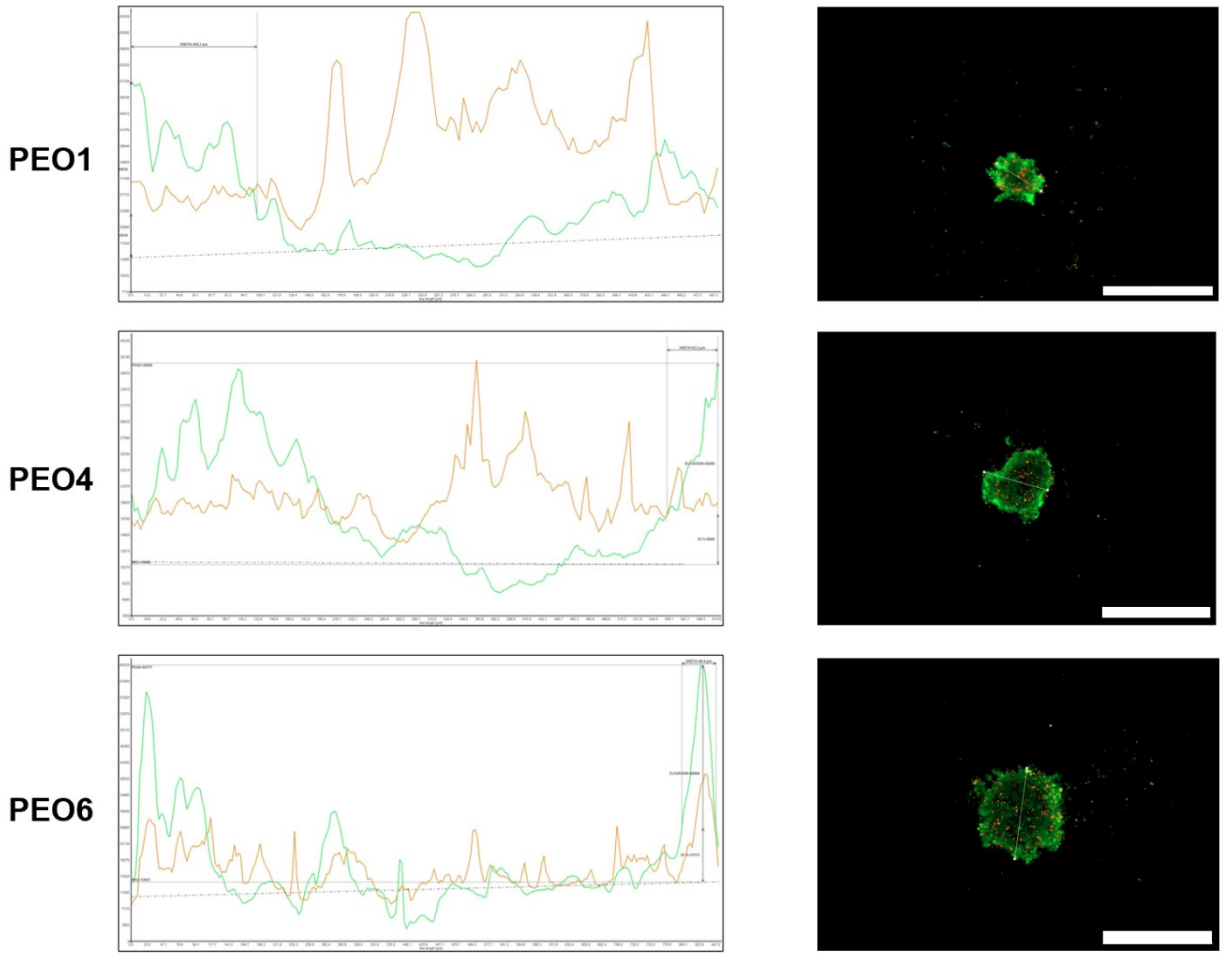

Figure S2.1. Green and red fluorescence intensities along the drawn white line passing through the spheroidal structures of PEO1, PEO4 and PEO6 cells 4 days after plating in 96-well ULAPs. Green fluorescence indicates live cells and red fluorescence indicates dead cells. Scale bars = 1000 μm.

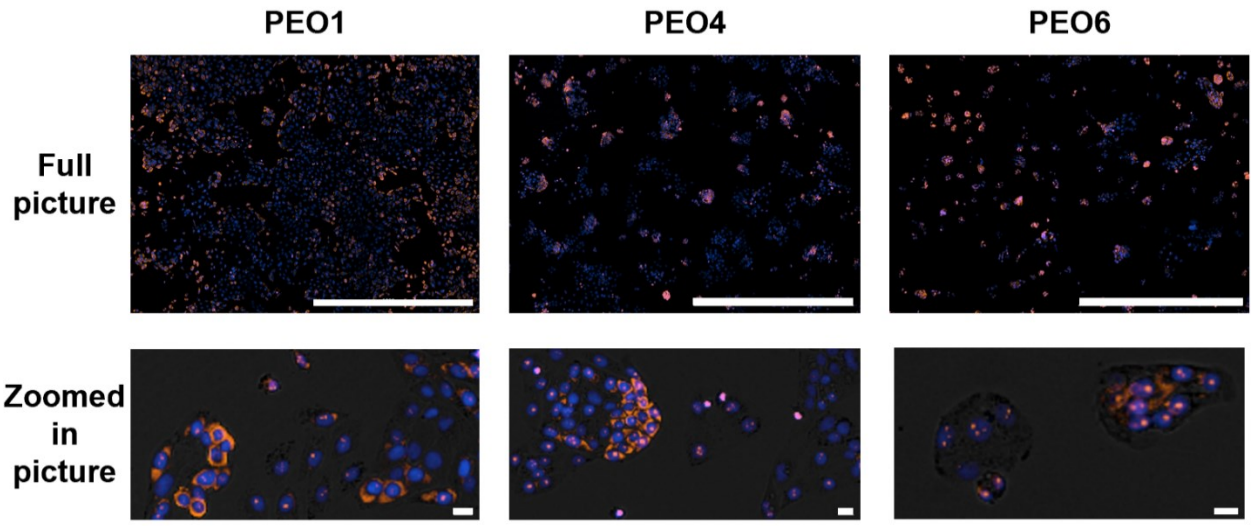

Figure S2.2. Live/Dead results of fixed PEO1, PEO4 and PEO6 cells four and seven days after plating in 96-well flat-bottom cell culture plates. Red fluorescence was used as the dead cell indicator and blue fluorescence for nuclear staining. Therefore, a purple color (i.e., a superposition of red and blue fluorescence) provides an accurate representation of dead cells. Scale bars in full pictures = 1000 µm and scale bars in zoomed in pictures = 20 µm.

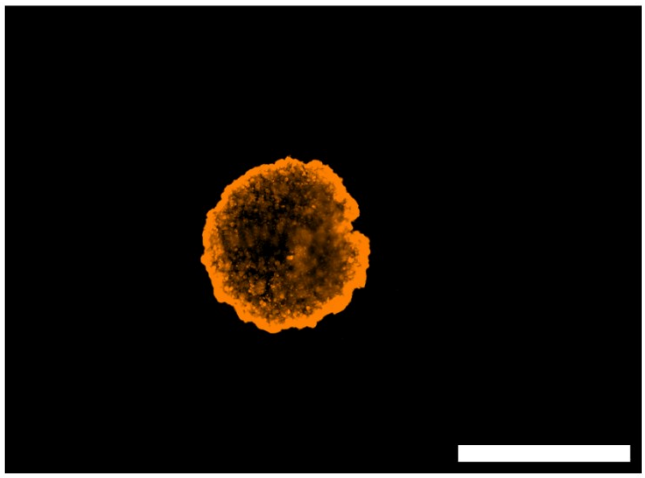

Figure S2.3. Live/Dead results of fixed PEO6 cells four days after plating in 96-well ULAPs. Green fluorescence indicates live cells, red fluorescence indicates dead cells. Scale bar = 1000 µm.

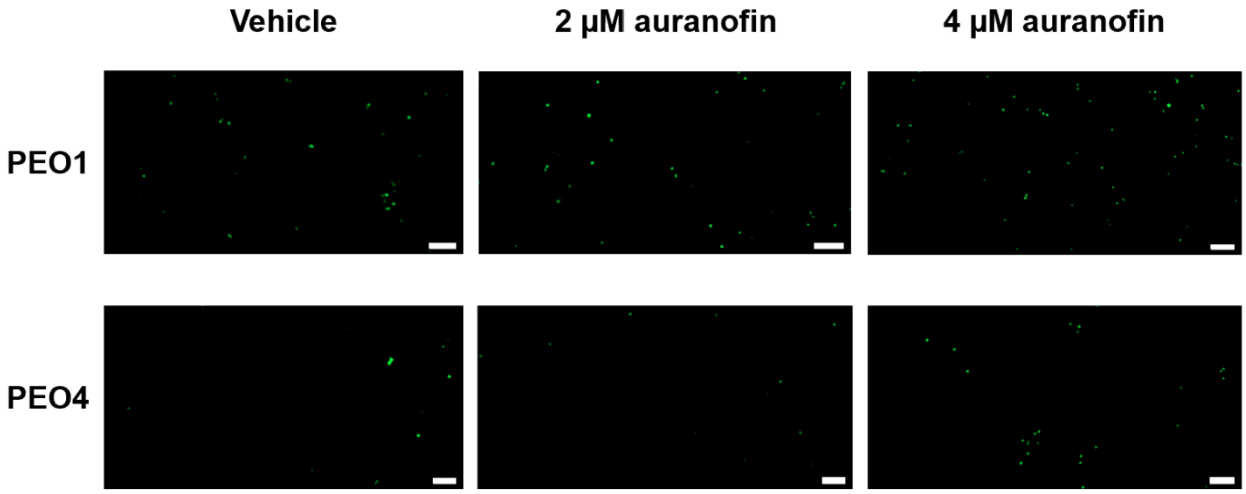

Figure S2.4. CellEvent Caspase-3/7 assay results in PEO1 and PEO4 cells exposed to the Caspase-3/7 Green Reagent and DMSO (i.e., the vehicle group), to the Caspase-3/7 Green Reagent, DMSO and 2 µM of auranofin and to the Caspase-3/7 Green Reagent, DMSO and 4 µM of auranofin in 96-well flat-bottom cell culture plates. Green fluorescence was used as the apoptosis indicator. Scale bars = 100 µm.

Chapter 3.

Preliminary Work on Patient-Derived Organoids

3.1 Patient-Derived Organoids

Another 3D model, which is gaining in popularity, is the organoid model. The organoid model, which contains a more complex diversity of cell types, constitutes a growing and promising area of research as organoids have been shown to partially resemble the organ in structure and function and histologically and genetically resemblance the tumor they are derived from[152-154]. However, organoids lack immune cells and blood vessels and are a costly model to generate[154, 155]. Therefore, researchers need to continue to push the boundaries of these current models for in-vitro work in the future[149].

Organoids have thus far been successfully generated from intestinal tissue as this was the first tissue-derived organoid type established and for multiple cancer types such as head and neck cancer, prostate cancer, stomach cancer, liver cancer, pancreatic cancer, breast cancer, etc. [162-165] Ovarian cancer organoids have also been successfully established in several laboratories[152, 157, 166]. However, different groups use different protocols and media compositions with different reported success rates.

Putting in place the appropriate series of steps for organoid maintenance and establishing the optimal media composition for stable long-term cultivation are required steps for an organoid development platform. Another part of the project focused on setting up a patient-derived organoids (PDOs) platform for ovarian cancer as another preclinical 3D model. Woking with spheroidal structures formed in ULAPs and with PDOs are two distinct processes. In ULAPs, already developed cell lines were grown in an anchorage independent manner without addition of any extracellular matrix. PDOs generation is based on the adaptation, in an anchorage dependent manner, of fresh tumor samples into Matrigel (i.e., serving as a matrix) and a defined media which promote stemness capacities in the tumor cells that adapt to these conditions. With regards to drug

testing, the existing work with 3D cell lines provides a platform to test and validate our drug-dosing protocol. While it has been established that there is variability in therapeutic response across models (2D monolayers, 3D spheroids, 3D ex-vivo tumors, mouse xenograft models), the 3D cell culture work would allow us to target potentially relevant concentration ranges for PDOs[146, 167]. The drug testing results obtained provide starting concentration ranges and confidence that ex-vivo drug response correlate with clinical response. We have established that cells in ULAPs are less sensitive to the drugs than cells in flat-bottom plates, and thus, that the more complex a system is, the less sensitive it is to drugs. Therefore, we hypothesize that higher drug concentrations than the ones we used will potentially be required in PDOs to obtain a clinically relevant response as PDOs are a more complex system than spheroidal structures formed in ULAPs.

A protocol and media composition unique to our group to generate PDOs for ovarian cancer have been developed. Protocols from different groups (the laboratory of Dr. Sarah Hill, the laboratory of Dr. Lorenzo Ferri and from the published protocol of Dr. Nina Maenhoudt and Dr. Hugo Vankelecom) were compared to establish the one to be used for PDOs generation[152, 168, 169]. A protocol adapted from the one Dr. Sarah Hill uses was developed and used for the first surgical samples processed (Protocol 4.1 in Appendix)[152]. Media compositions from different laboratories (the laboratory of Dr. Sarah Hill, the laboratory of Dr. Lorenzo Ferri and from the published protocol of Dr. Nina Maenhoudt and Dr. Hugo Vankelecom) were also compared to determine the best combination to use[152, 168, 169]. A study found that BMP suppression by Noggin and high-Wnt signalling activate the Wnt pathway leading to growth arrest of organoids[170]. Based on the results of the study suggesting that growth conditions needed to achieve stable, long-term expansion of HGSC organoids from primary tumor deposits require low-Wnt and no Noggin, we decided to not

add Wnt and Noggin in the media. The components forming the media used are listed in the "Suggested Plan" column in Table 4.1 in the Appendix and the media preparation steps, adapted from the ones Dr. Sarah Hill uses, are listed in Protocol 4.2 in the Appendix[152].

The laboratory of Dr. Lorenzo Ferri has successfully created 3D bioprinted models of gastric adenocarcinoma cells and has demonstrated that drug responses of these models recapitulate in-vivo patient drug response[171]. Julie Bérubé, who is part of the laboratory of Dr. Lorenzo Ferri, generously shared her knowledge and expertise on organoids development with us. I had the opportunity to watch her process fresh ovarian cancer samples and perform regular organoids maintenance steps. PDOs derived from a biopsy and a resection sample were successfully generated in the Ferri lab allowing me to gain experience on organoid generation and management. The biopsy-derived PDOs stopped growing at the second passage and the resection-derived PDOs stopped growing at the third passage. A possible explanation for the growth cessation could be the use of Wnt and Noggin in the media as seen in Table 4.1 in Appendix, which was not advised to be used in Hoffmann *et al*'s paper[170]. A picture of a PDO created in only 6 days from a HGSC patient (Patient A) with both homologous recombination deficiency and an innate resistance to PARPis can be found in Figure 3.1 below. A picture of PDOs created in only 5 days from a resection sample from Patient B can be found in Figure 3.2 below. PDOs media change was performed twice per week and passaging was performed every seven to ten days depending on the growth of the organoids.

Patient A is 56-year-old patient with stage IVB tubo-ovarian high-grade serous carcinoma. The patient is homologous recombination deficiency positive and *BRCA* negative. She presented with frequent abdominal bloating symptoms, new hot flash symptoms since menopause at 50 years old, a palpable umbilical nodule, right inguinal "pinch" discomfort, bladder/abdominal pressure and

frequent urination. CT scan was performed revealing a large pelvic mass of tubo-ovarian origin. Distant metastases were also highly suspected. CA125 levels were significantly elevated at 1,222 U/mL. An omental biopsy and immunohistochemistry findings were compatible with a tubo-ovarian high-grade serous carcinoma. Given the extent of disease, it was then recommended to proceed with neoadjuvant chemotherapy and she was found to be eligible for the OPAL-C clinical trial. The patient received one cycle of carboplatin/paclitaxel combination therapy. The overall treatment was well tolerated and no symptoms were found during treatment. The patient was then randomized to arm B where she received three cycles of neoadjuvant niraparib. Unfortunately, imaging demonstrated progression of disease (i.e., "unexpected non-responder" given patient's homologous recombination deficiency status), the patient came off the clinical trial. The patient had another omental biopsy done which was used for PDOs generation. Afterwards, the patient received three additional cycles of neoadjuvant carboplatin/paclitaxel. CT scans showed decreased disease burden. The patient then underwent interval debulking surgery after which pathology revealed high-grade serous carcinoma of the left fallopian tube involving bilateral ovaries. The patient's CA125 levels were 180 U/mL compared to 1,200 U/mL when the patient came off the clinical trial and more than 1,600 U/mL at diagnosis. It was then recommended that the patient continues adjuvant carboplatin/paclitaxel and may need more than six cycles.

Patient B is a 40-year-old pre-menopausal patient with stage IIIC2 high grade endometrioid ovarian cancer. Initially, the patient reported abdominal pain and bloating two years ago. All investigations were negative at that time. However, the abdominal pain worsened, and the patient began experiencing heavy menstrual bleeding, and thus, was assessed by gynecology. Ultrasound showed an endometrial mass. The patient underwent a hysteroscopy after which pathology revealed grade 1 endometrioid adenocarcinoma. The patient was referred to gynecology oncology

for management. The CA125 level of the patient at the first clinic visit was 130 U/mL. Surgery was strongly recommended because of the finding of either a metastatic endometrial cancer or a synchronous ovarian and endometrial cancer. The patient underwent a debulking surgery from which a resection sample was used for organoids generation (Fig.3.2). Final pathology confirmed stage IIIC2 high grade endometrioid ovarian cancer. The patient was approached to enroll a clinical trial and was randomized to the chemotherapy arm which receives carboplatin/paclitaxel for six cycles. The patient received one cycle and had a hypersensitivity reaction to paclitaxel on the first and second cycles. Patient was able to tolerate the rest of the infusions with pre-medications. The patient completed the six cycles of carboplatin/paclitaxel.

Morphologic and immunohistochemical analyses were also performed on the tumor sample of Patient A and the PDO generated from it (Fig.3.3). Comparison of the morphologic and immunohistochemical parameters of the PDO and parent tumor to assess their degree of similarity demonstrated concordance in staining of paired-box gene 8 (PAX8), the estrogen receptor (ER), p53, and Wilm's tumor gene 1 (WT1). Imaging for Patient A can be found in Figure 3.4 below.

So far, one fresh surgical sample from Patient C and one from Patient D have been used for organoid development by our group. The gynecology oncology team at the McGill University Health Center has helped with the sample collection and analysis. Dr. Alicia Goyeneche, Benjamin Forgie, Rewati Prakash and myself are part of the team that has contributed to the establishment of the organoid protocol used and the generation of the PDOs in the lab. Organoids are currently still growing and appear to be healthy, thereby suggesting that the protocol and media composition used might be effective for ovarian cancer PDO generation. The success we obtained with the organoids generated so far even after a first round of passaging may be a consequence of our

decision to not add Wnt and Noggin in the media as suggested by the findings of *Hoffmann et al*[170]. Pictures of PDOs generated by our group can be found in Figures 3.5 and 3.6 below.

Patient C is a 59-year-old patient with stage IIIC well-differentiated mucinous tubo-ovarian carcinoma. The patient started menopause at age 52, stopped smoking five or more years ago and has had no pregnancies. Initially, the patient had an incidental finding of left adnexal mass on CT during the work-up for a bariatric surgery. The patient was then referred for an ultrasound which showed a complex left adnexal mass around 13 cm in size, most likely consistent with mucinous or serous cystadenocarcinoma. The patient was then referred to gynecology oncology. The patient reported abdominal distension and discomfort as well as occasional urinary incontinence. The CA125 level of the patient at the first clinic visit was 459 U/mL. The patient underwent surgical debulking from which a sample was used for PDOs generation. The patient had disease remaining in the omentum and sigmoid colon. The tumor was found to be a stage 3C well-differentiated mucinous tubo-ovarian carcinoma with positive expression for PAX8 and negative expression for ER and WT1. P53 had a normal expression. Next-generation sequencing was requested by pathology. The patient experience post-operative ileus but otherwise recovered well. The CA125 level of the patient was later 142 U/mL and the patient has started their first cycle of adjuvant carboplatin/paclitaxel.

Patient D is a 50-year-old post-menopausal patient with stage IIIB high-grade serous tubo-ovarian carcinoma. The patient had a history of pelvic pain which was consulted for in the emergency room three years ago and an ultrasound at that time revealed a right ovarian cyst. The patient was then lost to follow-up and represented only in April 2023. An ultrasound was done and revealed that the cyst grew larger, and the tumor markers were elevated. The patient had an abdomen-pelvis CT and was then referred to gynecology oncology. The patient presented with

bilateral adnexal masses associated with a CA125 level at the first clinic visit of 7,921 U/mL. The patient was consented for primary debulking surgery and had a complete surgical resection to no visible residual disease. A tumor sample from the surgery was used for organoids generation. Pathology revealed that the diagnosis is bilateral tubo-ovarian high-grade serous carcinoma. Immunohistochemical tests showed tumor cells to be positive for WT1, PAX8 and ER. P53 had an abnormal (overexpression) pattern. The CA125 level at the first clinic visit post-surgery was 186 U/mL. The patient was recommended to begin adjuvant chemotherapy with six cycles of carboplatin/paclitaxel. The patient also consented for multi-gene panel testing and will do homologous recombination deficiency testing.

The long-term goal of this part of the project is to establish a workflow for the development of short-term HGSC PDOs that can be grown rapidly and tested with PARPis and other therapeutics to inform the optimal front-line treatment to use in each patient. Unique to this process to inform the personalization of front-line therapeutics for HGSC patients is the fact that PDOs will be generated to test drug efficacies for each individual patient. Tumor tissue will be obtained at two time points (untreated and at time of interval debulking surgery post-neoadjuvant therapy) (Fig.3.7). Organoids will be developed at both time points and validated by H&E and immunohistochemistry and compared to parent tumors. This will allow for correlation between clinical drug response and prediction from ex-vivo organoid experiments. Comparison between pre- and post-treated parent tumors and organoids will identify characteristics predictive of treatment response. The fidelity of organoids will be compared to parent tumors based on morphologic and immunohistochemical characteristics, and whole genome sequencing. Next Generation Sequencing allows for parallel sequencing to analyze numerous genes simultaneously in a single array with the potential to identify potentially targetable mutations to guide treatment[172,

[173]. The sequencing results would provide insight into signatures predictive of treatment response and differential profiles based on treatment received. This may clarify mechanisms associated with both platinum and PARPi resistance as well as potential signatures of unexpected responders to PARPi. If PDOs mirror the tumor they are derived from morphologically and cytologically and exhibit a treatment response correlated with that observed clinically, this will allow for patient specific analysis (i.e., precision medicine) of the most suitable frontline treatments within a short time period compatible with decision-making and has potential to improve prognosis of patients.

In addition, it would not only allow for the treatment of organoids with different drugs to determine which drug most effectively stops the cancer growth in the organoid from each patient, but also for testing of newer drugs that are under evaluation for ovarian cancer[98].

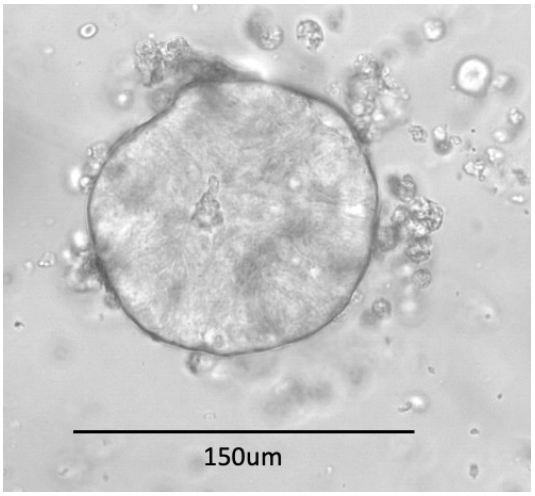

Figure 3.1. A PDO derived from a biopsy of Patient A, whose disease progressed after three cycles of PARPi in the upfront setting. The PDO shown is six days after sample collection. The picture was taken at 20x magnification. Fresh tumor specimen obtained at time of biopsy was dissociated mechanically and enzymatically, then embedded into single-cell suspension in Matrigel. PDOs were grown in ovarian-specific medium at 37 °C, 5% CO2 and 95% relative humidity.

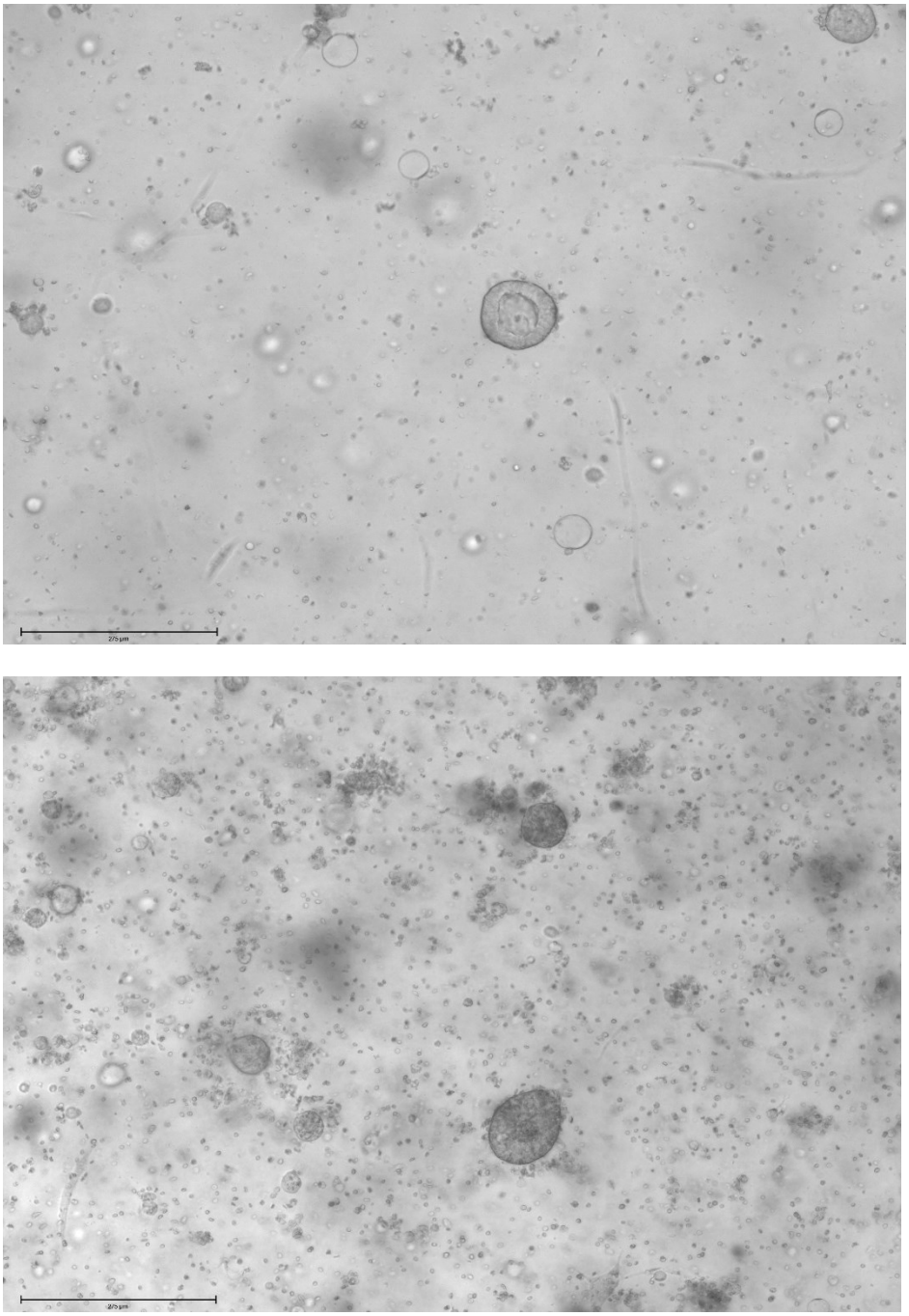

Figure 3.2. PDOs derived from a resection sample from Patient B. The PDOs shown are from five days after sample collection. The pictures were taken at 10x magnification. Fresh tumor specimen obtained at time of resection was dissociated mechanically and enzymatically, then embedded into single-cell suspension in Matrigel. PDOs were grown in ovarian-specific medium at 37 °C, 5% CO2 and 95% relative humidity.

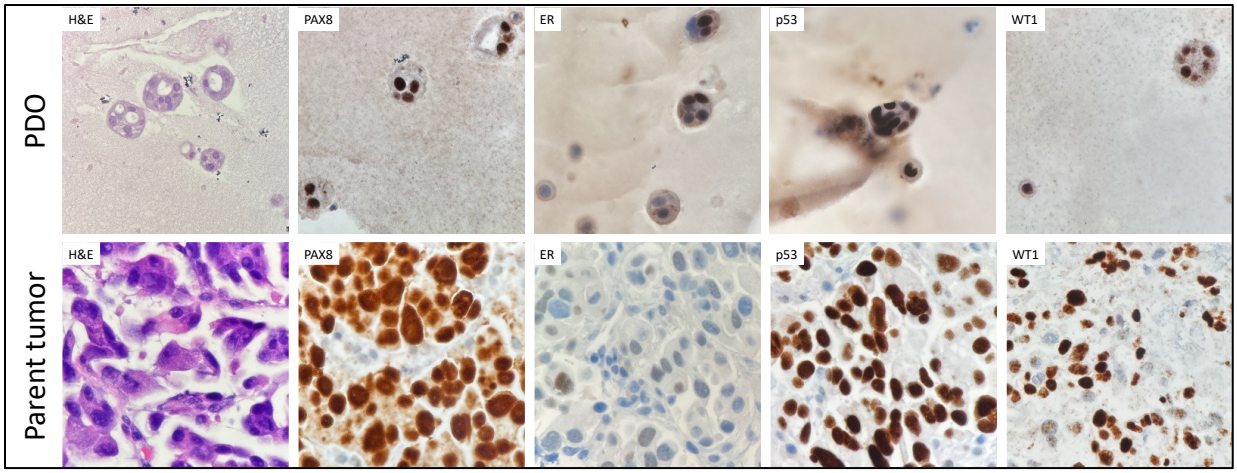

Figure 3.3. H&E and immunohistochemistry of Patient A who progressed on PARPi. Top and bottom rows show organoid and parent tumor respectively, demonstrating concordance in staining of PAX8, ER, p53, and WT1.

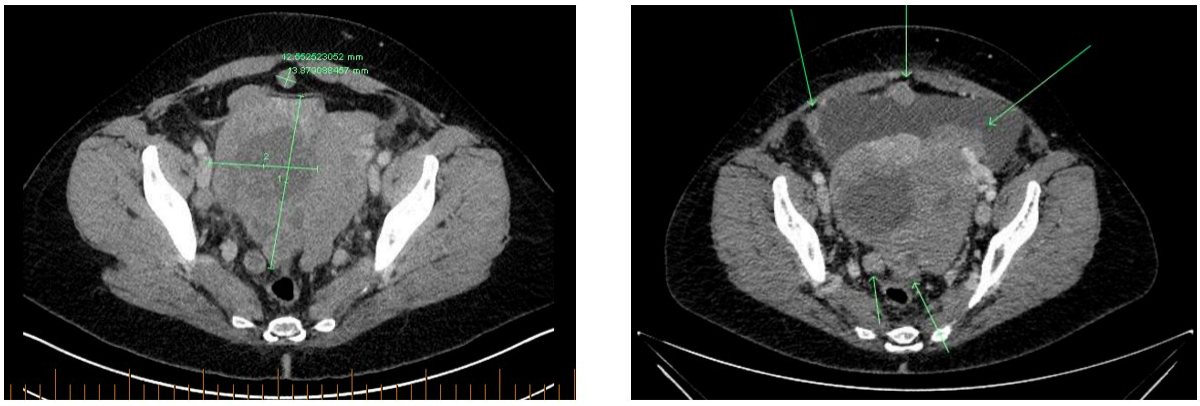

Figure 3.4. Patient A pelvic CT scan imaging. Patient with upfront PARPi before (left) and after (right) three cycles of every 21 days treatment demonstrating minimal change in primary ovarian tumor with development of ascites and progressive disease in other abdominal compartments. Organoid and IHC shown in Figures 3.1 and 3.3 respectively corresponds to this patient.

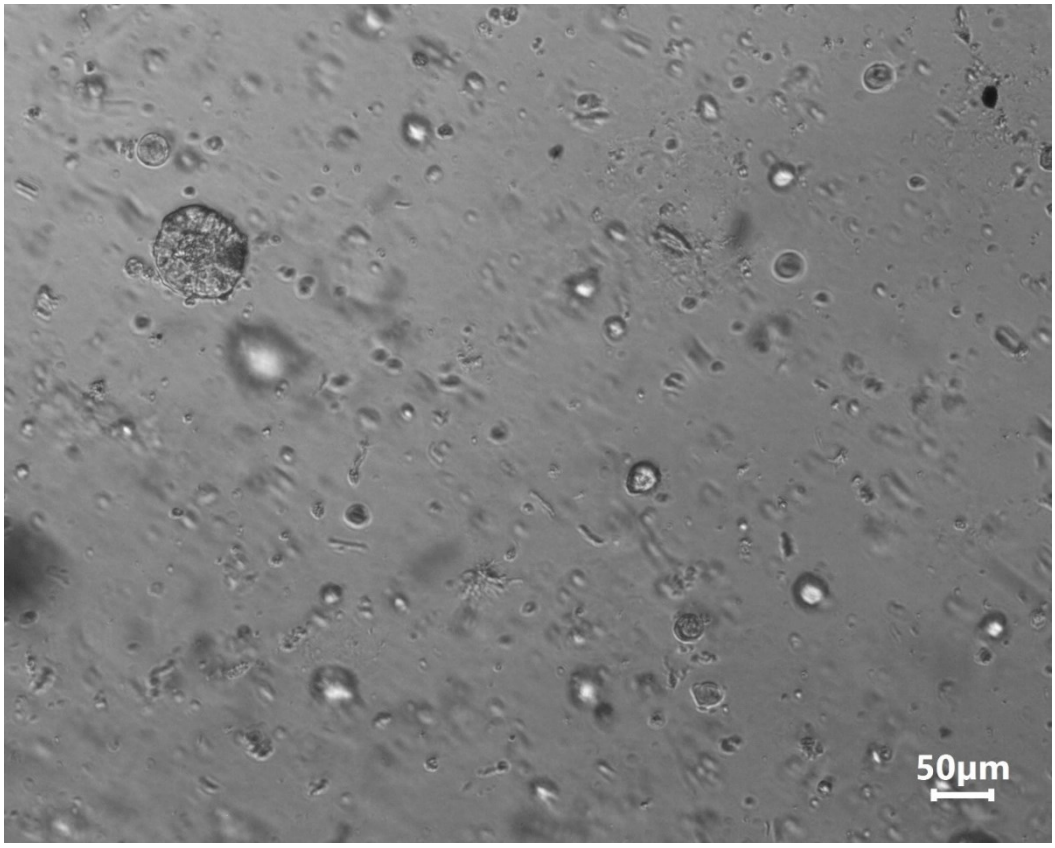

Figure 3.5. PDOs derived from a primary surgery of a patient (Patient C), who was treatment naive. The PDOs shown are from eleven days after sample collection. The picture was taken at 10x magnification.

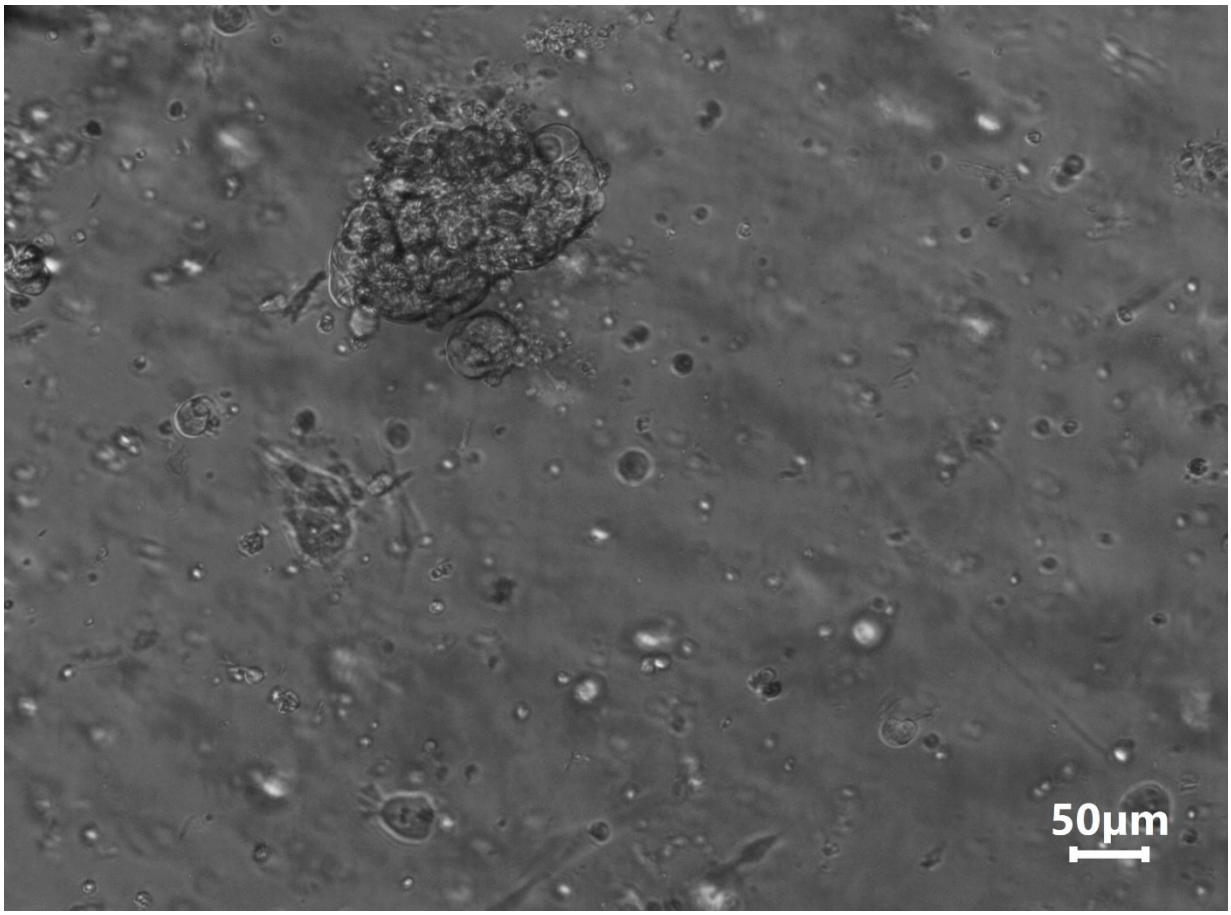

Figure 3.6. A PDO derived from a primary surgery of a patient (Patient D), who was treatment naive. The PDO shown is from six days after sample collection. The picture was taken at 10x magnification.

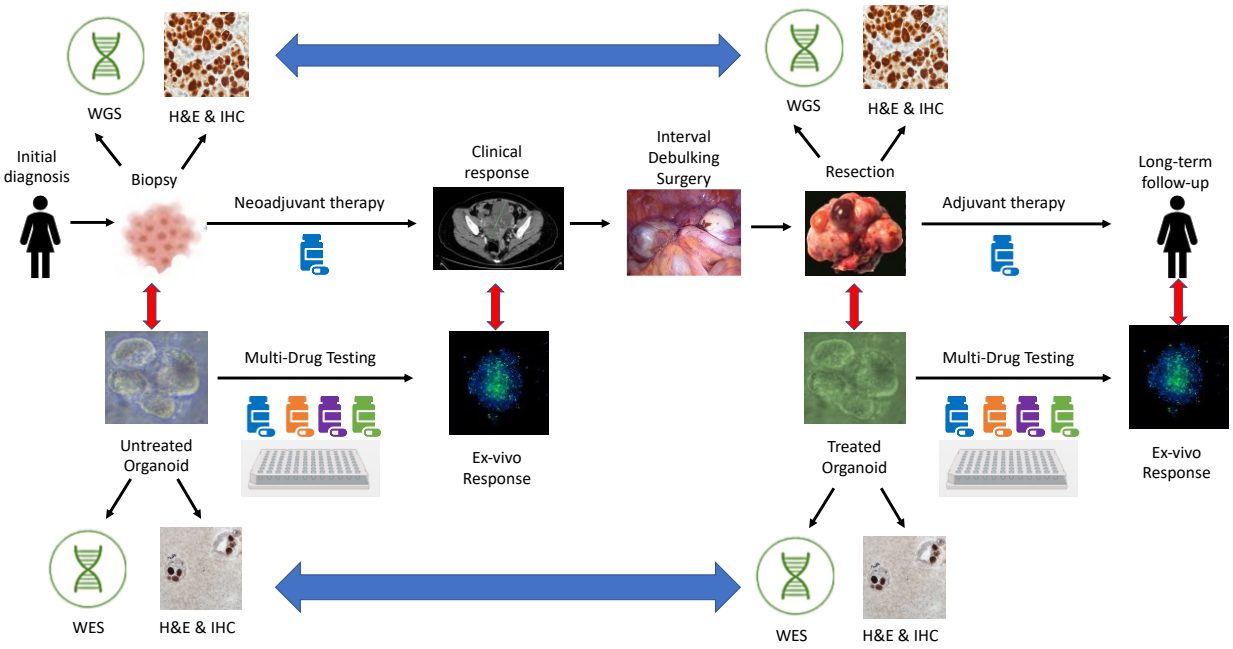

Fig. 3.7. Long-term goal of the organoid's development project with clinical flow of patient after initial diagnosis. Tumor tissue would be obtained at two time points (untreated and at time of interval debulking surgery post-neoadjuvant therapy). Organoids will be developed at both time points and validated by whole genome sequencing, H&E, and immunohistochemistry and compared to parent tumors. This also allows for correlation between clinical drug response and prediction from ex-vivo organoid experiments (red arrows). Furthermore, comparison of pre- and post-treatment tumor and organoids will provide insight into molecular signatures which may be predictive of response or resistance to therapy (blue arrows).

Chapter 4.
Conclusions and Future Works

The results obtained emphasize the idea that a more complex a model system may recapitulate in-vivo conditions and therapeutic responses more closely. Therefore, although the 2D culture system is a predominant preclinical method that can provide fast results, it may not accurately reflect the magnitude of the in-vivo drug effect when compared to a more complex 3D culture model. Overall, it has been reported that ovarian spheroids show morphological resemblance to multicellular aggregates in cancer ascites[174]. Analysis of spheroid versus monolayer ovarian cancer cells has demonstrated differences in the expression of several biomarkers relevant to disease, which could alter the tumorigenic properties of the cells. Ovarian cells in 3D culture have been found, in several studies, to be physiologically different from their 2D monolayer, suggesting that 3D growth is more informative in studying the properties of epithelial ovarian cancer cell lines.

4.1 Additional Data and Further Explanation

For the drug testing experiments in 3D, the Live/Dead assay was also performed once. PEO1, PEO4 and PEO6 cells were plated in ULAPs with 5,000 cells per well. The same drug concentrations, replicates and time points as for the drug testing experiments with the ATP quantitation assay were used. A summary of the results obtained can be found in figure 4.1 below. At 200 μM of carboplatin, no live (i.e., green) PEO1 cells are visible, only dead (i.e., red) cells are apparent compared to vehicle while live and dead PEO4 and PEO6 cells are visible compared to vehicle. The results provide further evidence that carboplatin has a greater effect on PEO1 cells and a lower effect on PEO4 and PEO6 cells, consistent with the platinum resistance which was expected to develop over the course of the disease. In addition, the results demonstrate that the

deaths caused by the drug exposures are occurring at the center of the spheroidal structures for PEO1, PEO4 and PEO6 cells and the three drugs.

The Live/Dead assay results in 3D showed that no dead cells were visible in the center of the spheroidal structures seven days after plating in ULAPs for PEO1 and PEO4 cells and four and seven days after plating for PEO6 cells (Fig.2.2B). However, apoptotic cells were apparent at the center of the spheroidal structures four and seven days after plating for all three cell lines as seen in Figure 2.3B. We speculate that the dead cells are not shown by the Live/Dead assay, but only by the CellEvent Caspase-3/7 assay because the apoptotic nuclei of dead cells are too small for EthD-1 to stain and fluoresce while the caspase 3/7 activity in the apoptotic cells can still be detected by the Caspase-3/7 Green Reagent.

4.2 Considerations Regarding the Use of ULAPs

Although the 3D cell culture technique used in this project for spheroids is used by many researchers, it has its own limitations[149]. When using ULAPs, careful consideration of what assays should be used is crucial to limit manipulations of the spheroidal structures in the wells, and thus, to avoid any external variables that could affect the results. If spheroidal structures are manipulated extensively, it could have a potential negative effect on the results since multiple aspirations of liquid from the wells and/or addition of reagents to the wells and/or accidental contacts between pipette tips and spherical structures could disturb the structures and affect morphological cellular behavior.

4.3 Limitations and Future Works

A first limitation is understanding the trend obtained in proliferation levels in 3D. The percentages of positive nuclear EdU indicate that the level of DNA synthesis in 2D of PEO1 is higher than that of PEO4, but do not significantly differ from that of PEO6. However, PEO1, PEO4 and PEO6 cells are known to have different doubling times with PEO1 cells being the fastest and PEO6 cells the slowest to divide[161]. To validate or refute our hypothesis that the time spent in the G2/M phase of the cell cycle, during which cell division occurs, could be longer for PEO4 and PEO6 than for PEO1, we could perform cell cycle analysis using flow cytometry and compare the time spent by PEO1, PEO4 and PEO6 in each phase of the cell cycle.

A second limitation is the growth of cells in 3D conditions without blood vessels which are present in-vivo. This limitation might be overcome by the development of more complex models adding endothelial cells or by applying the already existing organoid-on-a-chip model.

Appendix

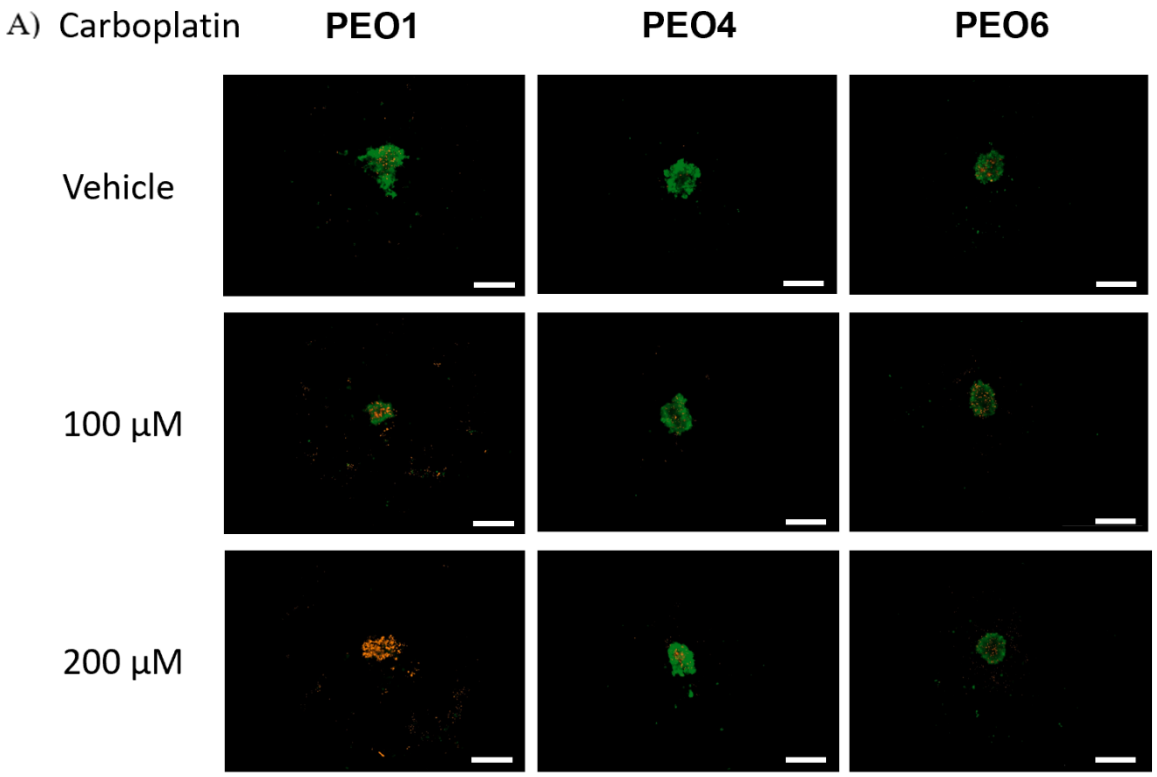
A) Carboplatin
PEO1
PEO4
PEO6
Vehicle
100 µM
200 µM

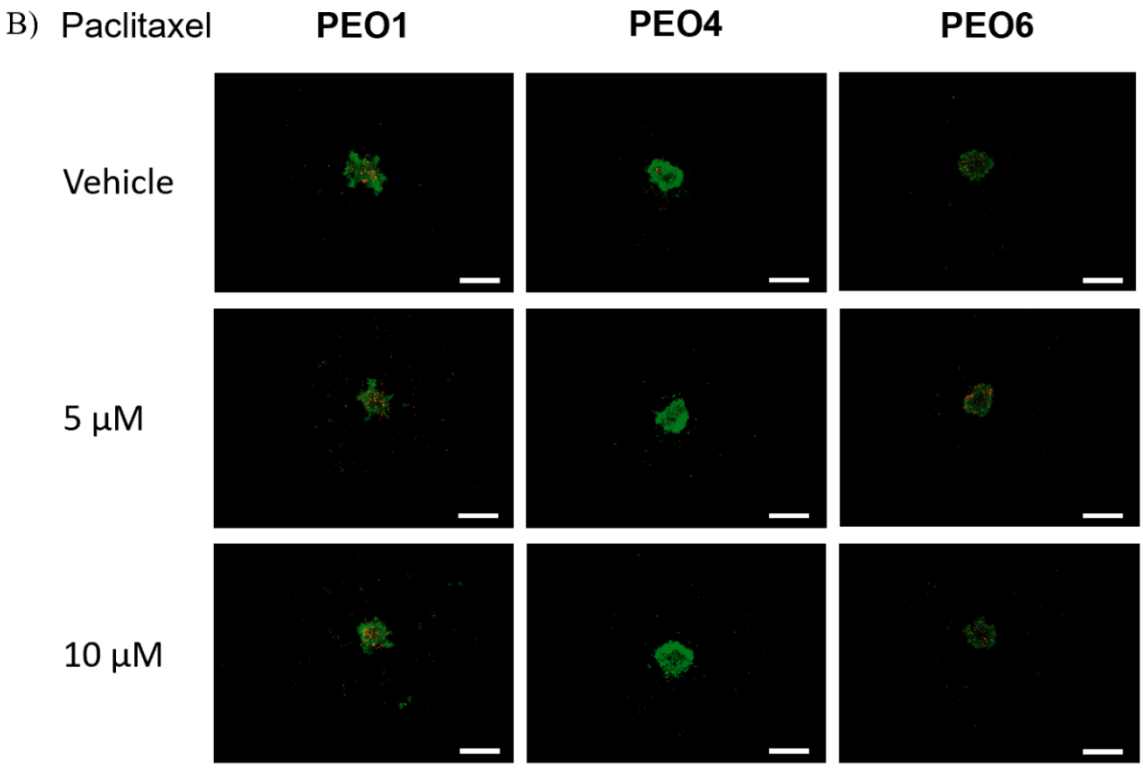
B) Paclitaxel
PEO1
PEO4
PEO6
Vehicle
5 µM
10 µM

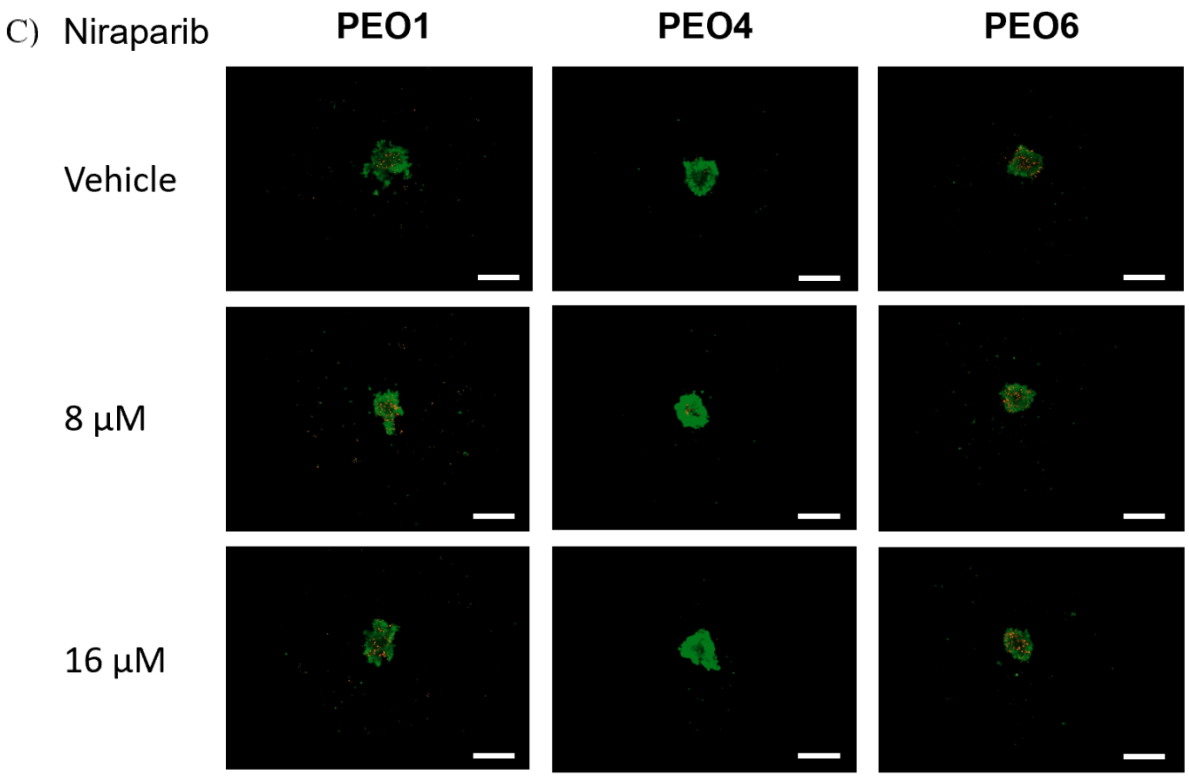

Figure 4.1. Live/Dead assay results of PEO1, PEO4 and PEO6 cells exposed to A) carboplatin, B) paclitaxel and C) niraparib in ultra-low attachment round-bottom plates.

	Laboratory of Dr.Sarah Hill	Laboratory of Dr.Lorenzo Ferri	Published Protocol of Dr.Nina Maenhoudt and Dr.Hugo Vankelecom	Suggested Plan
Advanced DMEM/F12	x	x	x	x
Antibiotic-Antimycotic	x (Penicillin + Streptomycin)	x (Penicillin + Streptomycin + Gentamicin + Normocin)	x (Penicillin + Streptomycin)	x
1X GlutaMAX Supplement	x	x		x
HEPES	x	x		x
R-spondin 1	x	x	x	
Noggin	x	x	x	
FGF2	x			
SB202190	x	x		x
A 83-01	x	x	x	x
EGF	x	x	x	x
FGF10	x	x		x
Prostaglandin E2	x	x		x
N-Acetyl-L-cysteine	x	x	x	x
Nicotinamide	x	x	x	x
B27 Supplement	x	x	x (B27 minus vitamin A)	x
Y-27632 dihydrochloride	**Determined to be unnecessary for culture maintenance**	x	x	
Recombinant Human FGF basic/FGF2/bFGF Protein				x
Forskolin				
β-Estradiol			x (17-β Estradiol)	
N-2 Supplement			x	
SB431542 hydrate				
Human Recombinant BMP-2				
L-glutamine			x	
SB203580			x	
IGF1			x	
HGF			x	
NRG1			x	
FGF7		x		
wnt		x		

Table 4.1. Comparison of media mixtures used by different groups for ovarian cancer patient-derived organoids generation.

1. Sample will be stored/transferred in base media on ice.
2. Divide sample into three sections, one will be for cryopreservation, one will be fixed for histological analysis, and one will be used for organoids generation.
3. When ready to begin, thaw at least one aliquot of 60 µL 50 000X, type II collagenase per 1-2 square cm of tumour. Add 50 µL to 5 mL base culture medium.
4. Dice the tumour to pieces of 2 mm or less using a scalpel. Then take the butt of a 10 mL syringe and crush the tumour as possible. You do not want solid pieces. You want as much mechanical disruption as possible.
5. Add up to 2 square cm of tumour tissue to 10 mL of base culture media with collagenase already added. Place the tube horizontally in the 37 °C shaker and shake for no longer than 30 minutes.
6. Dilute this homogenate 1:1 with base culture media, and filter through a 70 µM filter.
7. Spin the cell suspension at 300 xg for 5 min to create a pellet.
8. Wash with 1X red blood cell lysis buffer (900 µL base media: 100 µL 10X buffer) two to three times, and then wash once with base culture media. Count the viable cells.
9. Pellet the cells and mix the cell pellet with growth factor reduced Matrigel, such that there are approximately 10,000 or more cells per 10 µL droplet of Matrigel.
10. Rapidly plate the suspense into a 48-well plate with 15 µL of suspension per well located in the center of the well as a small, raised sphere.
11. Once done plating, place the plate at 37 °C for 2 minutes to let the Matrigel solidify.
12. Add 250 µL DR+++ media per well. Add media or PBS to the empty surrounding wells to prevent evaporation.
13. Ideally, the media should be changed every 3-4 days.

14. Once the organoids become confluent, you will need to split them. This is best done at 1:1.5 or 1:2.
15. To passage, scape the organoids and Matrigel out of the well along with the media, pipet into a 50 mL conical, and vigorously pipet. You want to break up the organoids to smaller clumps (NOT SINGLE CELLS). Alternatively, you can add 1mL of TYRPLE per 4 wells of organoids, incubate at 37 °C for 3 minutes, and then vigorously pipet until you don't see clumps any more. In either case, spin for 3 min at 3000 RPM, aspirate the media, and place on ice.
16. Add enough Matrigel to allow for a 1:1.5 – 1:2 split. Mix well. Add 15 µL of suspension per well in a 48 well plate. Let solidify as above. Add 250 µL DR+++ media per well.

Protocol 4.1. Protocol developed and used for the first surgical samples processed by our group. Adapted from the protocol used by Dr.Sarah Hill.

Make 50 mL aliquots of media. Store them at 4 degrees for up to one week. Once per week, make fresh dilutions of the following growth factors in base media to make the final media:

- SB202190-Dilute 40 µL stock solution in 80 µL base media for a 1:3 dilution
- A 83-01-Dilute 4 µL stock solution in 196 µL base media for a 1:50 dilution
- FGF10-Dilute 20 µL of stock solution in 80 µL base media for a 1:5 dilution
- EGF-Dilute 20 µL stock solution in 180 µL base media for a 1:10 dilution
- Prostaglandin E2-Dilute 20 µL stock solution in 180 µL base media for a 1:10 dilution

To make 50 mL of DR+++ media, add the following to 50mL of base media:

- 50 µL FGF2/FGF basic stock solution
- 50 µL SB202190 1:3 dilution
- 50 µL A 83-01 1:50 dilution
- 50 µL EGF 1:10 dilution
- 50 µL FGF10 1:50 dilution
- 50 µL Prostaglandin E2 1:10 dilution
- 125 µL N-Acetylcysteine stock solution
- 500 µL Nicotinamide stock solution
- 1000 µL B27 stock solution

Protocol 4.2. Media preparation steps used for the first surgical samples processed by our group. Adapted from the media preparation steps used by Dr.Sarah Hill.

Bibliography

[1] Momenimovahed Z, Tiznobaik A, Taheri S, Salehiniya H: Ovarian cancer in the world: epidemiology and risk factors. Int J Womens Health 2019, 11:287-99.
[2] Mazidimoradi A, Momenimovahed Z, Allahqoli L, Tiznobaik A, Hajinasab N, Salehiniya H, Alkatout I: The global, regional and national epidemiology, incidence, mortality, and burden of ovarian cancer. Health Sci Rep 2022, 5:e936.
[3] Bray F, Ferlay J, Soerjomataram I, Siegel RL, Torre LA, Jemal A: Global cancer statistics 2018: GLOBOCAN estimates of incidence and mortality worldwide for 36 cancers in 185 countries. CA Cancer J Clin 2018, 68:394-424.
[4] Coburn SB, Bray F, Sherman ME, Trabert B: International patterns and trends in ovarian cancer incidence, overall and by histologic subtype. Int J Cancer 2017, 140:2451-60.
[5] Organization IAfRoCWH: Cancer incidence and mortality statistics worldwide and by region. Edited by Ovary. The Global Cancer Observatory, 2020.
[6] Torre LA, Trabert B, DeSantis CE, Miller KD, Samimi G, Runowicz CD, Gaudet MM, Jemal A, Siegel RL: Ovarian cancer statistics, 2018. CA Cancer J Clin 2018, 68:284-96.
[7] Society AC: Key Statistics for Ovarian Cancer. American Cancer Society, 2023.
[8] National Cance Institute Surveillance E, and End Results Program: Cancer Stat Facts: Ovarian Cancer. National Cancer Institute, 2023.
[9] Badgwell D, Bast RC, Jr.: Early detection of ovarian cancer. Dis Markers 2007, 23:397-410.
[10] Doubeni CA, Doubeni AR, Myers AE: Diagnosis and Management of Ovarian Cancer. Am Fam Physician 2016, 93:937-44.
[11] Society CC: Survival statistics for ovarian cancer. Canadian Cancer Society.
[12] Huang J, Chan WC, Ngai CH, Lok V, Zhang L, Lucero-Prisno DE, Xu W, Zheng Z-J, Elcarte E, Withers M, Wong MCS, Universities oboNGHRGoAoPR: Worldwide Burden, Risk Factors, and Temporal Trends of Ovarian Cancer: A Global Study. Cancers 2022, 14:2230.
[13] Ng M, Freeman MK, Fleming TD, Robinson M, Dwyer-Lindgren L, Thomson B, Wollum A, Sanman E, Wulf S, Lopez AD, Murray CJL, Gakidou E: Smoking Prevalence and Cigarette Consumption in 187 Countries, 1980-2012. JAMA 2014, 311:183-92.
[14] Bray F, Loos AH, Tognazzo S, La Vecchia C: Ovarian cancer in Europe: Cross-sectional trends in incidence and mortality in 28 countries, 1953–2000. International Journal of Cancer 2005, 113:977-90.
[15] Prat J: FIGO's staging classification for cancer of the ovary, fallopian tube, and peritoneum: abridged republication. J Gynecol Oncol 2015, 26:87-9.
[16] Anzar N, Hasan MR, Akram M, Yadav N, Narang J: Systematic and validated techniques for the detection of ovarian cancer emphasizing the electro-analytical approach. Process Biochemistry 2020, 94:126-35.
[17] Kobel M, Kang EY: The Evolution of Ovarian Carcinoma Subclassification. Cancers (Basel) 2022, 14.
[18] Kim J, Park EY, Kim O, Schilder JM, Coffey DM, Cho CH, Bast RC, Jr.: Cell Origins of High-Grade Serous Ovarian Cancer. Cancers (Basel) 2018, 10.
[19] Cancer B: Ovary - Epithelial Carcinoma. Provincial Health Services Authority, 2023.
[20] Matulonis UA, Sood AK, Fallowfield L, Howitt BE, Sehouli J, Karlan BY: Ovarian cancer. Nat Rev Dis Primers 2016, 2:16061.
[21] Métairie M, Benoit L, Koual M, Bentivegna E, Wohrer H, Bolze P-A, Kerbage Y, Raimond E, Akladios C, Carcopino X, Canlorbe G, Uzan J, Lavoué V, Mimoun C, Huchon C, Koskas M,

Costaz H, Margueritte F, Dabi Y, Touboul C, Bendifallah S, Ouldamer L, Delanoy N, Nguyen-Xuan H-T, Bats A-S, Azaïs H: A Suggested Modification to FIGO Stage IV Epithelial Ovarian Cancer. Cancers 2023, 15:706.
[22] Javadi S, Ganeshan DM, Qayyum A, Iyer RB, Bhosale P: Ovarian Cancer, the Revised FIGO Staging System, and the Role of Imaging. AJR Am J Roentgenol 2016, 206:1351-60.
[23] Kanao H, Chang EJ, Matsuzaki S, Roman LD, Matsuo K: Survival effect of intra-operative tumor spillage during minimally invasive hysterectomy for early-stage endometrial cancer: a call for research. Int J Gynecol Cancer 2021, 31:308-9.
[24] KUIPER JJ, DE MAN RA, VAN BUUREN HR: Review article: management of ascites and associated complications in patients with cirrhosis. Alimentary Pharmacology & Therapeutics 2007, 26:183-93.
[25] Rezaei-Tazangi F, Roghani-Shahraki H, Khorsand Ghaffari M, Abolhasani Zadeh F, Boostan A, ArefNezhad R, Motedayyen H: The Therapeutic Potential of Common Herbal and Nano-Based Herbal Formulations against Ovarian Cancer: New Insight into the Current Evidence. Pharmaceuticals 2021, 14:1315.
[26] Ritch SJ, Telleria CM: The Transcoelomic Ecosystem and Epithelial Ovarian Cancer Dissemination. Front Endocrinol (Lausanne) 2022, 13:886533.
[27] Finch A, Shaw P, Rosen B, Murphy J, Narod SA, Colgan TJ: Clinical and pathologic findings of prophylactic salpingo-oophorectomies in 159 BRCA1 and BRCA2 carriers. Gynecologic Oncology 2006, 100:58-64.
[28] Trimble EL: The NIH Consensus Conference on Ovarian Cancer: Screening, Treatment, and Follow-up. Gynecologic Oncology 1994, 55:S1-S3.
[29] Eisen A, Rebbeck T, Lynch H, Lerman C, Ghadirian P, Dube M, Weber B, Narod S: Reduction in breast cancer risk following bilateral prophylactic oophorectomy in BRCA1 and BRCA2 mutation carriers. AMERICAN JOURNAL OF HUMAN GENETICS: UNIV CHICAGO PRESS 5720 SOUTH WOODLAWN AVE, CHICAGO, IL 60637-1603 USA, 2000. pp. 58-.
[30] Rebbeck T, Levin A, Eisen A: Reduction in breast cancer risk after bilateral prophylactic oophorectomy in BRCA1 mutation carriers. J Natl Cancer Inst 1998, 90:761-65.
[31] Kindelberger DW, Lee Y, Miron A, Hirsch MS, Feltmate C, Medeiros F, Callahan MJ, Garner EO, Gordon RW, Birch C, Berkowitz RS, Muto MG, Crum CP: Intraepithelial Carcinoma of the Fimbria and Pelvic Serous Carcinoma: Evidence for a Causal Relationship. The American Journal of Surgical Pathology 2007, 31:161-9.
[32] Neff RT, Senter L, Salani R: BRCA mutation in ovarian cancer: testing, implications and treatment considerations. Ther Adv Med Oncol 2017, 9:519-31.
[33] Chang HHY, Pannunzio NR, Adachi N, Lieber MR: Non-homologous DNA end joining and alternative pathways to double-strand break repair. Nature Reviews Molecular Cell Biology 2017, 18:495-506.
[34] Vítor AC, Huertas P, Legube G, de Almeida SF: Studying DNA Double-Strand Break Repair: An Ever-Growing Toolbox. Frontiers in Molecular Biosciences 2020, 7.
[35] Weterings E, Chen DJ: The endless tale of non-homologous end-joining. Cell Research 2008, 18:114-24.
[36] Creeden JF, Nanavaty NS, Einloth KR, Gillman CE, Stanbery L, Hamouda DM, Dworkin L, Nemunaitis J: Homologous recombination proficiency in ovarian and breast cancer patients. BMC Cancer 2021, 21:1154.
[37] Qiu S, Huang J: MRN complex is an essential effector of DNA damage repair. J Zhejiang Univ Sci B 2021, 22:31-7.

[38] Wang H, Shao Z, Shi LZ, Hwang PY, Truong LN, Berns MW, Chen DJ, Wu X: CtIP protein dimerization is critical for its recruitment to chromosomal DNA double-stranded breaks. J Biol Chem 2012, 287:21471-80.
[39] Karki R, Pandya D, Elston RC, Ferlini C: Defining "mutation" and "polymorphism" in the era of personal genomics. BMC Medical Genomics 2015, 8:37.
[40] Ramus SJ, Gayther SA: The contribution of BRCA1 and BRCA2 to ovarian cancer. Mol Oncol 2009, 3:138-50.
[41] Albertsen H, Plaetke R, Ballard L, Fujimoto E, Connolly J, Lawrence E, Rodriguez P, Robertson M, Bradley P, Milner B, et al.: Genetic mapping of the BRCA1 region on chromosome 17q21. Am J Hum Genet 1994, 54:516-25.
[42] Lin KK, Harrell MI, Oza AM, Oaknin A, Ray-Coquard I, Tinker AV, Helman E, Radke MR, Say C, Vo L-T: BRCA reversion mutations in circulating tumor DNA predict primary and acquired resistance to the PARP inhibitor rucaparib in high-grade ovarian carcinoma. Cancer discovery 2019, 9:210-9.
[43] Konstantinopoulos PA, Norquist B, Lacchetti C, Armstrong D, Grisham RN, Goodfellow PJ, Kohn EC, Levine DA, Liu JF, Lu KH: Germline and somatic tumor testing in epithelial ovarian cancer: ASCO guideline. Journal of clinical oncology: official journal of the American Society of Clinical Oncology 2020, 38:1222.
[44] Ngoi NYL, Tan DSP: The role of homologous recombination deficiency testing in ovarian cancer and its clinical implications: do we need it? ESMO Open 2021, 6:100144.
[45] Lakhani SR, Manek S, Penault-Llorca F, Flanagan A, Arnout L, Merrett S, McGuffog L, Steele D, Devilee P, Klijn JGM, Meijers-Heijboer H, Radice P, Pilotti S, Nevanlinna H, Butzow R, Sobol H, Jacquemier J, Lyonet DS, Neuhausen SL, Weber B, Wagner T, Winqvist R, Bignon Y-J, Monti F, Schmitt F, Lenoir G, Seitz S, Hamman U, Pharoah P, Lane G, Ponder B, Bishop DT, Easton DF: Pathology of Ovarian Cancers in BRCA1 and BRCA2 Carriers. Clinical Cancer Research 2004, 10:2473-81.
[46] Petrucelli N, Daly MB, Pal T: BRCA1- and BRCA2-Associated Hereditary Breast and Ovarian Cancer. GeneReviews(®). Edited by Adam MP, Mirzaa GM, Pagon RA, Wallace SE, Bean LJH, Gripp KW, Amemiya A. Seattle (WA): University of Washington, Seattle

[47] Zhang H, Liu T, Zhang Z, Payne SH, Zhang B, McDermott JE, Zhou J-Y, Petyuk VA, Chen L, Ray D: Integrated proteogenomic characterization of human high-grade serous ovarian cancer. Cell 2016, 166:755-65.
[48] Dougherty BA, Lai Z, Hodgson DR, Orr MC, Hawryluk M, Sun J, Yelensky R, Spencer SK, Robertson JD, Ho TW: Biological and clinical evidence for somatic mutations in BRCA1 and BRCA2 as predictive markers for olaparib response in high-grade serous ovarian cancers in the maintenance setting. Oncotarget 2017, 8:43653.
[49] Mohyuddin GR, Aziz M, Britt A, Wade L, Sun W, Baranda J, Al-Rajabi R, Saeed A, Kasi A: Similar response rates and survival with PARP inhibitors for patients with solid tumors harboring somatic versus Germline BRCA mutations: A Meta-analysis and systematic review. BMC cancer 2020, 20:1-9.
[50] Bankhead C, Collins C, Stokes-Lampard H, Rose P, Wilson S, Clements A, Mant D, Kehoe S, Austoker J: Identifying symptoms of ovarian cancer: a qualitative and quantitative study. BJOG: An International Journal of Obstetrics & Gynaecology 2008, 115:1008-14.

[51] Goff BA, Mandel L, Muntz HG, Melancon CH: Ovarian carcinoma diagnosis. Cancer 2000, 89:2068-75.
[52] Glance A: Ovarian cancer: an overview. Am Fam Physician 2009, 80:609-16.
[53] Zheng G, Yu H, Kanerva A, Försti A, Sundquist K, Hemminki K: Familial risks of ovarian cancer by age at diagnosis, proband type and histology. PLOS ONE 2018, 13:e0205000.
[54] Cancer CGoESoO: Ovarian cancer and oral contraceptives: collaborative reanalysis of data from 45 epidemiological studies including 23 257 women with ovarian cancer and 87 303 controls. The Lancet 2008, 371:303-14.
[55] Fasching PA, Beckmann MW: Hormones and genetics caught in the crossfire of preventive medicine. The Lancet Oncology 2007, 8:5-6.
[56] Gadducci A, Sergiampietri C, Tana R: Alternatives to risk-reducing surgery for ovarian cancer. Annals of Oncology 2013, 24:viii47-viii53.
[57] Kotsopoulos J, Lubinski J, Gronwald J, Cybulski C, Demsky R, Neuhausen SL, Kim-Sing C, Tung N, Friedman S, Senter L, Weitzel J, Karlan B, Moller P, Sun P, Narod SA, Group tHBCCS: Factors influencing ovulation and the risk of ovarian cancer in BRCA1 and BRCA2 mutation carriers. International Journal of Cancer 2015, 137:1136-46.
[58] Walker JL, Powell CB, Chen L-m, Carter J, Bae Jump VL, Parker LP, Borowsky ME, Gibb RK: Society of Gynecologic Oncology recommendations for the prevention of ovarian cancer. Cancer 2015, 121:2108-20.
[59] Schrijver LH, Antoniou AC, Olsson H, Mooij TM, Roos-Blom M-J, Azarang L, Adlard J, Ahmed M, Barrowdale D, Davidson R, Donaldson A, Eeles R, Evans DG, Frost D, Henderson A, Izatt L, Ong K-R, Bonadona V, Coupier I, Faivre L, Fricker J-P, Gesta P, van Engelen K, Jager A, Menko FH, Mourits MJE, Singer CF, Tan YY, Foretova L, Navratilova M, Schmutzler RK, Ellberg C, Gerdes A-M, Caldes T, Simard J, Olah E, Jakubowska A, Rantala J, Osorio A, Hopper JL, Phillips K-A, Milne RL, Beth Terry M, Noguès C, Engel C, Kast K, Goldgar DE, van Leeuwen FE, Easton DF, Andrieu N, Rookus MA, Noguès C, Laborde L, Pontois P, Breysse E, Berline M, Stoppa-Lyonnet D, Gauthier-Villars M, Buecher B, Colas C, Caron O, Noguès C, Mouret-Fourme E, Saule C, Colas C, Fricker J-P, Lasset C, Bonadona V, Dussard S, Berthet P, Faivre L, Luporsi E, Mari V, Gladieff L, Gesta P, Chieze-Valéro S, Moretta J, Sobol H, Eisinger F, Popovici C, Longy M, Grivelli L, Colas C, Soubrier F, Benusiglio P, Coupier I, Pujol P, Corsini C, Morin-Meschin M-E, Lortholary A, Adenis C, Maillez A, Nguyen TD, Delnatte C, Abadie C, Tinat J, Tennevet I, Maugard C, Bignon Y-J, Gay Bellile M, Penet C, Dreyfus H, Cohen-Haguenauer O, Gilbert B, Venat-Bouvet L, Leroux D, Legrand C, Dreyfus H, Zattara-Cannoni H, Layet V, Lacaze E, Fert-Ferrer S, Bera O, Gilbert-Dussardier B, Tougeron D, Lallaoui H, Tinat J, Rookus MA, Hogervorst FBL, van Leeuwen FE, Adank MA, Schmidt MK, Jenner DJ, Collée JM, van den Ouweland AMW, Hooning MJ, Boere IA, van Asperen CJ, Devilee P, van der Luijt RB, van Cronenburg TCTEF, Wevers MR, Mensenkamp AR, Ausems MGEM, Koudijs MJ, van de Beek I, van Engelen K, Gille JJP, Gómez García EB, Blok MJ, de Boer M, Berger LPV, van der Hout AH, Mourits MJE, de Bock GH, Siesling S, Verloop J, van den Broek EC: Oral contraceptive use and ovarian cancer risk for BRCA1/2 mutation carriers: an international cohort study. American Journal of Obstetrics and Gynecology 2021, 225:51.e1-.e17.
[60] Narod SA, Risch H, Moslehi R, Dørum A, Neuhausen S, Olsson H, Provencher D, Radice P, Evans G, Bishop S, Brunet J-S, Ponder BAJ, Klijn JGM: Oral Contraceptives and the Risk of Hereditary Ovarian Cancer. New England Journal of Medicine 1998, 339:424-8.

[61] Tanha K, Mottaghi A, Nojomi M, Moradi M, Rajabzadeh R, Lotfi S, Janani L: Investigation on factors associated with ovarian cancer: an umbrella review of systematic review and meta-analyses. J Ovarian Res 2021, 14:153.
[62] Tempany CM, Zou KH, Silverman SG, Brown DL, Kurtz AB, McNeil BJ: Staging of advanced ovarian cancer: comparison of imaging modalities--report from the Radiological Diagnostic Oncology Group. Radiology 2000, 215:761-7.
[63] Goerg C, Schwerk WB: Peritoneal carcinomatosis with ascites. American Journal of Roentgenology 1991, 156:1185-7.
[64] Mitchell DG, Javitt MC, Glanc P, Bennett GL, Brown DL, Dubinsky T, Harisinghani MG, Harris RD, Horowitz NS, Pandharipande PV, Pannu HK, Podrasky AE, Royal HD, Shipp TD, Siegel CL, Simpson L, Wong-You-Cheong JJ, Zelop CM: ACR appropriateness criteria staging and follow-up of ovarian cancer. J Am Coll Radiol 2013, 10:822-7.
[65] Tsili AC, Tsampoulas C, Charisiadi A, Kalef-Ezra J, Dousias V, Paraskevaidis E, Efremidis SC: Adnexal masses: accuracy of detection and differentiation with multidetector computed tomography. Gynecol Oncol 2008, 110:22-31.
[66] Kawamoto S, Urban BA, Fishman EK: CT of epithelial ovarian tumors. Radiographics 1999, 19 Spec No:S85-102; quiz S263-4.
[67] Pannu HK, Horton KM, Fishman EK: Thin section dual-phase multidetector-row computed tomography detection of peritoneal metastases in gynecologic cancers. J Comput Assist Tomogr 2003, 27:333-40.
[68] Bristow RE, Duska LR, Lambrou NC, Fishman EK, O'Neill MJ, Trimble EL, Montz FJ: A model for predicting surgical outcome in patients with advanced ovarian carcinoma using computed tomography. Cancer 2000, 89:1532-40.
[69] Qayyum A, Coakley FV, Westphalen AC, Hricak H, Okuno WT, Powell B: Role of CT and MR imaging in predicting optimal cytoreduction of newly diagnosed primary epithelial ovarian cancer. Gynecol Oncol 2005, 96:301-6.
[70] Hricak H, Chen M, Coakley FV, Kinkel K, Yu KK, Sica G, Bacchetti P, Powell CB: Complex adnexal masses: detection and characterization with MR imaging--multivariate analysis. Radiology 2000, 214:39-46.
[71] Rieber A, Nüssle K, Stöhr I, Grab D, Fenchel S, Kreienberg R, Reske SN, Brambs HJ: Preoperative diagnosis of ovarian tumors with MR imaging: comparison with transvaginal sonography, positron emission tomography, and histologic findings. AJR Am J Roentgenol 2001, 177:123-9.
[72] Forstner R, Hricak H, Occhipinti KA, Powell CB, Frankel SD, Stern JL: Ovarian cancer: staging with CT and MR imaging. Radiology 1995, 197:619-26.
[73] Low RN, Barone RM, Lucero J: Comparison of MRI and CT for predicting the Peritoneal Cancer Index (PCI) preoperatively in patients being considered for cytoreductive surgical procedures. Ann Surg Oncol 2015, 22:1708-15.
[74] Kubik-Huch RA, Dörffler W, von Schulthess GK, Marincek B, Köchli OR, Seifert B, Haller U, Steinert HC: Value of (18F)-FDG positron emission tomography, computed tomography, and magnetic resonance imaging in diagnosing primary and recurrent ovarian carcinoma. Eur Radiol 2000, 10:761-7.
[75] Yoshida Y, Kurokawa T, Kawahara K, Tsuchida T, Okazawa H, Fujibayashi Y, Yonekura Y, Kotsuji F: Incremental benefits of FDG positron emission tomography over CT alone for the preoperative staging of ovarian cancer. AJR Am J Roentgenol 2004, 182:227-33.

[76] Sheng XG, Zhang XL, Fu Z, Li HQ, Li QS, Ma ZF, Li DP, Chen ZY: [Value of positron emission tomography-CT imaging combined with continual detection of CA125 in serum for diagnosis of early asymptomatic recurrence of epithelial ovarian carcinoma]. Zhonghua Fu Chan Ke Za Zhi 2007, 42:460-3.
[77] Cho SM, Ha HK, Byun JY, Lee JM, Kim CJ, Nam-Koong SE, Lee JM: Usefulness of FDG PET for assessment of early recurrent epithelial ovarian cancer. AJR Am J Roentgenol 2002, 179:391-5.
[78] Iagaru AH, Mittra ES, McDougall IR, Quon A, Gambhir SS: 18F-FDG PET/CT evaluation of patients with ovarian carcinoma. Nucl Med Commun 2008, 29:1046-51.
[79] García-Velloso MJ, Jurado M, Ceamanos C, Aramendía JM, Garrastachu MP, López-García G, Richter JA: Diagnostic accuracy of FDG PET in the follow-up of platinum-sensitive epithelial ovarian carcinoma. Eur J Nucl Med Mol Imaging 2007, 34:1396-405.
[80] Chung HH, Kang WJ, Kim JW, Park NH, Song YS, Chung JK, Kang SB, Lee HP: Role of [18F]FDG PET/CT in the assessment of suspected recurrent ovarian cancer: correlation with clinical or histological findings. Eur J Nucl Med Mol Imaging 2007, 34:480-6.
[81] Funicelli L, Travaini LL, Landoni F, Trifirò G, Bonello L, Bellomi M: Peritoneal carcinomatosis from ovarian cancer: the role of CT and [^{18}F]FDG-PET/CT. Abdom Imaging 2010, 35:701-7.
[82] Castro-Mesta JF, González-Guerrero JF, Barrios-Sánchez P, Villarreal-Cavazos G: Bases and foundations of the treatment of peritoneal carcinomatosis: Review article. Medicina Universitaria 2016, 18:98-104.
[83] Charkhchi P, Cybulski C, Gronwald J, Wong FO, Narod SA, Akbari MR: CA125 and Ovarian Cancer: A Comprehensive Review. Cancers (Basel) 2020, 12.
[84] Gupta D, Lis CG: Role of CA125 in predicting ovarian cancer survival - a review of the epidemiological literature. Journal of Ovarian Research 2009, 2:13.
[85] Bast RC, Jr., Feeney M, Lazarus H, Nadler LM, Colvin RB, Knapp RC: Reactivity of a monoclonal antibody with human ovarian carcinoma. The Journal of Clinical Investigation 1981, 68:1331-7.
[86] Funston G, Mounce LT, Price S, Rous B, Crosbie EJ, Hamilton W, Walter FM: CA125 test result, test-to-diagnosis interval, and stage in ovarian cancer at diagnosis: a retrospective cohort study using electronic health records. British Journal of General Practice 2021, 71:e465-e72.
[87] Woodward ER, Sleightholme HV, Considine AM, Williamson S, McHugo JM, Cruger DG: Annual surveillance by CA125 and transvaginal ultrasound for ovarian cancer in both high-risk and population risk women is ineffective. Bjog 2007, 114:1500-9.
[88] Nañez A, Stram DA, Garcia C, Powell CB: Ovarian cancer surveillance in the clinical follow up of women with known BRCA1 or BRCA2 pathogenic variants in a large health care system. Gynecologic Oncology 2021, 163:134-41.
[89] Hellström I, Raycraft J, Hayden-Ledbetter M, Ledbetter JA, Schummer M, McIntosh M, Drescher C, Urban N, Hellström KE: The HE4 (WFDC2) protein is a biomarker for ovarian carcinoma. Cancer Res 2003, 63:3695-700.
[90] Dochez V, Caillon H, Vaucel E, Dimet J, Winer N, Ducarme G: Biomarkers and algorithms for diagnosis of ovarian cancer: CA125, HE4, RMI and ROMA, a review. Journal of Ovarian Research 2019, 12:28.
[91] Drapkin R, von Horsten HH, Lin Y, Mok SC, Crum CP, Welch WR, Hecht JL: Human Epididymis Protein 4 (HE4) Is a Secreted Glycoprotein that Is Overexpressed by Serous and Endometrioid Ovarian Carcinomas. Cancer Research 2005, 65:2162-9.

[92] Yanaranop M, Anakrat V, Siricharoenthai S, Nakrangsee S, Thinkhamrop B: Is the Risk of Ovarian Malignancy Algorithm Better Than Other Tests for Predicting Ovarian Malignancy in Women with Pelvic Masses? Gynecologic and Obstetric Investigation 2016, 82:47-53.
[93] Wilailak S, Chan KKL, Chen C-A, Nam J-H, Ochiai K, Aw T-C, Sabaratnam S, Hebbar S, Sickan J, Schodin BA, Charakorn C, Sumpaico WW: Distinguishing benign from malignant pelvic mass utilizing an algorithm with HE4, menopausal status, and ultrasound findings. J Gynecol Oncol 2015, 26:46-53.
[94] Romagnolo C, Leon AE, Fabricio ASC, Taborelli M, Polesel J, Del Pup L, Steffan A, Cervo S, Ravaggi A, Zanotti L, Bandiera E, Odicino FE, Scattolo N, Squarcina E, Papadakis C, Maggino T, Gion M: HE4, CA125 and risk of ovarian malignancy algorithm (ROMA) as diagnostic tools for ovarian cancer in patients with a pelvic mass: An Italian multicenter study. Gynecologic Oncology 2016, 141:303-11.
[95] Chen X, Zhou H, Chen R, He J, Wang Y, Huang L, Sun L, Duan C, Luo X, Yan H: Development of a multimarker assay for differential diagnosis of benign and malignant pelvic masses. Clin Chim Acta 2015, 440:57-63.
[96] Van Gorp T, Cadron I, Despierre E, Daemen A, Leunen K, Amant F, Timmerman D, De Moor B, Vergote I: HE4 and CA125 as a diagnostic test in ovarian cancer: prospective validation of the Risk of Ovarian Malignancy Algorithm. Br J Cancer 2011, 104:863-70.
[97] Matulonis UA: Management of newly diagnosed or recurrent ovarian cancer. Clin Adv Hematol Oncol 2018, 16:426-37.
[98] Leung SOA, Konstantinopoulos PA: Advances in the treatment of platinum resistant epithelial ovarian cancer: an update on standard and experimental therapies. Expert Opin Investig Drugs 2021, 30:695-707.
[99] Lukanović D, Kobal B, Černe K: Ovarian Cancer: Treatment and Resistance to Pharmacotherapy. Reproductive Medicine 2022, 3:127-40.
[100] Arab M, Jamdar F, Sadat Hosseini M, Ghodssi- Ghasemabadi R, Farzaneh F, Ashrafganjoei T: Model for Prediction of Optimal Debulking of Epithelial Ovarian Cancer. Asian Pac J Cancer Prev 2018, 19:1319-24.
[101] Sonnichsen DS, Relling MV: Clinical pharmacokinetics of paclitaxel. Clin Pharmacokinet 1994, 27:256-69.
[102] Hirte H, Poon R, Yao X, May T, Ethier JL, Petz L, Speakman J, Elit L: Neoadjuvant and Adjuvant Systemic Therapy for Newly Diagnosed Stage II-IV Epithelial Ovary, Fallopian Tube, or Primary Peritoneal Carcinoma: A Practice Guideline. Curr Oncol 2022, 29:231-42.
[103] Vergote I, Trope CG, Amant F, Kristensen GB, Ehlen T, Johnson N, Verheijen RH, van der Burg ME, Lacave AJ, Panici PB, Kenter GG, Casado A, Mendiola C, Coens C, Verleye L, Stuart GC, Pecorelli S, Reed NS, European Organization for R, Treatment of Cancer-Gynaecological Cancer G, Group NCT: Neoadjuvant chemotherapy or primary surgery in stage IIIC or IV ovarian cancer. N Engl J Med 2010, 363:943-53.
[104] Kehoe S, Hook J, Nankivell M, Jayson GC, Kitchener H, Lopes T, Luesley D, Perren T, Bannoo S, Mascarenhas M, Dobbs S, Essapen S, Twigg J, Herod J, McCluggage G, Parmar M, Swart A-M: Primary chemotherapy versus primary surgery for newly diagnosed advanced ovarian cancer (CHORUS): an open-label, randomised, controlled, non-inferiority trial. The Lancet 2015, 386:249-57.
[105] Onda T, Satoh T, Saito T, Kasamatsu T, Nakanishi T, Nakamura K, Wakabayashi M, Takehara K, Saito M, Ushijima K, Kobayashi H, Kawana K, Yokota H, Takano M, Takeshima N, Watanabe Y, Yaegashi N, Konishi I, Kamura T, Yoshikawa H: Comparison of treatment

invasiveness between upfront debulking surgery versus interval debulking surgery following neoadjuvant chemotherapy for stage III/IV ovarian, tubal, and peritoneal cancers in a phase III randomised trial: Japan Clinical Oncology Group Study JCOG0602. Eur J Cancer 2016, 64:22-31.
[106] Fagotti A, Ferrandina MG, Vizzielli G, Pasciuto T, Fanfani F, Gallotta V, Margariti PA, Chiantera V, Costantini B, Gueli Alletti S, Cosentino F, Scambia G: Randomized trial of primary debulking surgery versus neoadjuvant chemotherapy for advanced epithelial ovarian cancer (SCORPION-NCT01461850). Int J Gynecol Cancer 2020, 30:1657-64.
[107] Sousa GFd, Wlodarczyk SR, Monteiro G: Carboplatin: molecular mechanisms of action associated with chemoresistance. Brazilian Journal of Pharmaceutical Sciences 2014, 50.
[108] Khanna C, Rosenberg M, Vail DM: A Review of Paclitaxel and Novel Formulations Including Those Suitable for Use in Dogs. Journal of Veterinary Internal Medicine 2015, 29:1006-12.
[109] Sharp DJ, Rogers GC, Scholey JM: Microtubule motors in mitosis. Nature 2000, 407:41-7.
[110] Ledermann JA: First-line treatment of ovarian cancer: questions and controversies to address. Ther Adv Med Oncol 2018, 10:1758835918768232.
[111] du Bois A, Lück HJ, Meier W, Adams HP, Möbus V, Costa S, Bauknecht T, Richter B, Warm M, Schröder W, Olbricht S, Nitz U, Jackisch C, Emons G, Wagner U, Kuhn W, Pfisterer J: A randomized clinical trial of cisplatin/paclitaxel versus carboplatin/paclitaxel as first-line treatment of ovarian cancer. J Natl Cancer Inst 2003, 95:1320-9.
[112] Falandry C, Rousseau F, Mouret-Reynier M-A, Tinquaut F, Lorusso D, Herrstedt J, Savoye A-M, Stefani L, Bourbouloux E, Sverdlin R, D'Hondt V, Lortholary A, Brachet P-E, Zannetti A, Malaurie E, Venat-Bouvet L, Trédan O, Mourey L, Pujade-Lauraine E, Freyer G, sein GdINplÉdCdlOed: Efficacy and Safety of First-line Single-Agent Carboplatin vs Carboplatin Plus Paclitaxel for Vulnerable Older Adult Women With Ovarian Cancer: A GINECO/GCIG Randomized Clinical Trial. JAMA Oncology 2021, 7:853-61.
[113] Leung D, Price ZK, Lokman NA, Wang W, Goonetilleke L, Kadife E, Oehler MK, Ricciardelli C, Kannourakis G, Ahmed N: Platinum-resistance in epithelial ovarian cancer: an interplay of epithelial–mesenchymal transition interlinked with reprogrammed metabolism. Journal of Translational Medicine 2022, 20:556.
[114] Davis A, Tinker AV, Friedlander M: "Platinum resistant" ovarian cancer: what is it, who to treat and how to measure benefit? Gynecol Oncol 2014, 133:624-31.
[115] van Zyl B, Tang D, Bowden NA: Biomarkers of platinum resistance in ovarian cancer: what can we use to improve treatment. Endocrine-Related Cancer 2018, 25:R303-R18.
[116] Reles A, Wen WH, Schmider A, Gee C, Runnebaum IB, Kilian U, Jones LA, El-Naggar A, Minguillon C, Schönborn I, Reich O, Kreienberg R, Lichtenegger W, Press MF: Correlation of p53 mutations with resistance to platinum-based chemotherapy and shortened survival in ovarian cancer. Clin Cancer Res 2001, 7:2984-97.
[117] Yang-Hartwich Y, Soteras MG, Lin ZP, Holmberg J, Sumi N, Craveiro V, Liang M, Romanoff E, Bingham J, Garofalo F, Alvero A, Mor G: p53 protein aggregation promotes platinum resistance in ovarian cancer. Oncogene 2015, 34:3605-16.
[118] Patch A, Christie E, Etemadmoghadam D, Garsed D, George J, Fereday S, Nones K, Cowin P, Alsop K, Bailey P: Whole-genome characterization of chemoresistant ovarian cancer. Nature 2015, 521:489-94.
[119] Wei S, Balch C, Paik H, Kim Y, Baldwin R, Liyanarachchi S, Li L, Wang Z, Wan J, Davuluri R: Prognostic DNA methylation biomarkers in ovarian cancer. Clinical Cancer Research 2006, 12:2788-94.

[120] Barakat B, Wang Q, Han C, Milum K, Yin D, Zhao Q, Wani G, Arafa el S, El-Mahdy M, Wani A: Overexpression of DDB2 enhances the sensitivity of human ovarian cancer cells to cisplatin by augmenting cellular apoptosis. International Journal of Cancer 2010, 127:977-88.
[121] Vang S, Wu H, Fischer A, Miller D, MacLaughlan S, Douglass E, Comisar L, Steinhoff M, Collins C, Smith P: Identification of ovarian cancer metastatic miRNAs. PLoS ONE 2013, 8:e58226.
[122] Steg A, Bevis K, Katre A, Ziebarth A, Dobbin Z, Alvarez R, Zhang K, Conner M, Landen C: Stem cell pathways contribute to clinical chemoresistance in ovarian cancer. Clinical Cancer Research 2012, 18:869-81.
[123] Marchini S, Fruscio R, Clivio L, Beltrame L, Porcu L, Fuso Nerini I, Cavalieri D, Chiorino G, Cattoretti G, Mangioni C: Resistance to platinum-based chemotherapy is associated with epithelial to mesenchymal transition in epithelial ovarian cancer. European Journal of Cancer 2013, 49:520-30.
[124] Chebouti I, Kasimir-Bauer S, Buderath P, Wimberger P, Hauch S, Kimmig R, Kuhlmann J: EMT-like circulating tumor cells in ovarian cancer patients are enriched by platinum-based chemotherapy. Oncotarget 2017, 8:48820-31.
[125] O'Connor MJ: Targeting the DNA Damage Response in Cancer. Mol Cell 2015, 60:547-60.
[126] Rose PG: First-Line Chemotherapy for Ovarian Cancer: Inferences From Recent Studies. Oncologist 2016, 21:1286-90.
[127] Moore K, Colombo N, Scambia G, Kim BG, Oaknin A, Friedlander M, Lisyanskaya A, Floquet A, Leary A, Sonke GS, Gourley C, Banerjee S, Oza A, Gonzalez-Martin A, Aghajanian C, Bradley W, Mathews C, Liu J, Lowe ES, Bloomfield R, DiSilvestro P: Maintenance Olaparib in Patients with Newly Diagnosed Advanced Ovarian Cancer. N Engl J Med 2018, 379:2495-505.
[128] Ledermann J, Harter P, Gourley C, Friedlander M, Vergote I, Rustin G, Scott C, Meier W, Shapira-Frommer R, Safra T, Matei D, Macpherson E, Watkins C, Carmichael J, Matulonis U: Olaparib Maintenance Therapy in Platinum-Sensitive Relapsed Ovarian Cancer. New England Journal of Medicine 2012, 366:1382-92.
[129] Hess LM, Brnabic A, Mason O, Lee P, Barker S: Relationship between Progression-free Survival and Overall Survival in Randomized Clinical Trials of Targeted and Biologic Agents in Oncology. J Cancer 2019, 10:3717-27.
[130] Pujade-Lauraine E, Ledermann JA, Selle F, Gebski V, Penson RT, Oza AM, Korach J, Huzarski T, Poveda A, Pignata S, Friedlander M, Colombo N, Harter P, Fujiwara K, Ray-Coquard I, Banerjee S, Liu J, Lowe ES, Bloomfield R, Pautier P, Korach J, Huzarski T, Byrski T, Pautier P, Friedlander M, Harter P, Colombo N, Pignata S, Scambia G, Nicoletto M, Nussey F, Clamp A, Penson R, Oza A, Poveda Velasco A, Rodrigues M, Lotz J-P, Selle F, Ray-Coquard I, Provencher D, Prat Aparicio A, Vidal Boixader L, Scott C, Tamura K, Yunokawa M, Lisyanskaya A, Medioni J, Pécuchet N, Dubot C, de la Motte Rouge T, Kaminsky M-C, Weber B, Lortholary A, Parkinson C, Ledermann J, Williams S, Banerjee S, Cosin J, Hoffman J, Penson R, Plante M, Covens A, Sonke G, Joly F, Floquet A, Banerjee S, Hirte H, Amit A, Park-Simon T-W, Matsumoto K, Tjulandin S, Kim JH, Gladieff L, Sabbatini R, O'Malley D, Timmins P, Kredentser D, Laínez Milagro N, Barretina Ginesta MP, Tibau Martorell A, Gómez de Liaño Lista A, Ojeda González B, Mileshkin L, Mandai M, Boere I, Ottevanger P, Nam J-H, Filho E, Hamizi S, Cognetti F, Warshal D, Dickson-Michelson E, Kamelle S, McKenzie N, Rodriguez G, Armstrong D, Chalas E, Celano P, Behbakht K, Davidson S, Welch S, Helpman L, Fishman A, Bruchim I, Sikorska M, Słowińska A, Rogowski W, Bidziński M, Śpiewankiewicz B, Casado Herraez A, Mendiola Fernández C, Gropp-Meier M, Saito T, Takehara K, Enomoto T, Watari H, Choi CH, Kim B-G,

Kim JW, Hegg R, Vergote I: Olaparib tablets as maintenance therapy in patients with platinum-sensitive, relapsed ovarian cancer and a BRCA1/2 mutation (SOLO2/ENGOT-Ov21): a double-blind, randomised, placebo-controlled, phase 3 trial. The Lancet Oncology 2017, 18:1274-84.
[131] Penson RT, Valencia RV, Cibula D, Colombo N, Leath CA, 3rd, Bidzinski M, Kim JW, Nam JH, Madry R, Hernandez C, Mora PAR, Ryu SY, Milenkova T, Lowe ES, Barker L, Scambia G: Olaparib Versus Nonplatinum Chemotherapy in Patients With Platinum-Sensitive Relapsed Ovarian Cancer and a Germline BRCA1/2 Mutation (SOLO3): A Randomized Phase III Trial. J Clin Oncol 2020, 38:1164-74.
[132] Gonzalez-Martin A, Pothuri B, Vergote I, DePont Christensen R, Graybill W, Mirza MR, McCormick C, Lorusso D, Hoskins P, Freyer G, Baumann K, Jardon K, Redondo A, Moore RG, Vulsteke C, O'Cearbhaill RE, Lund B, Backes F, Barretina-Ginesta P, Haggerty AF, Rubio-Perez MJ, Shahin MS, Mangili G, Bradley WH, Bruchim I, Sun K, Malinowska IA, Li Y, Gupta D, Monk BJ, Investigators PE-OG-: Niraparib in Patients with Newly Diagnosed Advanced Ovarian Cancer. N Engl J Med 2019, 381:2391-402.
[133] Thorsell AG, Ekblad T, Karlberg T, Löw M, Pinto AF, Trésaugues L, Moche M, Cohen MS, Schüler H: Structural Basis for Potency and Promiscuity in Poly(ADP-ribose) Polymerase (PARP) and Tankyrase Inhibitors. J Med Chem 2017, 60:1262-71.
[134] Valabrega G, Scotto G, Tuninetti V, Pani A, Scaglione F: Differences in PARP Inhibitors for the Treatment of Ovarian Cancer: Mechanisms of Action, Pharmacology, Safety, and Efficacy. Int J Mol Sci 2021, 22.
[135] Coleman RL, Fleming GF, Brady MF, Swisher EM, Steffensen KD, Friedlander M, Okamoto A, Moore KN, Efrat Ben-Baruch N, Werner TL, Cloven NG, Oaknin A, DiSilvestro PA, Morgan MA, Nam J-H, Leath CA, Nicum S, Hagemann AR, Littell RD, Cella D, Baron-Hay S, Garcia-Donas J, Mizuno M, Bell-McGuinn K, Sullivan DM, Bach BA, Bhattacharya S, Ratajczak CK, Ansell PJ, Dinh MH, Aghajanian C, Bookman MA: Veliparib with First-Line Chemotherapy and as Maintenance Therapy in Ovarian Cancer. New England Journal of Medicine 2019, 381:2403-15.
[136] Liu J, Gunderson C, Hendrickson A, Ratner E, Diver E, Moroney J, Arend R, Louie-Gao M, Wang S, Luptakova K, Konecny G: Abstract CT157: An open-label Phase II study of combination of TSR-042, bevacizumab, and niraparib in patients with platinum-resistant ovarian cancer (OC): Cohort A of the OPAL trial, 2019.
[137] Reck M, Rodríguez-Abreu D, Robinson AG, Hui R, Csőszi T, Fülöp A, Gottfried M, Peled N, Tafreshi A, Cuffe S, O'Brien M, Rao S, Hotta K, Leiby MA, Lubiniecki GM, Shentu Y, Rangwala R, Brahmer JR: Pembrolizumab versus Chemotherapy for PD-L1–Positive Non–Small-Cell Lung Cancer. New England Journal of Medicine 2016, 375:1823-33.
[138] Jimmy Belotte BF, Amanda J. Baines, Ahmed YoussefAgha, Luis Rojas-Espaillat, Ana Godoy Ortiz, Diane Provencher, Raúl Márquez Vázquez, Lucia González Cortijo, Xing Zeng: Open-label, Phase 2, Randomized Controlled Multicenter Study Comparing Niraparib Versus Platinum-Taxane Doublet Chemotherapy

as Neoadjuvant Treatment in Participants With Homologous Recombination-Deficient Stage III/IV Ovarian Cancer: Trial in Progress. 2023.
[139] Gunti S, Hoke ATK, Vu KP, London NR, Jr.: Organoid and Spheroid Tumor Models: Techniques and Applications. Cancers (Basel) 2021, 13.
[140] Choi Y, Lee S, Kim K, Kim SH, Chung YJ, Lee C: Studying cancer immunotherapy using patient-derived xenografts (PDXs) in humanized mice. Exp Mol Med 2018, 50:1-9.

[141] Hou X, Du C, Lu L, Yuan S, Zhan M, You P, Du H: Opportunities and challenges of patient-derived models in cancer research: patient-derived xenografts, patient-derived organoid and patient-derived cells. World J Surg Oncol 2022, 20:37.
[142] Invrea F, Rovito R, Torchiaro E, Petti C, Isella C, Medico E: Patient-derived xenografts (PDXs) as model systems for human cancer. Current Opinion in Biotechnology 2020, 63:151-6.
[143] Byrne AT, Alférez DG, Amant F, Annibali D, Arribas J, Biankin AV, Bruna A, Budinská E, Caldas C, Chang DK: Interrogating open issues in cancer precision medicine with patient-derived xenografts. Nature Reviews Cancer 2017, 17:254-68.
[144] Yang J, Huang S, Cheng S, Jin Y, Zhang N, Wang Y: Application of Ovarian Cancer Organoids in Precision Medicine: Key Challenges and Current Opportunities. Front Cell Dev Biol 2021, 9:701429.
[145] Jung J, Seol HS, Chang S: The Generation and Application of Patient-Derived Xenograft Model for Cancer Research. Cancer Res Treat 2018, 50:1-10.
[146] Brodeur MN, Simeone K, Leclerc-Deslauniers K, Fleury H, Carmona E, Provencher DM, Mes-Masson A-M: Carboplatin response in preclinical models for ovarian cancer: comparison of 2D monolayers, spheroids, ex vivo tumors and in vivo models. Scientific Reports 2021, 11:18183.
[147] Heredia-Soto V, Redondo A, Berjon A, Miguel-Martin M, Diaz E, Crespo R, Hernandez A, Yebenes L, Gallego A, Feliu J, Hardisson D, Mendiola M: High-throughput 3-dimensional culture of epithelial ovarian cancer cells as preclinical model of disease. Oncotarget 2018, 9:21893-903.
[148] Millard M, Yakavets I, Zorin V, Kulmukhamedova A, Marchal S, Bezdetnaya L: Drug delivery to solid tumors: the predictive value of the multicellular tumor spheroid model for nanomedicine screening. Int J Nanomedicine 2017, 12:7993-8007.
[149] Tomas E, Shepherd TG: Insights into high-grade serous carcinoma pathobiology using three-dimensional culture model systems. Journal of Ovarian Research 2023, 16:70.
[150] Sainz-Arnal P, Pla-Palacín I, Sánchez-Romero N, Almeida M, Morini S, Solanas E, Lue A, Serrano-Aulló T, Baptista PM: Chapter 62 - Bioengineering of Liver Tissue. Principles of Regenerative Medicine (Third Edition). Edited by Atala A, Lanza R, Mikos AG, Nerem R. Boston: Academic Press, 2019. pp. 1101-13.
[151] Melissaridou S, Wiechec E, Magan M, Jain MV, Chung MK, Farnebo L, Roberg K: The effect of 2D and 3D cell cultures on treatment response, EMT profile and stem cell features in head and neck cancer. Cancer Cell Int 2019, 19:16.
[152] Hill SJ, Decker B, Roberts EA, Horowitz NS, Muto MG, Worley MJ, Jr., Feltmate CM, Nucci MR, Swisher EM, Nguyen H, Yang C, Morizane R, Kochupurakkal BS, Do KT, Konstantinopoulos PA, Liu JF, Bonventre JV, Matulonis UA, Shapiro GI, Berkowitz RS, Crum CP, D'Andrea AD: Prediction of DNA Repair Inhibitor Response in Short-Term Patient-Derived Ovarian Cancer Organoids. Cancer Discov 2018, 8:1404-21.
[153] Yao Y, Xu X, Yang L, Zhu J, Wan J, Shen L, Xia F, Fu G, Deng Y, Pan M, Guo Q, Gao X, Li Y, Rao X, Zhou Y, Liang L, Wang Y, Zhang J, Zhang H, Li G, Zhang L, Peng J, Cai S, Hu C, Gao J, Clevers H, Zhang Z, Hua G: Patient-Derived Organoids Predict Chemoradiation Responses of Locally Advanced Rectal Cancer. Cell Stem Cell 2020, 26:17-26.e6.
[154] Fang Z, Li P, Du F, Shang L, Li L: The role of organoids in cancer research. Experimental Hematology & Oncology 2023, 12:69.
[155] Kim J, Koo BK, Knoblich JA: Human organoids: model systems for human biology and medicine. Nat Rev Mol Cell Biol 2020, 21:571-84.
[156] Rodrigues J, Heinrich MA, Teixeira LM, Prakash J: 3D In Vitro Model (R)evolution: Unveiling Tumor–Stroma Interactions. Trends in Cancer 2021, 7:249-64.

[157] Kopper O, de Witte CJ, Lõhmussaar K, Valle-Inclan JE, Hami N, Kester L, Balgobind AV, Korving J, Proost N, Begthel H, van Wijk LM, Revilla SA, Theeuwsen R, van de Ven M, van Roosmalen MJ, Ponsioen B, Ho VWH, Neel BG, Bosse T, Gaarenstroom KN, Vrieling H, Vreeswijk MPG, van Diest PJ, Witteveen PO, Jonges T, Bos JL, van Oudenaarden A, Zweemer RP, Snippert HJG, Kloosterman WP, Clevers H: An organoid platform for ovarian cancer captures intra- and interpatient heterogeneity. Nature Medicine 2019, 25:838-49.
[158] Goyeneche A, Lisio M-A, Fu L, Srinivasan R, Valdez Capuccino J, Gao Z-h, Telleria C: The Capacity of High-Grade Serous Ovarian Cancer Cells to Form Multicellular Structures Spontaneously along Disease Progression Correlates with Their Orthotopic Tumorigenicity in Immunosuppressed Mice. Cancers 2020, 12:699.
[159] Stukova M, Hall MD, Tsotsoros SD, Madigan JP, Farrell NP, Gottesman MM: Reduced accumulation of platinum drugs is not observed in drug-resistant ovarian cancer cell lines derived from cisplatin-treated patients. Journal of Inorganic Biochemistry 2015, 149:45-8.
[160] Cooke SL, Ng CK, Melnyk N, Garcia MJ, Hardcastle T, Temple J, Langdon S, Huntsman D, Brenton JD: Genomic analysis of genetic heterogeneity and evolution in high-grade serous ovarian carcinoma. Oncogene 2010, 29:4905-13.
[161] Ritch SJ, Noman ASM, Goyeneche AA, Telleria CM: The metastatic capacity of high-grade serous ovarian cancer cells changes along disease progression: inhibition by mifepristone. Cancer Cell International 2022, 22:397.
[162] Verduin M, Hoeben A, De Ruysscher D, Vooijs M: Patient-Derived Cancer Organoids as Predictors of Treatment Response. Frontiers in Oncology 2021, 11.
[163] Millen R, De Kort WWB, Koomen M, van Son GJF, Gobits R, Penning de Vries B, Begthel H, Zandvliet M, Doornaert P, Raaijmakers CPJ, Geurts MH, Elias SG, van Es RJJ, de Bree R, Devriese LA, Willems SM, Kranenburg O, Driehuis E, Clevers H: Patient-derived head and neck cancer organoids allow treatment stratification and serve as a tool for biomarker validation and identification. Med 2023, 4:290-310.e12.
[164] Zhao Z, Chen X, Dowbaj AM, Sljukic A, Bratlie K, Lin L, Fong ELS, Balachander GM, Chen Z, Soragni A, Huch M, Zeng YA, Wang Q, Yu H: Organoids. Nature Reviews Methods Primers 2022, 2:94.
[165] Xu H, Lyu X, Yi M, Zhao W, Song Y, Wu K: Organoid technology and applications in cancer research. Journal of Hematology & Oncology 2018, 11:116.
[166] Nanki Y, Chiyoda T, Hirasawa A, Ookubo A, Itoh M, Ueno M, Akahane T, Kameyama K, Yamagami W, Kataoka F, Aoki D: Patient-derived ovarian cancer organoids capture the genomic profiles of primary tumours applicable for drug sensitivity and resistance testing. Scientific Reports 2020, 10:12581.
[167] St-Georges-Robillard A, Cahuzac M, Péant B, Fleury H, Lateef MA, Ricard A, Sauriol A, Leblond F, Mes-Masson A-M, Gervais T: Long-term fluorescence hyperspectral imaging of on-chip treated co-culture tumour spheroids to follow clonal evolution. Integrative Biology 2019, 11:130-41.
[168] Maenhoudt N, Vankelecom H: Protocol for establishing organoids from human ovarian cancer biopsies. STAR Protocols 2021, 2:100429.
[169] Karakasheva TA, Kijima T, Shimonosono M, Maekawa H, Sahu V, Gabre JT, Cruz-Acuña R, Giroux V, Sangwan V, Whelan KA, Natsugoe S, Yoon AJ, Philipone E, Klein-Szanto AJ, Ginsberg GG, Falk GW, Abrams JA, Que J, Basu D, Ferri L, Diehl JA, Bass AJ, Wang TC, Rustgi AK, Nakagawa H: Generation and Characterization of Patient-Derived Head and Neck, Oral, and Esophageal Cancer Organoids. Curr Protoc Stem Cell Biol 2020, 53:e109.

[170] Hoffmann K, Berger H, Kulbe H, Thillainadarasan S, Mollenkopf HJ, Zemojtel T, Taube E, Darb-Esfahani S, Mangler M, Sehouli J, Chekerov R, Braicu EI, Meyer TF, Kessler M: Stable expansion of high-grade serous ovarian cancer organoids requires a low-Wnt environment. Embo j 2020, 39:e104013.
[171] Flores-Torres S, Peza-Chavez O, Kuasne H, Munguia-Lopez JG, Kort-Mascort J, Ferri L, Jiang T, Rajadurai CV, Park M, Sangwan V, Kinsella JM: Alginate-gelatin-Matrigel hydrogels enable the development and multigenerational passaging of patient-derived 3D bioprinted cancer spheroid models. Biofabrication 2021, 13.
[172] Idos GE, Kurian AW, Ricker C, Sturgeon D, Culver JO, Kingham KE, Koff R, Chun NM, Rowe-Teeter C, Lebensohn AP, Levonian P, Lowstuter K, Partynski K, Hong C, Mills MA, Petrovchich I, Ma CS, Hartman AR, Allen B, Wenstrup RJ, Lancaster JM, Brown K, Kidd J, Evans B, Mukherjee B, McDonnell KJ, Ladabaum U, Ford JM, Gruber SB: Multicenter Prospective Cohort Study of the Diagnostic Yield and Patient Experience of Multiplex Gene Panel Testing For Hereditary Cancer Risk. JCO Precis Oncol 2019, 3.
[173] Wang J, Dean DC, Hornicek FJ, Shi H, Duan Z: RNA sequencing (RNA-Seq) and its application in ovarian cancer. Gynecol Oncol 2019, 152:194-201.
[174] Ciucci A, Buttarelli M, Fagotti A, Scambia G, Gallo D: Preclinical models of epithelial ovarian cancer: practical considerations and challenges for a meaningful application. Cellular and Molecular Life Sciences 2022, 79:364.